Litho–structural Controls on the Groundwater Flow System and Hydrogeochemical Setup of the Mekelle Outlier and Surrounding Areas, Nothern Ethiopia

Ermias Hagos Girmay

A Thesis Submitted to

The School of Earth Sciences

Presented in Partial Fulfillment of the Requirements for the Degree of

Doctor of Philosophy in Hydrogeology

Addis Ababa University

Addis Ababa, Ethiopia

September 2015

Addis Ababa University

School of Graduate Studies

This is to certify that the thesis prepared by Ermias Hagos Girmay, entitled: *Litho-stratigraphic and Structural controls on the Groundwater Flow Dynamics and Hydrogeochemical setting of the Mekelle Outlier and Surrounding Areas, Nothern Ethiopia* and submitted in partial fulfillment of the requirements for the Degree of Doctor of Philosophy in Hydrogeology complies with the regulations of Addis Ababa University and meets the accepted standards with respect to originality and quality.

Signed by the Examining Committee:

External Examiner_____ Signature_____ Date _____

Internal Examiner _____ Signature_____ Date _____

Principal Advisor _____ Signature_____ Date _____

Co-Avdisor _____ Signature_____ Date _____

Co-Avdisor _____ Signature_____ Date _____

_____

Chaired by the School Graduate Program Coordinator

ABSTRACT

Litho-stratigraphic and Structural controls on the Groundwater Flow Dynamics and Hydrogeochemical setting of the Mekelle Outlier and Surroundings, Northern Ethiopia

Ermias Hagos Girmay

PhD thesis, Addis Ababa University, 2015

The study area (Mekelle outlier and surroundings) is located in the north-eastern part of the Tekeze River Basin, northern Ethiopia. It constitutes a wide range of lithologic units with ages ranging from Neoproterozoic to Quaternary. The older WNW-ESE oriented normal faults, younger NNE-SSW directed lineaments and associated fractures and the N-S trending foliations and lineations associated with the Negash synclinorium are prominent structures in the area. The isotopic signatures ($\delta^{18}O$, $\delta^{2}H$ and tritium) and patterns of dissolved-ion concentrations in the groundwater, coupled with understanding of the three-dimensional geological framework, are used to conceptualize the groundwater flow model and recharge-discharge mechanisms in this complex hydrogeological environment.

The basement rocks, glacial deposits and dolerites in the study area are characterized by shallow and localized aquifers mostly associated with faults and shear zones. Boreholes drilled into these rock formations have well yields mostly less than 5 L/s. The Agula Shale and the upper part of Antalo Limestone are dominated with shale and marl units although gypsum and thin beds of limestone are also minor constituents found as intercalation. They are mostly intruded by dolerite sills and to a lesser extent dolerite dykes. Although they are affected by intense joints, the

groundwater occurrence and flow in this upper part of the sedimentary section is limited due to clay dominated lithology. Wells and springs have low discharges hardly exceeding 2 L/s. At the contact zones with the dolerite intrusions, discharge rates of 12-40 L/s are common. Whereas the Adigrat Sandstone and the lower part of Antalo Limestone are characterized by extensive/semi-regional aquifers with boreholes' yield of up to 60 L/s.

A pattern of high discharge springs, higher boreholes' yield and transmissivity values parallel to the major faults and lineaments and at the contacts between the Mesozoic sedimentary rocks and the Mekelle dolerite is observed. Based on the piezometric map, along with the relatively more depleted isotopic compositions, higher d-excess, and lower dissolved-ion concentrations of the groundwater samples, the highland areas (northwest, north, east and south of the study area) are characterized as recharge areas, while the narrow major river valleys of Giba, Illala, Chelekot and Fucea Mariam are found to be discharge areas. The groundwater divide between the Tekeze and the Denakil basins coincides with the surface-water divide line of these two basins.

Most groundwater samples lay close to the Addis Ababa LMWL indicating meteoric origin. Slight shifts of some samples from this line are attributed to the altitude effect and the isotopic exchanges of rain droplets with the local air mass that have different isotopic composition (more depleted and higher d-excess) from that of Addis Ababa. This effect also results to a smaller slope of the LMWL of the study area ($\delta^2H = 6\times\delta^{18}O + 9.8$; $R^2 = 0.8$). The equation for the evaporation line for the area is $\delta^2H = 4.47\delta^{18}O + 6.42$; $R^2 = 0.8$. The $\delta^{18}O$ of shallow groundwater at different altitudes indicates a depletion rate of -0.51 ‰/100m towards highlands.

In most cases, groundwater feeds the semi-perennial streams and rivers in the area. But isotopic signatures in some wells indicate that there are localities where river flow and seepage from

micro-dams locally feed the adjacent aquifers. Double isotopic measurement of groundwater samples from wells in the summer and dry seasons indicates a significant amount interflow (throughflow) that is pumped in wells during the summer season and disappears shortly after the rainy season passed.

The lithostratigraphic, geomorphologic, isotopic and hydrochemical settings observed in this study indicate that three groundwater flow systems (shallow/local, intermediate and deep/semi-regional) can exist here. Tritium data indicate that the groundwater in the study area has generally short residence time and is dependent on modern precipitation. The range observed in the study area (1.73 to 3.66 TU) indicates components of pre- and post-1952 recharge.

ACKNOWLEDGEMENTS

In the first place, I would like to highly acknowledge the Addis Ababa University, Ruhr Universitat Bochum (Germany) and German Academic Exchange Service (DAAD) for their financial, logistical and laboratory support to the accomplishment of this PhD research work.

My deepest gratitude goes to Professor Tenalem Ayenew who has been my principal advisor for the whole period of my PhD study. His guidance, kind advises and supports towards the scientific achievements presented in this thesis were highly valuable. Thanks a lot, Prof.

My co-advisors Dr. Seifu Kebede (Head of the School of Earth Sciences) and Dr. Mulugeta Alene (Graduate program coordinator of the School of Earth Sciences) are also highly acknowledged for their continuous scientific contributions to this PhD research work and all their kind support.

I am thankful to the highly valuable advises and scientific reviews of my research outputs by Prof. Dr. Stefan Wohnlich and Prof. Dr. Frank Wisotzky during my eight months stay at the Ruhr Universitat Bochum (RUB). Without the free access to their hydrochemical laboratory facilities, this PhD work would not have been completed fast. The brotherly approach, patience and carefulness of Mr. Richard Nicholas during our laboratory analysis activities allowed me to gain important experience. The cheerful and learning time with all other colleagues at the RUB will stay in my heart forever.

The PhD advisory committee and School Graduate Committee members of the School of Earth Sciences are highly appreciated for their serious follow-up and approval of necessary budgetary, logistical and laboratory facilities. I am thankful to all the high caliber academic staff and lab assistants of the school for sharing their rich knowledge and encouragements. I am also grateful to the kind support from Prof. Teketel Yohannes (Former Associate Dean for Research and Graduate Programs in the College of Natural Sciences, AAU) during my enrolment as PhD student and his subsequent follow-ups. The kind support from the administrative staff and registrar of the AAU is highly appreciated. The patience and efforts

from the driver Ato Dibabe during my field work in the remote and highly rugged topography of my study area is highly acknowledged.

The Ministry of Water and Energy, Federal Water Works Design and Supervision Enterprise, Geological Survey of Ethiopia, DH-consult, Tigray Region Bureau of Water and Energy and Water Works Construction Enterprise, Mekelle Town Water Supply Authority, Mekelle University, Wereda water supply bureaus and different towns water supply offices in all parts of my study area, Tekeze Drilling Enterprise, Relief Society of Tigray, Tigray Region Office of Science and Technology are acknowledged for free access to secondary data and support letters.

My wife Rahel Meaza and my children Yonatan and Silvana were always my source of strength during my stay in the PhD study. My father and mother and all my brothers and sisters were also always on my side. Thank you all.

It is difficult to list down all colleagues, friends and relatives who were helping me in many ways. Therefore, asking their apologies, I would like to forward them all big thanks.

Table of contents

List of figures

List of tables

List of annexes

List of abbreviation and symbols

ANS	Arabian Nubian Shield
BH	Borehole
DW	Deep Well
EC	Electrical Conductivity
eg	example
EIGS	Ethiopian Institute of Geological Survey
EELSS	Electrolytic Enrichment and Liquid Scintillation Spectrometry
EMA	Ethiopian Mapping Authority
Fm	Formation
FWWDSE	Federal Water Works Design and Supervision Enterprise
GIS	Geographic Information System
GMWL	Global Meteoric Water Line
GPS	Global Positioning System
HCA	Hierarcical Cluster Analysis
HDW	Hand Dug Well
IAEA	International Atomic Energy Agency
IWMI	International Water Management Institute
ITCZ	Inter Tropical Convergence Zone
LMWL	Local Meteoric Water Line
LWIA	Liquid-Water Isotope Analyzer
mbgl	meters below ground level
MER	Main Ethiopian Rift

MWR	Ministry of Water Resources
NBE	Nile Basin in Ethiopia
SG	Sub-Group
SMOW	Standard Mean Ocean Water
SP	Spring
SRTM	Shuttle Radar Terrain Mission
SWL	Static Water Level
TDS	Total Dissolved Solids
TRB	Tekeze River Basin
USGS	United States Geological Survey

1. Background

1.1. Rationale

Groundwater occurrence in the earth's geological formations is basically heterogeneous. Hence, the knowledge of how these earth materials are formed and the changes they have undergone is vital to understand the distribution of geological materials of varying hydraulic conductivity and porosity (Fetter, 1994; Tenalem Ayenew and Tamiru Alemayehu, 2001; Tamiru Alemayehu, 2006; Newman et al., 2010; Singhal and Gupta, 2010; Seifu Kebede, 2013). Such geological expertise in a multifaceted hard rock and tectonic setting should therefore come as a *priory* while trying to conceptualize the groundwater flow system and hydrogeochemical characteristics of an area. The expertise includes knowledge about metamorphic and sedimentary facies and architecture, the tectonic settings and the genesis of aquifers. This helps as a source of knowledge to interpret results from isotopic, hydrochemical and other hydrogeological data; to fill data gaps and ultimately to establish more precise conceptual hydrogeological models.

The environmental isotopes ^{18}O and ^{2}H are widely used as tracers to investigate various hydrogeological processes (such as origin, movement, mixing, evaporation, groundwater recharge and basin hydrology) to improve our understanding of the modern hydrological cycle at local, regional and global scales (Clark and Fritz 1997; Rietti-Shati et al. 2000; Kendall and Coplen 2001; Gibson et al. 2005). These studies provide base-level information, as the ^{18}O and ^{2}H isotopes systematically vary after evaporation from seawater, condensation during atmospheric transportation of water vapor, and evaporation from the surface water and groundwater after precipitation.

A number of researches in the Ethiopian Rift Valley and the Blue Nile Basins have shown that the patterns of $\delta^{18}O$, $\delta^{2}H$ and ^{3}H isotopic compositions in water can provide a useful tool for hydrological investigations (Darling et al. 1996; Tenalem Ayenew, 1998, 2003; Seifu Kebede, 2004; Seifu Kebede et al., 2005, 2008, 2012; Molla Demelle et al., 2006, 2007; Andarge Yitbarek et al., 2012; Wakgari Furi et al., 2011; Shimelis Weldesenbet, 2012), while there are no similar studies undertaken in the Tekeze and Denakil basins, where the study area resides.

Accordingly, these environmental isotopes (^{18}O, ^{2}H and ^{3}H) and hydrochemical data coupled with geological expertise of the study area have been employed to construct conceptual groundwater flow models. Within these models, the current study has tried to solve many controversial ideas forwarded in the previous studies (Beyth and Shachnai 1970; Tesfaye and Gebretsadik 1982; Abdelwassie Hussein 2000; Samuel Yihdego 2003 and Teklay Zereay 2007; FWWDSE/Federal Water Works Design and Supervision Enterprise 2007; Tesfamichael 2009; DH-consult 2010) regarding the groundwater flow dynamics within the Mekelle sedimentary outlier and its close surroundings.

1.2. Summary of previous hydrogeological works and ongoing debates in the Mekelle outlier and close surroundings

Most of the previous hydrogeological studies are done using conventional hydrogeological techniques with an overall goal of solving the immediate and intermediate water demand problems of the Mekelle town focusing on delineating and quantifying potential groundwater localities to propose new well fields.

The master plan study done in the area (MWR, 1998) has focused on organizing the available previous data and assessing the water resources potential of the focus areas at reconnaissance

level. Most of the M.sc thesis works at different universities within Ethiopia and abroad have focused on the Aynalem, Illala and small catchments around Mekelle. They emphasized on the localized and shallow groundwater dynamism and the problems associated with identifying and evaluating groundwater potential areas for the Mekelle and other smaller towns.

A more comprehensive scientific PhD dissertation (Tesfamichael, 2009) that is done on the Giba river basin has intensively applied remote sensing for geological and land use mapping and groundwater flow modeling with the aim of estimating the different components of water balance in the area.

Hydrogeological investigation of the Federal Water Works Design and Supervision Enterprise (2007) and the DH-consult (2010) have covered relatively large areas. They have generated large volumes of data and forwarded some important hypothesis into the regional geological and hydrogeological characteristics of the area. Their works were largely dependent on conventional hydrogeological techniques with an overall goal of assessing, delineating and quantifying potential groundwater resources in the area and to propose on management aspects.

In the previous works there are two diverging views about the groundwater flow system in the area. Some of them have tried to indicate that there is only local flow system where precipitation is the only source of recharge to the area and discharge is only through springs/wetlands and rivers that follow the nearly E-W trending faults (Beyth et. al., 1970, Tesfamichael Gebreyohannes, 2009 and DH-consult, 2010). Whereas others tried to show that there are inter-catchment/inter-basin groundwater transfers with possibility of intermediate to regional flow systems (Tesfaye Cherinet and Gebretsadik Eshete, 1982; FWWDSE, 2007; Abdelwassie Hissein, 2000; Samuel Yihdego, 2003 and Teklay Zereay, 2007). In the second group, Tesfaye

Chernet and Gebretsadik Eshete (1982) and the FWWDSE (2007) concluded that there are both regionally extended aquifers and structurally (N-S trending faults) controlled inter-basin transfers whereas Abdelwassie Hussein (2000), Samuel Yihdego (2003) and Teklay Zereay (2007) who studied around the Aynalem well-field rely on the cross-catchment semi-regional structures (N-S trending faults) for the localized inter-catchment groundwater transfers. Almost all of the authors have recommended a much more detailed analysis of the litho-structural controls on the hydrodynamics of the area by using systematically selected sampling points for detailed structural analysis and robust hydrochemical and environmetal isotope techniques.

Another debate is on whether the shale in the study area can serve as aquifer or not. Most previous studies considered the shale to be mainly characterized by very less permeability. But the study of Nata Tadesse and Muruts Hagos (2010) in the Hantebet catchment within the Mekelle Outlier has articulated that irrespective of the nature of the rock; the fractures and joints seems effective as conduits for groundwater movement particularly for the shale which is rather considered impermeable. This conclusion is made from their observations on productive shallow wells drilled into the fractured shale.

In addition, there is a debate on the distribution of salinity in the groundwaters. Even though, almost all the pervious investigators have hypothesized that the sources of high salinity to groundwaters in the area are the gypsum layers within the Agula shale unit (Abdelwassie Hussein, 2000; Samuel Yihdego, 2003; FWWDSE, 2007; Teklay Zereay, 2007; Tesfamichael Gebreyohannes, 2009; DH-consult, 2010) which are encountered in many wells and there is linear correlation between the concentration of SO_4^{--} and salinity. But on the other hand low salinity waters are detected at depths below 200 meters (FWWDSE, 2007; DH-consult, 2010). The Federal Water Works Design and Supervision Enterprise (2007) has concluded that the

upper aquifer in the Aynalem area which bears groundwater with relatively higher salinity is characterized by a closed basin nature which is separated from the lower (deeper) regional aquifer by thick impermeable dolerite layer while DH-consult (2010) indicated that there is salinity stratification with low values at the shallow depths and increasing with depth until it turns back to lower values below 200m. Both have used resistivity and SP well logging for their conclusion. On the other hand, the area is highly dissected by deep penetrating regional faults and intensive jointing which could interconnect the lithologically different aquifers at different levels in the stratigraphy. The spatial and vertical salinity distributions and the patterns of hydrochemical variability in relation to the flow dynamics and respective rock-water reactions are not well studied in the previous studies except with respect to quality and changes in water type.

1.3. Statement of the Problem

The area is characterized by a semi-arid climate and uni-modal type of rainfall (rainy months: June, July and August). Similar to other arid and semiarid regions, most rivers and springs in the study area significantly decrease their discharge to unreliable levels (for domestic and small-scale irrigation water supply) starting from the early or mid months of the dry season and usually they become dry in the late months of the dry season. Therefore, hand dug and machine drilled wells are the main source of water supply for domestic, irrigation and industrial uses in almost all parts of the area. Lowering of groundwater levels, significant decrease of wells discharge and high salinity and hardness of the groundwater are the common challenges in the area.

The study area is comprised of a wide range of rock formations with various geochemical compositions and a range of primary and secondary permeabilities that complicate our

understanding of the groundwater flow system and its hydrochemical characteristics. The roles of regional and local geological structures on the dynamics of the groundwater in the study area are not well understood.

The stratigraphy and tectonics of the interface zone is complex (rocks are laterally discontinuous, aquifer compositions are heterogeneous, aquifer hydrodynamic characteristics are variable). Even the same rock type at different locations can have variable hydrodynamic and geochemical characteristics depending on its genesis, age and position in the stratigraphic sequence and the geological history it has passed. Accordingly, the lateral and vertical groundwater flow systems in these diverse rock formations that are spatially and vertically heterogeneous are also so complex that conventional hydrogeological techniques that focus in the assessment and quantification of potential groundwater reservoirs for immediate and intermediate domestic water supply applied in the previous works simplify the situation and could not outline persuasive conceptual models.

Therefore, a close and systematic insight using modern and reliable scientific techniques into the roles of the various structural, litho-stratigraphic and geochemical settings is essential. Addressing what role the difference in the nature of the interface zones play on the groundwater flow pattern and hydrogeochemical evolution between aquifers of different rock formations is also vital. Accordingly, the findings of this research can help to have a much better conceptualization and model of the overall hydrodynamics and hydrogeochemical variability within the study area.

This research work has used a converging approach from the results of litho-stratigraphic, structural, hydrogeochemical and isotopic (both stable and radioactive) analysis of systematically

selected samples. The collected data is thoroughly interpreted using different scientific techniques (refer the methodology section).

In general, the results of this research work can play a vital role in adding significant knowledge and disclose reliable insights into the hydrogeology of the Mekelle outlier and its surroundings. It can also help to advance our understanding and propose solutions to specific problems (such as, declining groundwater levels and drying-up of production wells due to over pumping and recurrent droughts, and the frequent encounter of highly saline/hard waters in production wells in many parts of the research area).

1.4. Research questions

The following research questions are relevant to this work.

- What are the roles of the different lithological units and geological structures (Faults, Joints and dolerite intrusions) on the groundwater flow dynamics?
- Which of the groundwater flow systems (local, intermediate or regional) exist in the Mekelle outlier and surroundings?
- How, when and where is the groundwater in the area recharged and how does it discharge?
- How does the groundwater chemistry evolve when it flows from recharge to discharge areas in the different rock units and geological structures?

1.5. Objectives

1.5.1. General objective

Investigate the roles of litho-stratigraphic and tectonic structures on the hydrodynamics and hydrogeochemical settings of the groundwater within the Mekelle outlier and adjacent areas.

1.5.2. Specific objectives

The specific objectives of this research work were as follows:

- Lithostratigraphic and structural analysis with reference to their control on the hydrodynamics and hydrochemistry of the Mekelle outlier.
- Outline the local, intermediate and regional groundwater flow systems.
- Investigate the recharge-discharge mechanism of the Mekelle outlier and its hydraulic interconnection with the adjacent areas of the Tekeze basin.
- Investigate the rock-water interaction and hydrogeochemical evolution of the groundwater along identified flow lines.

1.6. Structure of the Thesis

This thesis comprises nine chapters. Chapter 1 describes the overall background of this research work including the rationale, pre-existing debates and the research problem, questions and objetives. In chapter 2, the details of approaches and methodology followed in this study are presented. Chapter 3 indicates the location, physiography and climatic conditions of the study area.

Chapter 4 includes the regional and local geology. It starts by describing the regional geologic and tectonic history of Ethiopia and an overview of the geology and hydrogeology of the Tekeze River basin in which the study area is a part. The last section of this chapter is all about the local geology of the study area (Mekelle Outlier and close surroundings).

Chapter 5 deals with the hydrogeology of the study area. Within this chapter, section 5.1 states the hydrostratigraphic features in the study area. Section 5.2 presents the major structural settings and their implication on the distribution of aquifers, groundwater occurrence and possible recharge-discharge mechanisms. And section 5.3 shows the distribution of aquifer hydraulic properties.

Chapter 6 is devoted to the hydrochemistry and isotope hydrology in this research. Sections 6.1 to 6.6 of this chapter present the data and interpretations of the stable isotopes and tritium in water samples that are collected from surface-water and groundwater in different (systematically selected) locations of the study area. Section 6.7 deals with the hydrochemical characteristics of different aquifers in the staratigraphic section and implications about the groundwater flow dynamics.

Chapter 7 shows the inference about the regional groundwater flow directions from static-water-level data and the total-dissolved-solids and d-excess distribution maps.

Chapter 8 summerizes the aquifer systems and their recharge-discharge mechanisms and provides the conceptual groundwater flow model of the Mekelle Paleozoic Mesozoic outlier and surroundings from the converging evidence of the different datasets. The final chapter 9 gives concluding remarks and recommendations.

2. Approach and methodology

In the first place, the relevant previous works in the study area and surroundings were reviewed in detail. This helped to assess the pre-existing level of knowledge in the area; to pinpoint the debates that were not clearly answered; and to identify gaps which need further work regarding the hydrogeological system in the Mekelle outlier and surroundings. This step has given a clue about the type, volume and distribution of reliable pre-existing data (geological, hydrogeological …) that can be used in this study. Side by side, review of relevant up-to-date scientific publications were further assessed in order to gain new knowledge, skills and techniques of scientific approaches.

An exhaustive survey of previous geological knowledge in the study area (Tesfamichael Gebreyohannes et al., 2009; DH-consult, 2010) and new field observations, lithologic logs, geophysical data, digital satellite image interpretations and visual observations from Google Earth Map were employed to produce a modified geological map (scale 1:50000) and geological cross-sections (vertical exaggeration of 5.0).

For the interpretation of satellite images, four Landsat ETM digital images (path numbers 168 and 169; raw numbers 50 and 51) of the years 1999 and 2000 have been mosaiced and processed in the ENVI software version 4.2. The color composite image of bands 7-4-2 was selected to delineate the lithologic contacts. Directional filters at 45º and 135º with a sun angle of 45º were used to enhance the major lineament directions and to plot the major geological structures. The US Geological Survey (USGS) SRTM data of 90 meters resolution is used to produce a shaded digital elevation model of the area and to extract profile sections along selected lines for producing the geological cross sections. The data of lithologic contacts, structures and the

geological cross-sections extracted in the ENVI software have been exported in shape files to the ArcGIS v10 software and shaded with standard shades and symbols. Finally, geological map layouts for print are prepared in the ArcGIS environment.

During the field work, traverse lines were selected along the pathways of the Giba and Zamra Rivers and their tributaries; parallel to and across the regional faults of the Wukro, Mekelle, Chelekot and Fucea Mariam (*Fig 13*). This helped to observe and describe the overall geological, structural and hydrogeological setting of the area and to take GPS locations as ground control points for satellite image interpretation. Field assessment and measurements of fractures and sets of fractures were done for structural analysis and to characterize their role in the hydrodynamic properties of the rocks in the area.

In this research, a total of 114 water samples were collected (25 samples from deep wells, with depth 90 to 350 mbgl (meters below ground level); 36 samples from shallow wells, with depth 45 to 80 mbgl; 6 samples from hand dug wells, with depth 12 to 18 mbgl; 33 samples from springs, and 14 samples from river water). Twenty of the samples were collected at the end of the rainy season (end of August to early October, 2012; summer samples) and the other 94 samples were collected in April, 2013 (close to the end of the dry season; winter samples).

The locations of water sampling points (*Fig 1*) were systematically selected based on the following criteria:

- in a way to have representation from different rock formations in the stratigraphic column
- from recharge and discharge areas, and along expected groundwater circulation paths

- their location with respect to different geologic structures (such as faults and dolerite sills and dykes)

The water samples from wells were collected either from the pumped water (continuously functioning hand pumps and submersible pumps) or from the artesian flow on some wells. Spring and river water samples were collected from points of strong flow and no interference from humans or animals, facing opposite to the flow directions. The sampling bottles were repeatedly rinsed with the water to be sampled and then completely filled leaving no space for air. The rubber stoppers were tightly closed and plastered in order to avoid isotopic exchange with the air. The water samples were then kept in cool and dark place both during transportation and in the laboratory.

The laboratory analyses for the stable isotopes were undertaken within one month time and that of tritium within five months time of arrival at the laboratory of the Addis Ababa University (School of Earth Sciences). All of the 114 samples were analyzed for ^{18}O and ^{2}H using a liquid-water isotope analyzer (LWIA) and 35 systematically selected samples were analyzed for activities of tritium using electrolytic enrichment and liquid scintillation spectrometry (EELSS).

Some hydrochemical parameters such as pH, electrical conductivity (EC) and temperature were measured during the field work. The carbonate species (CO_3 and HCO_3) of the 94 samples collected in April were measured upon arrival in the hydrogeology laboratory of the Addis Ababa University by using titration method. These samples were also taken to the hydrogeology laboratory of the Ruhr Universitat Bochum and analyzed for the major cations and anions. The samples were prepared in two separate 50 milli-liter sample bottles, one for the cation analysis

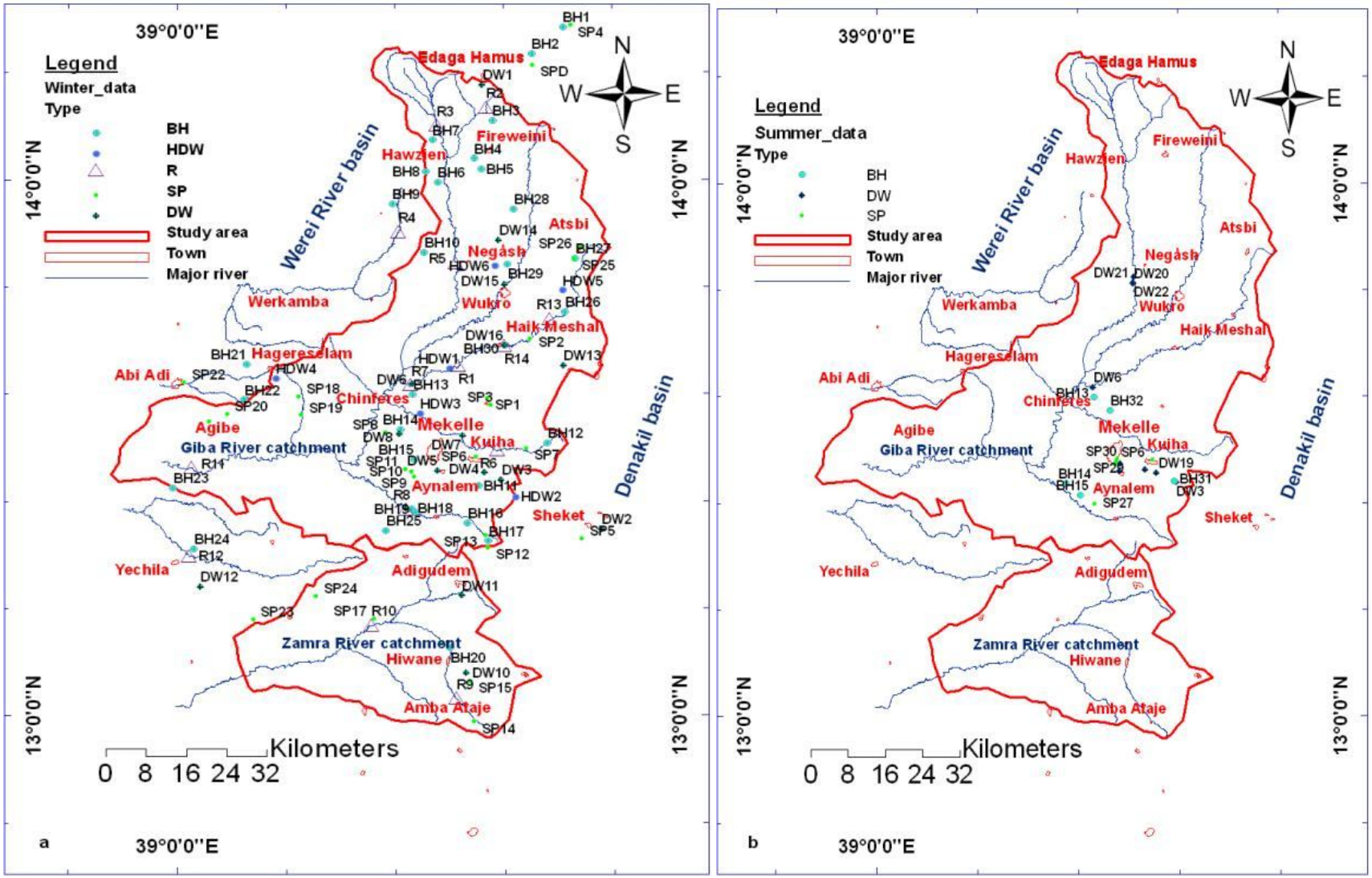

Fig 1 *Locations of water sampling points collected in the (a) winter and (b) summer seasons*

and the other for the anion analysis. Each sample being filtered with 0.25µm filter papers and 0.5 ml of diluted HNO_3 solution was added as preservative in the samples for cations analysis. The concentrations of major cations (K^+, Na^+, $Ca2^+$, and Mg^{2+}), major anions (Cl^-, HCO_3^-, NO_3^-, and SO_4^{2-}) and trace anions (F^- and Br^-) were determined by ionic chromatography (ICS1000 DIONEX chromatograph).

A qualitative and semi-quantitative evaluation of the oxygen and hydrogen stable isotopes results is made by using graphical techniques with reference to some pre-defined patterns of the Standard Mean Oceanic Water Line and Local Meteoric Water Lines and with respect to the sample's location in the different components of the hydrologic system and aquifers. AquaChem version 4.0 (Waterloo Hydrogeologic Inc, 2003) and Microsoft Excel 2007 (Microsoft Corporation 1985) are employed for the graphical analyses.

Cluster analysis is used to characterize samples into groups of statistically distinct hydrochemical properties that are significant in the hydrogeologic context. The Statistica Release 7.0 (StatSoft, Inc. 1995) commercial software package is employed for this purpose. Comparisons based on major-ion chemistry (Li^+, Na^+, K^+, Mg^{2+}, Ca^{2+}, HCO_3^-, SO_4^{2-}, F^-, Cl^-, NO_3^-), EC and altitude of the water samples was made and the samples are grouped according to their 'similarity' to each other. The classification of samples according to their parameters is termed Q-mode classification. In this study, Q-mode Hierarcical Cluster Analysis (HCA) is used to classify the samples into distinct hydrochemical groups and hence to better constrain the hydrochemical interpretation.

In general, the resulting stable isotope data are interpreted by plotting them with the global meteoric water line (GMWL), which was created for the first time by Craig (1961), and the local

meteoric water line (LMWL) of Addis Ababa (Seifu Kebede et al., 2005). The variations in stable isotope and electrical conductivity values of water samples with respect to altitude, depth and geology are critically analyzed by using cross plots and observing their spatial distribution on maps. Static water level and d-excess iso-maps and preliminary cluster analysis of major ions chemistry data of samples from this study (analyzed in the hydrochemical laboratory of the Department of Applied Geology in the Ruhr Universitat Bochum, Germany) are also employed as additional information.

Afterwards, the observed patterns are used to identify recharge and discharge areas, different groundwater flow systems and the surface-water/groundwater interaction trends. The tritium data are utilized to see the relative residence time of the groundwater and to compare it with the interpretations made using stable isotopes and electrical conductivity data. The final results and interpretations are then squeezed to formulate a three-dimensional conceptual hydrogeological framework of the Mekelle Mesozoic sedimentary outlier and its close surroundings.

3. Description of the study area

3.1. Location

The study area is found in the northern part of the Northwestern Ethiopian Plateau. It is geographically located between 38º48ʾ-40º23ʾ east longitudes and 12º55ʾ-14º17ʾ north latitudes. It builds the western shoulder of the Red Sea-Afar Rift at the northern edge of the East African Rift System, and constitutes the northeastern part of Tekeze River Basin (tributary of the Nile Basin) adjucent to the Denakil Depression *(Fig 2)*.

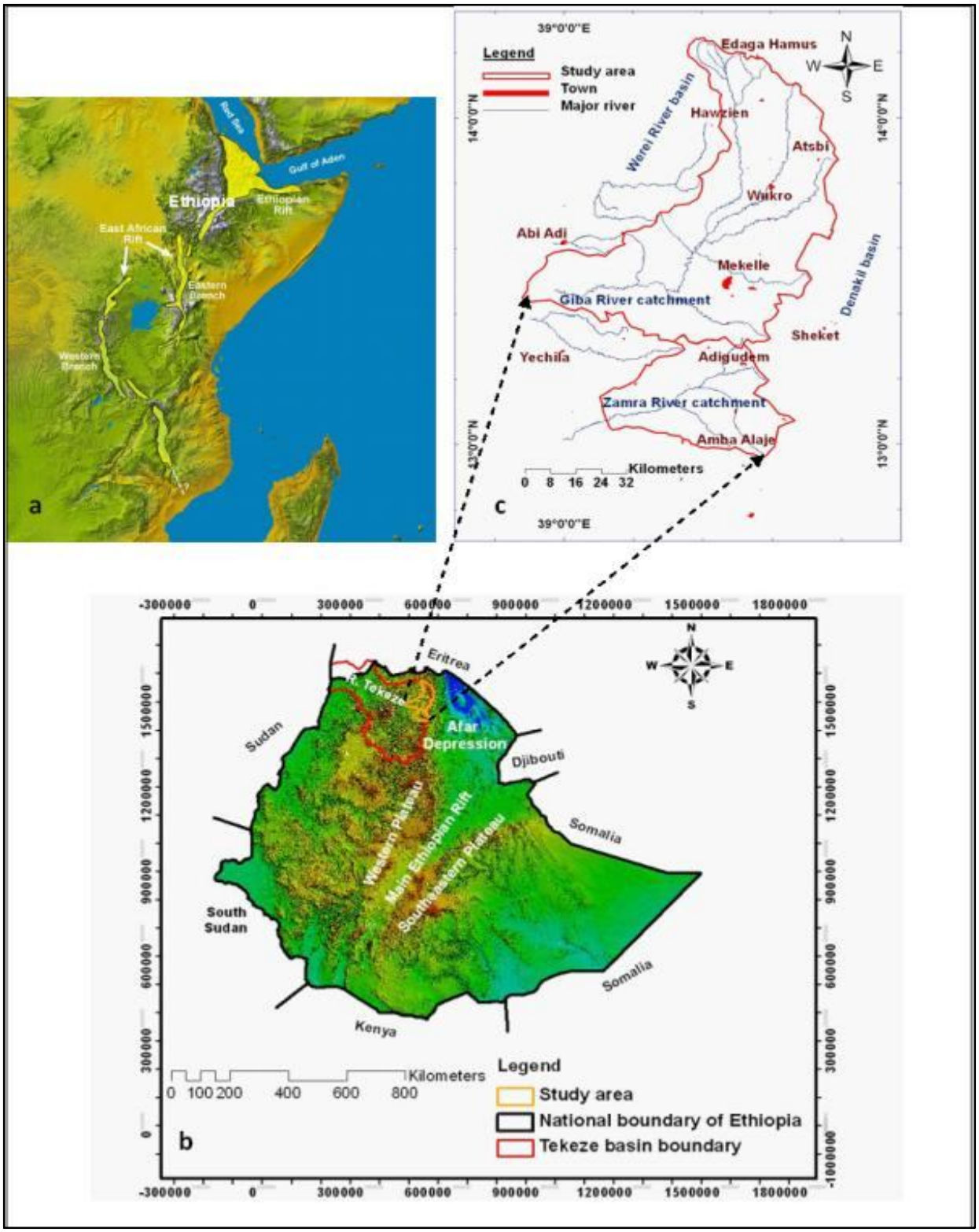

Fig 2 *Location map of (a) major geological features of Ethiopia, and (b) the watershed boundary and (c) major rivers of the study area*

The area is accessed by the main asphalt road from Addis Ababa (the capital city of Ethiopia) and the eastern part of the area is crossed from South to North by this asphalt road which passes through Mekelle town. Most part of the study area is accessed by all-weather roads *(Fig 3b).*

3.2. Physiography

The study area has variable topography. The altitude ranges from 1250 masl in the southwestern lowlands to over 3000 m in the highlands along the boundary of the study area (*Fig 3a*). In general, the study area can broadly be divided into three physiographic regions: the highland; intermountain valleys and grabens; and the southwestern lowlands. Significant portion of the basin belongs to the Ethiopian highlands at altitudes over 2000 m amsl, located west of the Afar Rift. This region is a flat-topped plateau with intervening large volcanic mountains which form water divides and act as regional groundwater recharge zones. The highland areas are deeply cut by the major rivers and their tributaries (*Fig 3a*).

The drainage pattern in the study area is dominantly parallel trellies type indicating the control of the major faults over the drainage pattern (*Fig 3a*). Dendritic pattern is also observed in the upper most catchments of the major rivers which are mostly covered either by basement rocks or Shale or hard volcanic rocks. The major rivers form deep canyons and gorges with steep and narrow river valleys. These valleys are discharge areas where many springs emanate along the contacts of the different rock units (mainly between the Mesozoic sedimentary rocks and the dolerite/Trap series volcanics) and talus deposits. These areas have high surface runoff and are characterized by waterfalls and rapids.

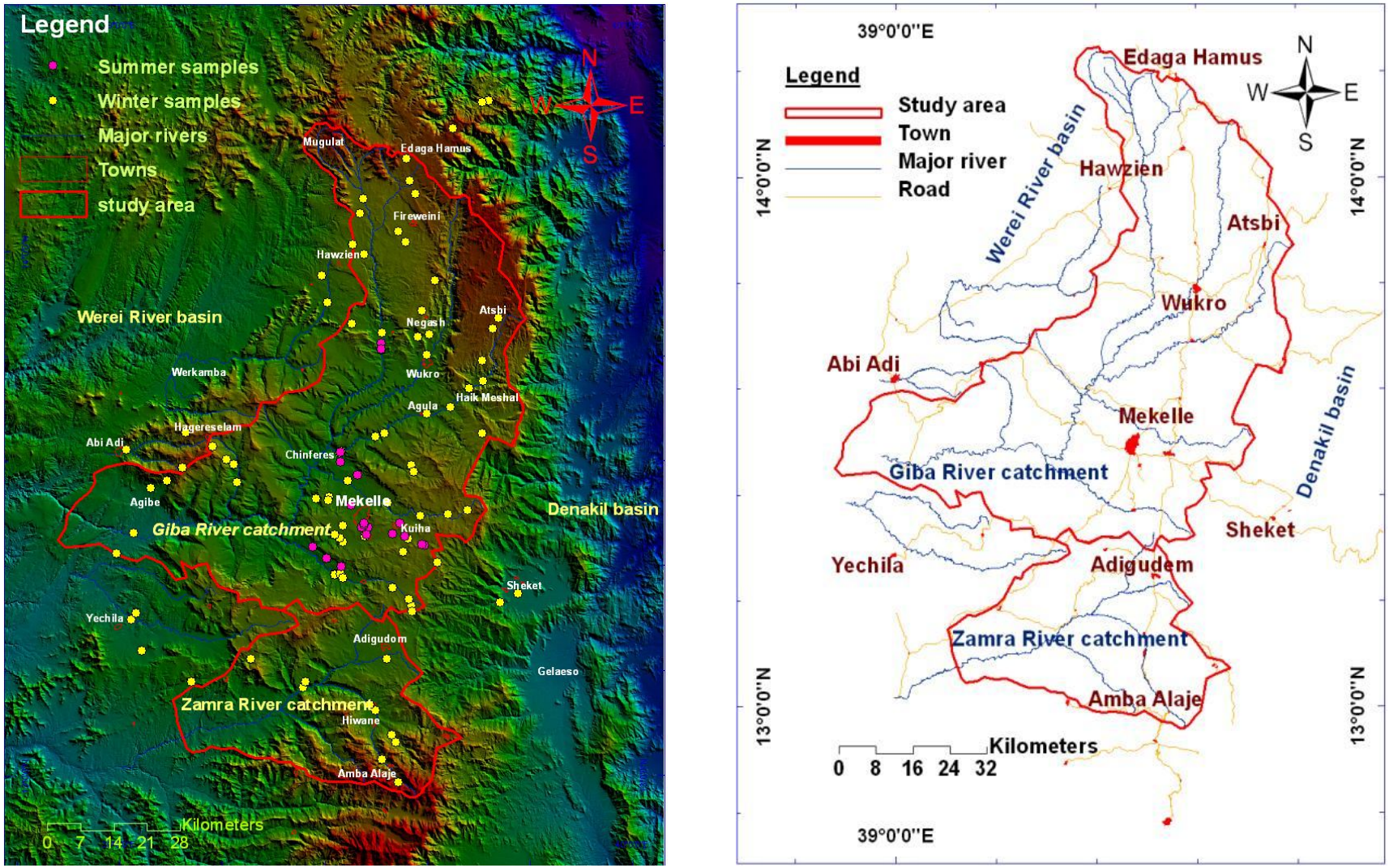

Fig 3 *(a) JPEG Digital Elevation model of the study area (Note: data derived from the Shuttle Radar Terrain Mission (SRTM)) and (b) Simplified map of the study are*

3.3. Climate

The climate in the study area varies significantly in space and time. There is a general agreement that the North Ethiopian rainfall regime is under the influence of both the Indian and the Atlantic Ocean monsoons (Griffiths, 1972; Daniel Gemechu, 1977 and Telford, 1998 in Seifu Kebede and Travi, 2012). The flow of the monsoon moisture to the region is controlled by the seasonal migration of the Inter Tropical Convergence Zone (ITCZ), which interacts with the different physiographic features of the basin. In summer (June to September) the ITCZ is located in northern of the study area and it is under the influence of the southwesterly and southerly monsoon flows (*Fig 4*). Between October and March the ITCZ is located south of Ethiopia. This results in northerly flow of dry and cold air from the Arabian continent (Daniel Gemechu, 1977 in Seifu Kebede and Travi, 2012).

In general the study area is characterized by a semi-arid climate and uni-modal type of rainfall (rainy months: June, July and August). The air temperature varies from an average daily minimum of 6 ^{o}C in the Amba Alaje, Hagereselam and Atsbi highlands to an average daily maximum of 33 ^{o}C in the western and eastern lowland areas. Similarly, the annual average precipitation varies between 450 mm in the lowland areas and 970 mm in the highland areas. Using the WetSpass model, Tesfamichael Gebreyohannes (2009) has estimated a mean annual potential evapotranspiration and a mean annual groundwater recharge of 462 mm and 37 mm respectively for the Giba river basin (*Fig 3*). Similar to other arid and semiarid regions, most rivers and springs in the study area significantly decrease their discharge to unreliable levels (for domestic and small-scale irrigation water supply) starting from the early or mid months of the dry season and usually they become dry in the late months of the dry season.

Table 1 Climate classification based on altitude and temperature (Daniel Gemechu, 1977)

Altitude (m.a.s.l)	Mean annual Temperature (^{o}C)	Description	Local name of climatic classes
3,300 and above	10 or less	Cool	Kur
2,300 - 3,300	10 – 15	Cool temperate	Dega
1,500 - 2,300	15 – 20	Temperate	Weina Dega
500 - 1,500	20 – 25	Warm temperate	Kola
Below 500	25 and above	Hot	Bereha

All the above classes exist in the study area. The highlands belong to Dega, and Weina Dega; while the lowlands are Kola and Bereha.

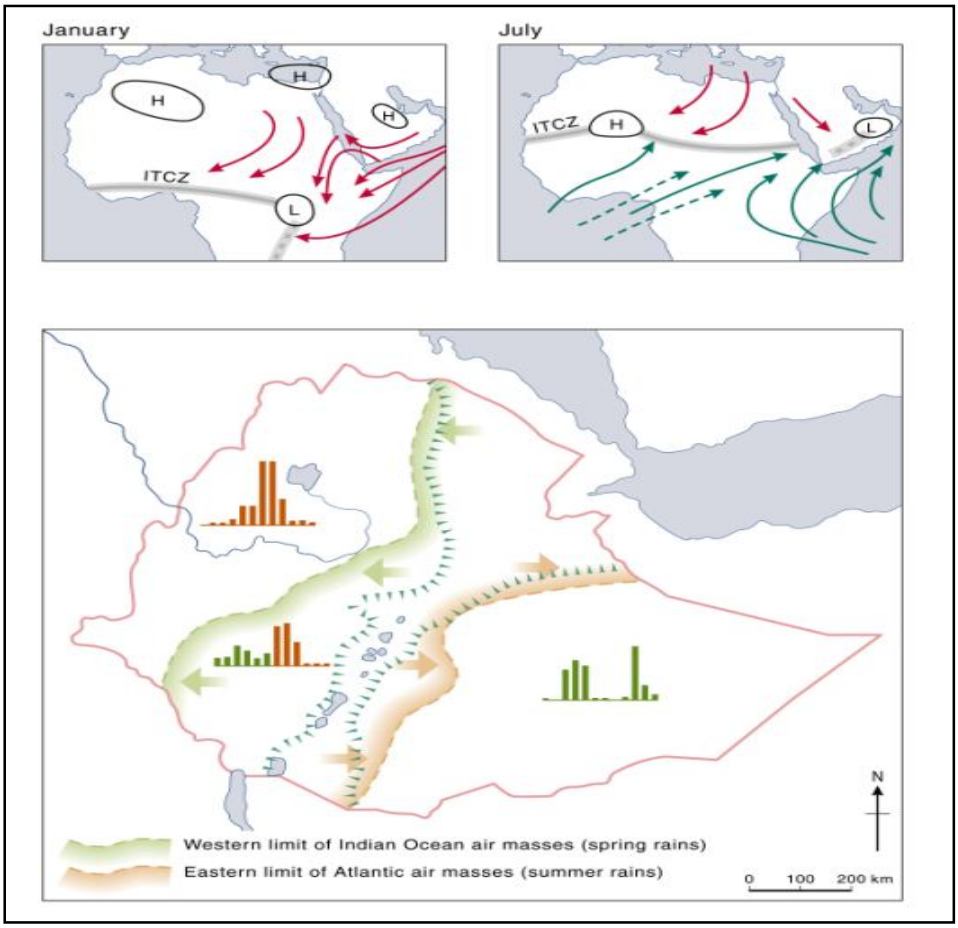

Fig 4 *Seasonal migration of the Intertropical Convergence Zone and its impact on rainfall seasonality in Ethiopia* (FWWDSE, 2009)

4. Geology

4.1. Regional Geology

Ethiopia can be divided into three major physiographic regions widely known as the western plateau with associated lowlands, the southeastern plateau and its peripheral lowlands and the Ethiopian Rift system including the Afar Depression. The Ethiopian plateau is underlain at depth by Precambrian rocks which are considered to be a continuation of two folded belts, the Mozambique belt and the Arabian-Nubian Shield. This Precambrian basement is covered for the most part by glacial and marine sediments of Permian to Paleocene period and Tertiary volcanic rocks with related sediments. The Cenozoic volcanic succession is split apart by parts of the Great East African Rift System in Ethiopia (i.e. The Afar Depression, Main Ethiopian Rift and related southern rifts) (EIGS, 1996).

Precambrian basement exposures are found in areas not intensively affected by Cenozoic volcanism and rifting and where the Phanerozoic cover rocks have been eroded away. Precambrian rocks outcrop in four major regions around the plateau margins. These areas are in Tigray region in the north; along the Sudan border in Benishangul-Gumuz, Wollega, Gambela and Kefa regions (in the west); in Borena and Bale regions in the south and in Harerghe region in the east. Two major litho-tectonic assemblages have been recognized in the Precambrian basement in Ethiopia similar to those recognized in the neighboring countries of northeast Africa and Arabian Peninsula. These are blocks of gneissic terrains and metamorphosed volcanosedimentary belts associated with minor ultramafic bodies and intrusives ranging in composition from mafic to granitic (EIGS, 1996).

The blocks of gneissic terrains which are considered to be generally older than the volcano-sedimentary belts they commonly enclose high grade heterogeneous orthogneisses and paragneisses, at upper amphibolite to granulite facies metamorphism. Metamorphic facies in the low grade volcano-sedimentary succession, however, typically ranges from greenschist to lower amphibolite facies. The most conspicuous foliation trend is north-south with deviations to northeast and northwest. These trends are characteristics of both the low grade volcano-sedimentary succession and the high grade rocks. The boundaries between the gneissic and volcano-sedimentary sequences are typically of tectonic origin. Sheared, mylonitized and highly tectonically deformed rocks occur particularly along the contacts between the gneissic and the low grade volcano - sedimentary belts (EIGS, 1996).

The Precambrian contains a wide variety of sedimentary, volcanic and intrusive rocks which have been metamorphosed to varying degrees. The tract of land along the Ethio-Sudan border in the west is underlain by gneisses and migmatites known as Baro Group. It is flanked on the east by a large tract of land underlain by the relatively low grade volcano-sedimentary succession known as Birbir, Tulu Dimtu, Tsaliet, Tembien Groups and Didikama and Shiraro Formations and associated plutonic rocks. The volcano-sedimentary successions are bordered by a terrain of predominantly gneissic rocks and migmatites to the east. In the southern part of the country another volcano-sedimentary belt (Adola Group) with its attendant intrusives occurs enclosed by gneissic terranes of Early Proterozoic to Archaean age (EIGS, 1996).

Following the Proterozoic to Early Paleozoic; tectonic and magmatic activity and peneplanation of the metamorphic basement took place until Carboniferous and Permian (Kazmin, 1972). Late Paleozoic to Early Mesozoic sediments such as Enticho Sandstone, Edaga Arbi Glacials in northern Ethiopia (Dow et al., 1971), Permian Sandstones in western and southern Ethiopia

(Davidson, 1983), Waju Sandstone in eastern Ethiopia (Kazmin, 1972, 1975) and Gum Sandstone in southern Ethiopia (Belay, 1978) accumulated- in shallow basins and narrow channels cut in the Precambrian basement. Paleozoic continental sediments are also wide spread in Tigray, Harar regions and in the Abay River Gorge (Kazmin, 1972, 1975).

Two major transgression-regression cycles took place during the Mesozoic era (Kazmin, 1972). The first transgression started in the Early Jurassic or Late Triassic from the Ogaden region in the Southeast towards northwest and reached its maximum extent in Kimmeridgian. During this time Adigrat Formation consisting mainly of sandstone and minor lenses of siltstone; Hamanilei Formation consisting mainly of limestone and dolomite; Abay Formation consisting of limestone, sandstone, gypsum and shale; Urandab and Antalo Formation consisting mainly of fossilferous limestones were deposited.

The transgressive sea appears to have reached as far west as 36°E 1ongitude. The regression of the sea started towards the end of Jurassic depositing lagoonal facies of the Agula Formation, which consists of black shale, marl and claystone with beds of limestone, gypsum and dolomite in the Mekelle area in northern Ethiopia. In the Late Cretaceous the second regression event took place depositing continental sediments predominantly composed of interbedded shale, siltstone and sandstone of the Amaba Aradom Formation.

Following the Late Mesozoic – Early Tertiary transgression of the sea from the south-east, an epierogenic uplift of Afro-Arabia (East Africa together with Arabian Peninsula and the intervening regions now occupied by the Red sea and Gulf of Aden) occurred on an immense scale. According to Mohr (1962) the magnitude of the uplift was such that nowhere in the world outside the orogenic belts have basement rocks been uplifted to such an elevation as that

associated with the East African swell. The cause of the major uplift is related to a mantle plume whose decompression melting generated enormous quantities of basaltic magma in the lithosphere and resulted in the formation of a classic continental flood basalt province. The upraised and uparched crust fissuring under tension permitted the ascension of voluminous basaltic magma (Mohr, 1983) to form the Trap Series of Ethiopia.

The Ethiopian flood basalts (or traps) cover an area of about 600,000 km^2 with a layer of basaltic and felsic volcanic rocks. The thickness of this layer is highly variable but reaches 2km in some regions. The volcanic and shallow intrusive rocks have a total volume of about 350,000 km^3 (Mohr, 1983 and Mohr & Zanettin, 1988). But, the Plio-Quaternary volcanics (Late Tertiary) are largely restricted in the rift valley and the Tana basin (Chorowicz et al., 1998). The felsic volcanic strata, capping the flood basalt sequences, are preferentially localized on or near the border fault, indicating that the age of the rhylites actually dates the onset of rifting in the southern Red Sea and Northern main Ethiopian rift. This clearly shows that rifting provides a mechanism for generation of large volumes of felsic magmatism (Dereje Ayalew, 2005).

The mineralogical and chemical composition of the flood basalts is relatively uniform. Most are aphyric to sparsely phyric, and contain phenocryst of plagioclase and clinopyroxene with or without olivine. Most have tholeitic to transitional compostions (Mohr, 1983; Mohr & Zabettin, 1988; Pik et al., 1998). Interlayered with the flood basalts, particularly at upper stratigraphic levels, are felsic lavas and pyroclastic rocks of rhyolitic or less commonly trachytic compositions (Dereje Ayalew et al., 1999).

Except along its margins and in major river valleys, the entire Ethiopian volcanic plateau currently stands above 2000m in altitude. According to Jestin and Huchon (1992) and Menzies

et al. (1992), the uplift took place concurrently with or very soon after eruption of the flood basalts (30 Ma) and since that time the high altitudes have been maintained. It is most unlikely that this uplift is due to the thermal or compositional influence of Oligocene plume, which should have dissipated by now. Instead, the present elevation of the plateau is normally attributed to dynamic support from a thermally anomalous up-welling portion of the present upper mantle (Kieffer et al., 2004). The Ethiopian volcanic plateau is not a thick monotonous, rapidly erupted pile of undeformed, flat lying tholeiitic basalts. Instead, it consists of a number of volcanic centers with different magmatic character and with a large range of ages.

Superimposed on the long uplifted swell of Afro-Arabia, with its axis approximately oriented north-south, parts of the Great East African Rift System started to develop in the Miocene. Rifting began from the presently oceanic Red Sea and Gulf of Aden Rifts which join with the younger and continental Main Ethiopian Rift (MER) at the complex proto-oceanic Afar triple junction (Afar Depression). The MER, which is an important segment of the continental East African Rift, dies out or bifurcates further south into the Lake Turkana and Lake Stifane Rifts and the Reireba proto-rift south of Lake Chamo (EIGS, 1996).

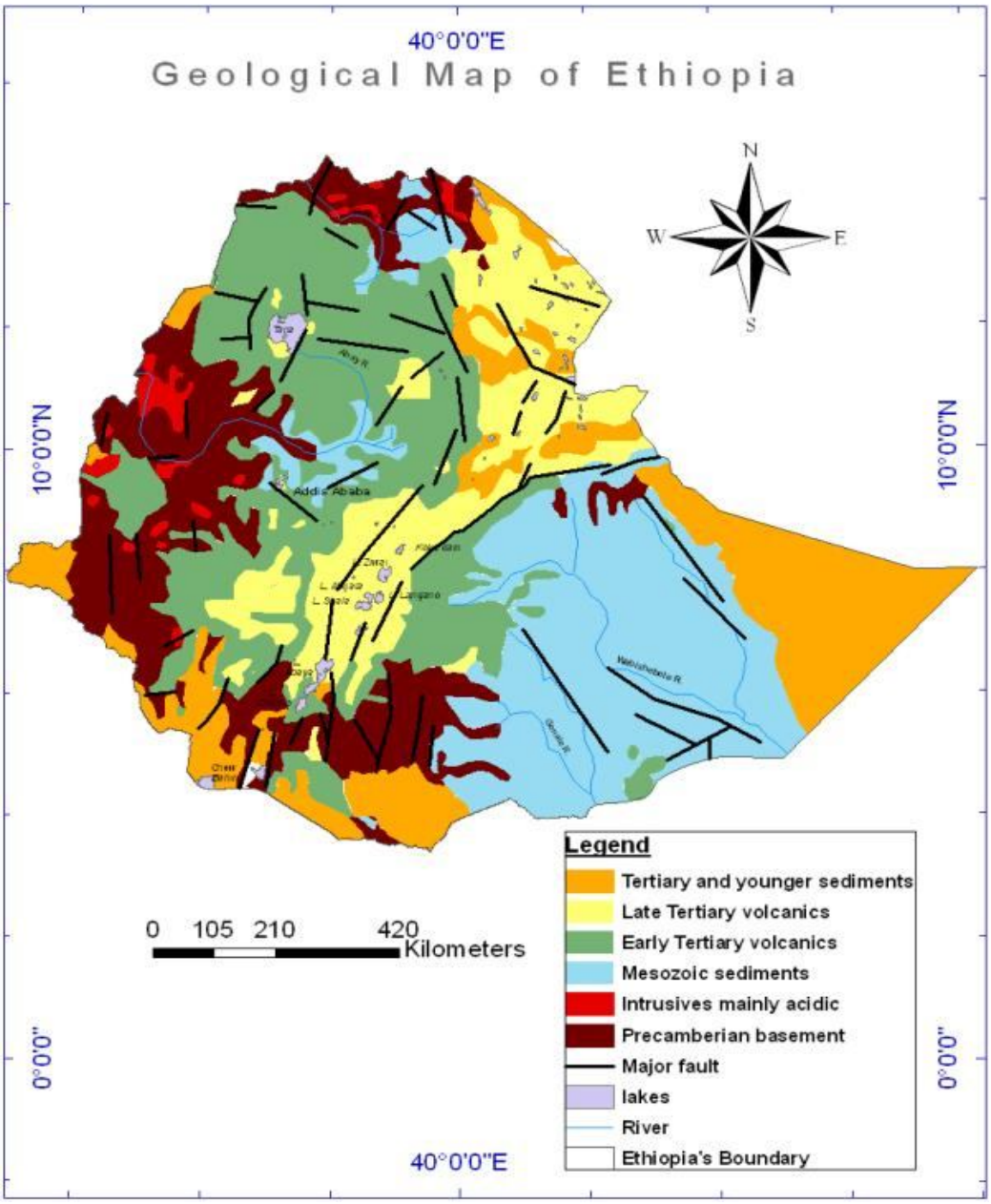

Fig 5 *Simplified geological map of Ethiopia (Modified from EIGS, 1996)*

In the course of the development of parts of the Great East African Rift System in Ethiopia, a variety of continental sedimentary basins were developed since Miocene. In the Afar Depression, sediments originating from the rapid erosion of the steep escarpments together with abundant volcanic products tended to fill the depression but tectonic deepening was more rapid than

volcano-sedimentary infilling. Moreover, the nature of the sediments was dependent on whether the basins are marginal or axial. Evaporite beds have also been formed during the restricted marine invasion of the northern Afar Depression (Danakil Depression). Plio-Pleistocene fluvo-lacustrine sediments are also widespread in the Ethiopian Rift. In the MER, lacustrine sedimentation is wide spread during the pluvial periods of the Quaternary. The present Rift Valley Lakes are therefore remnants of larger ancestral lakes, which covered most parts of the developing rift floor (EIGS, 1996).

4.1.1. Overview of the regional geology and hydrogeology of the Tekeze River Basin

The Tekeze-Atbara River Basin (TRB), in which the study area resides, is part of the Nile Basin in Ethiopia (NBE). It is found in northern Ethiopia between $11^0 40'$ and $14^0 51'$N latitudes and $36^0 40'$ and $39^0 50'$E longitudes. This basin is surrounded by the main Blue Nile (Abay), Angereb, Denakil and the Mereb River Basins (*Fig 6*).

It has a rugged topography (*Fig 7*) with a catchment area of 70000 km^2. The altitude ranges from 500 m in most of the western lowlands to over 4000 m in the Siemen Mountain chains. Significant portion of the basin (70%) belongs to Ethiopian highlands at altitudes over 1,500 m amsl (*Fig 7*). The western lowlands are found in a strip of about 150 km long and 30 km to 100 km wide along the Sudanese border. Here the elevation varies from 500 m to 1000 m and the topography is almost flat or slightly undulating.

The length of Tekeze River, from its source at springs near Lalibela down to the Sudanese border is more than 750 km. The river slope is quite steep in the mountainous stretch (>1.5%), but decreases gradually to 0.3%, and then less than 0.1% in the low lands.

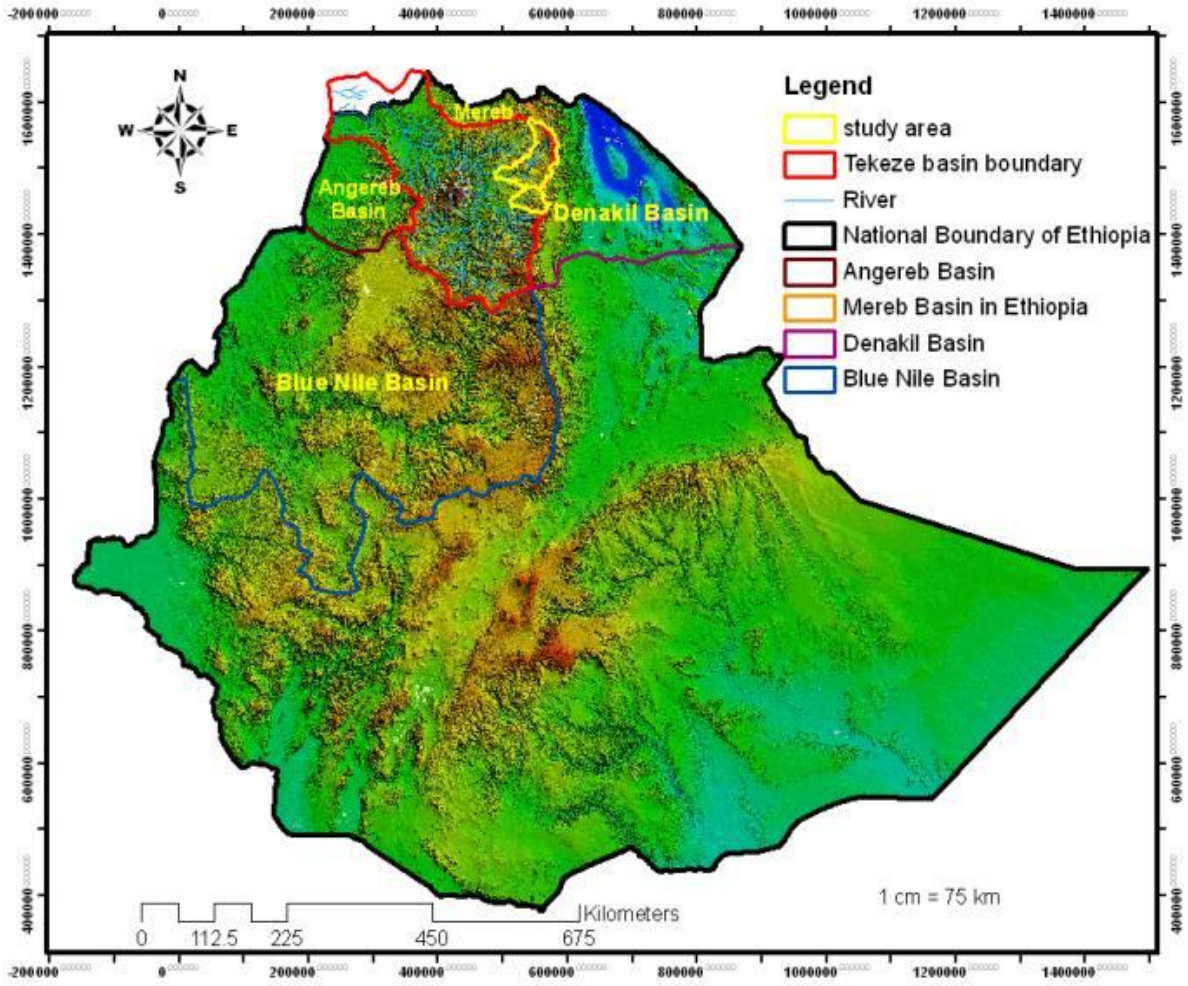

Fig 6 *Location map, watershed boundary and major rivers of the TRB*

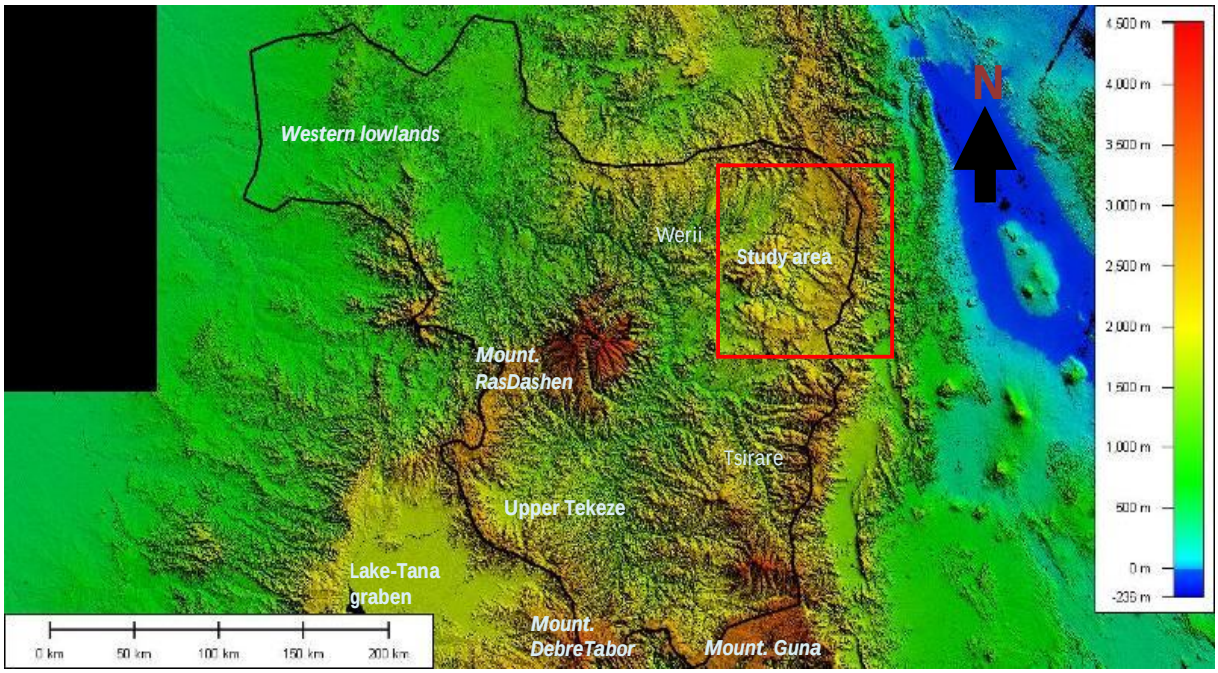

Fig 7 *JPEG Digital Elevation model of the TRB (Elevation legend expressed in metres) Note: data derived from the Shuttle Radar Terrain Mission (SRTM)*

4.1.1.1. Geological setting of the TRB

The TRB constitutes diversified rock types ranging from Neoproterozoic Basement to Quaternary sediments (*Fig 8*) and is characterized by complex tectonic structures. The hydrodynamics of the Tekeze River Basin is strongly controlled by the type of rocks and associated geological structures.

4.1.1.1.1. Neoproterozoic Basement unit

The Neoproterozoic Basement unit is exposed in TRB where all the younger rocks have been removed by erosion. It is composed of low grade metavolcanics, metagraywackes, slates, schists, carbonates and plutonic rocks (Arkin et al., 1971; Beyth, 1971; Garland, 1980; Trekegn Tadesse, 1997; Mulugeta Alene, 1998; Mulugeta Alene et al., 2000, 2006). The rocks are also categorized

into the older and largely metavolcanic unit (the Tsaliet Group) and the younger dominantly metasedimentary unit (the Tambien Group). Both units belong to the Arabian-Nubian Shield (ANS) that developed during the East African Orogeny.

The ANS is considered to have evolved through the opening and closure of oceanic basin, formation and accretion of island arcs, followed by terrain amalgamation and collision processes (Stern, 1994; Meert, 2003). As a result, the basement rocks of TRB possess tectonic fabric as well as low grade metamorphic features. The rocks have been subjected to two major, N-S and E-W, regional compressions producing various folding phases and pervasive foliations and associated lower greenschist facies metamorphism.

In general, the Neoproterozoic metamorphic and associated intrusive rocks in the TRB are usually supposed to have lower permeability and groundwater potential. Mostly they are neglected or less studied in previous hydrogeological investigations in the region. But wells drilled into these rocks where tectonic structures and/or weathering prominently affect them, are sometimes found to be considerably productive and many rural communities and small towns in the area get their water supplies from such rocks.

4.1.1.1.2. Paleozoic and Mesozoic Sedimentary Unit

The flat-lying Phanerozoic sedimentary cover rocks of the TRB fall under two major episodes of deposition: deposition in Paleozoic era or in Mesozoic era (Danielli, 1943; Bosellini et al., 1997). The Paleozoic formations are localized in the Tekeze basin and not common in other parts of Ethiopia. They are essentially constituted of Enticho Sandstone and Edaga Arbi glacial deposits with measured thickness of 150-180 m (Beyth, 1972).

The Enticho Sandstone is the lowermost unmetamorphosed sedimentary unit in the TRB unconformably overlying the basement unit and generally forms flat-topped plateaus and sometimes mesas. It is characterised by white, medium to coarse grained sandstone, coarsely cross-bedded with silty beds and some ferruginous layers. It also exhibits calcareous sandstone, with lenses of polymicritic conglomerates, pebbles and large granite boulders.

The Edaga Arbi Tillite consists of poorly sorted, unstratified and poorly consolidated sediments forming small conical hills or irregular slopes. It is exposed in the western and northern margins of the Mekelle Outlier (*Fig 8*).

In most cases, the Enticho Sandstone is found interfingered with Edaga Arbi Tillite beds hence these rocks are not considered as separate stratigraphic horizons, rather as two different facies of the same age (Tesfamichael Gebreyohannes et al., 2009).

Overlying the Paleozoic rocks is a Mesozoic sedimentary sequence of marine and continental facies. These rocks outcrop dominantly in the Mekelle Outlier and in the incised valleys of the Upper Tekeze and its major tributaries. The Mesozoic succession includes the Adigrat Sandstone, the Antalo Limestone and Agula Shale and the Amba Aradem Formation (*Fig 9*) (Merla and Minucci, 1938; Danielli, 1943; Bossellini et al., 1997).

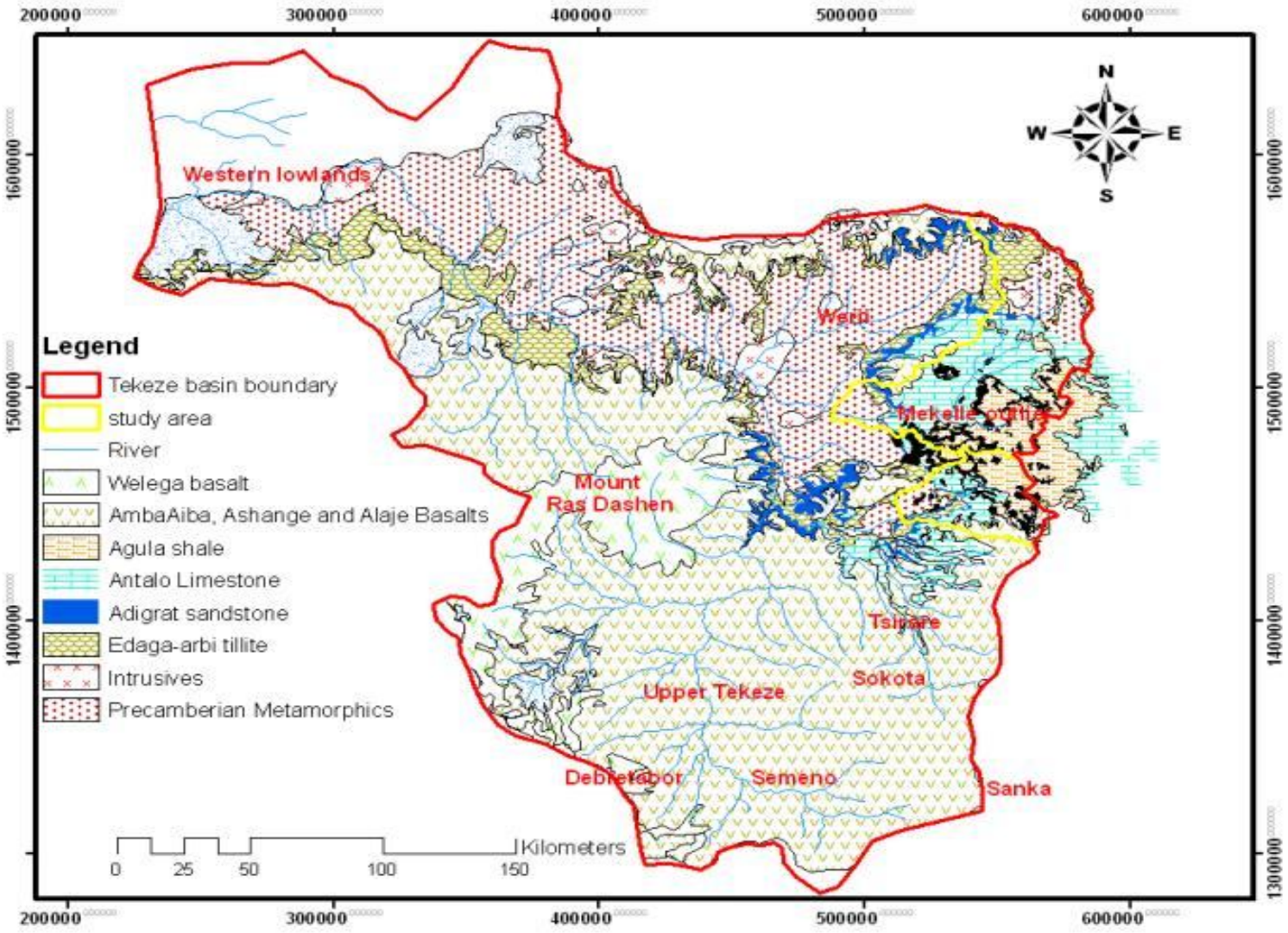

Fig 8 *Simplified geological map of the TRB (Modified from EIGS, 1993)*

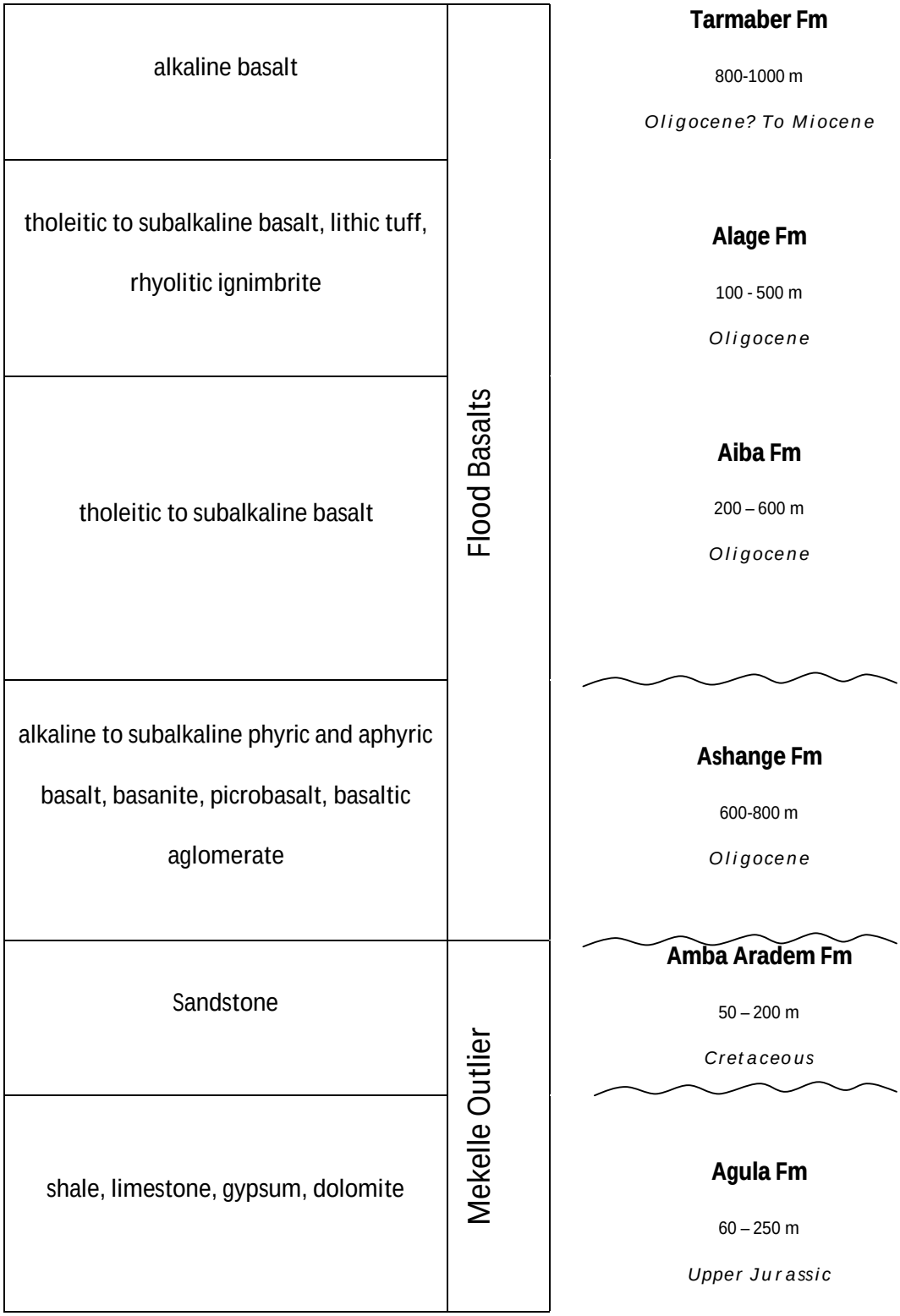
alkaline basalt
tholeitic to subalkaline basalt, lithic tuff, rhyolitic ignimbrite
tholeitic to subalkaline basalt
alkaline to subalkaline phyric and aphyric basalt, basanite, picrobasalt, basaltic aglomerate
Flood Basalts
Sandstone
shale, limestone, gypsum, dolomite
Mekelle Outlier
Tarmaber Fm
800-1000 m
Oligocene? To Miocene
Alage Fm
100 - 500 m
Oligocene
Aiba Fm
200 – 600 m
Oligocene
Ashange Fm
600-800 m
Oligocene
Amba Aradem Fm
50 – 200 m
Cretaceous
Agula Fm
60 – 250 m
Upper Jurassic

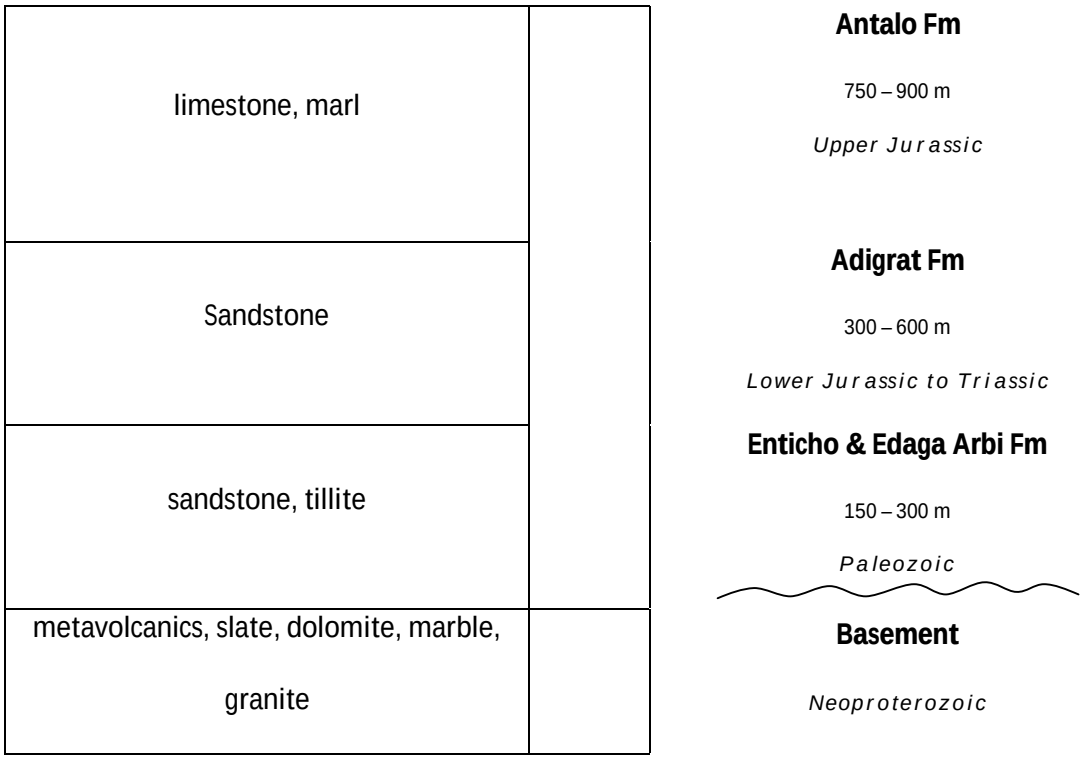

Fig 9 *Simplified stratigraphy of the Mekelle Outlier and northern Ethiopia flood basalt province (after Arkin et al., 1971; Beyth, 1972; Merla et al., 1979)*

The Adigrat Sandstone in TRB is described as Triassic to Collovian in age and fluviatile in origin (Bosellini et al., 1997). It has variable thickness ranging from about 80 m to 700 m (Beyth, 1972). It is mostly massive and thickly bedded with frequently observed cross-bedding. It is mostly white or grey to red, fine- to medium-grained and well sorted. It generally shows an intercalation of conglomerate, silt-shale, laterite and carbonate beds. It contains largely quartz grains and clasts, and subordinate amounts of K-feldspar, muscovite and clay minerals. The lithic fragments are mostly metamorphic and include quartzite, elongated granite, gneiss, phyllites and schists. The sandstone is not well cemented and it is unfossiliferous except for some silicified wood (Worash Getaneh, 2002).

The Antalo Limestone is largely composed of limestone, marls and shales constituting a classical depositional sequence on a gently sloping ramp of Neoproterozoic shield during Jurassic transgression which was punctuated by periodic regression. The boundary between the Adigrat Sandstone and the overlying Antalo Limestone is transitional, marked by the occurrence of 20 to 30 m thick shale, calcarenite and sandstone. The Antalo Limestone has been subdivided into several depositional sequences and parasequences, i.e. thickening and shallowing up cycle, showing systematic vertical and lateral changes. Its thickness is well over 800 m and based on its abundant foraminiferal fauna, the age of the Antalo Limestone is considered Late Oxfordian – Early Kimmeridgian (Bosellini et al., 1997). The Agula Shale is the upper marly part of the carbonate succession which includes some shale but mostly marlstone, coquinoid limestone, quartz sandstone and gypsum. The boundary between Antalo and Agula formations is transitional and arbitrary. The thickness of Agula Shale is estimated, at least locally, to be 300 m and its deposition is the result of a regional regression towards the end of Jurassic and beginning of Cretceous (Bosellini et al., 1997).

The Amba Aradem Formation (also called 'Upper Sandstone') is the youngest Mesozoic unit, Late Cretaceous, which unconformably overlies the Agula Shale and is overlain by Tertiary Trap basalts (Danielli, 1943). In TRB it is 100-200 m thick and consists of fluviatile sandstone and shale. It shows fining-upward cycles and coarsens towards the southern margin of the Mekelle Outlier (Bosellini et al., 1997).

4.1.1.1.3. Cenozoic Volcanics

In Ethiopia, the earliest and most extensive groups of volcanic rocks are the Trap Series, erupted from fissures during the Early and Middle Tertiary (Pik et al., 1998). Huge shield volcanoes

consisting mainly of basalt lava were developed on the Ethiopian plateau during the Miocene and Pliocene (Kazmin, 1979) forming the large mountains of Ethiopia including Ras Dashen, Choke and Guna.

In Early Cenozoic, eruptions of flood lavas occured from fissures and centres and then covered the great part of the Mesozoic sedimentary rocks. According to the former classifications, the volcanic eruptions were believed to come in four major formations, all diachronous: from bottom to top, Ashange (Eocene), Aiba (32-25Ma), Alaji (32-15Ma) and Termaber (30-13Ma) (Mohr, 1983; Mohr and Zanettin, 1988). The whole volcanic sequence has been emplaced with no apparent development of paleosoil and erosional surfaces (Rochette et al., 1998).

Based on recent finding that the Ashange, Aiba, Alaji and Tarmaber basalts has been rapidly erupted in the period of 29-31 Ma BP with no major difference in their chemistry (dominantly tholeiitic), the Ethiopian Flood Basalt has been subdivided into two stratigraphic units, mainly depending on textural and geomorphologic characteristics. These are the basal basalt sequence forming gentle and rugged terrain corresponding to the Ashange basalts, and the upper basalt sequence forming the plateau corresponding to the Aiba-Alaji-Tarmaber sequences. The other two younger units (< 20 Ma) within this recent classification are the broad based shield volcanic deposits capping the plateau and quaternary scoria basalts associated with the shields (Kieffer et al., 2004).

The basal basaltic sequence is marked by its tilted appearance, more brecciated, deep weathering, thin layering (< 10 m), smooth topography and cross cutting sets of dykes. Within this unit there are minor intercalations of acid products (such as volcanic ash, rhyolites, and ignimbrites). In contrast the Aiba and Alaji formations are marked by their low degree of weathering, thick

layering and cliff forming topography. Frequent lacustrine deposits have been marked in the Aiba formation as evidenced by lenses of diatomites and porcelain lithologies particularly surrounding the Sekota area. The Termaber formation is marked by its jointing, thick layering, cliff forming topography with flat tops (Seifu Kebede, 2013).

The southern and south-eastern part of the Tekeze basin is covered with these Tertiary Trap series volcanics (*Fig 8*). Particularly, most of the Upper Tekeze sub-basin is underlain by volcanic piles accounting for its larger part of the landscape (Seifu Kebede, 2013). These rocks form one of the most productive aquifers in the basin.

Numerous small, hypabyssal intrusions of dolerite, trachyte, phonolite, microsyenite, and micro-granite also occur throughout Ethiopia, both within the Precambrian basement and the Phanerozoic cover rocks, sediments and pre and post-rift volcanic successions (Kazmin, 1972; Davidson, 1983). Particularly in TRB clusters of dolerite dykes and sills occur within the Mesozoic sediments (Arkin et al., 1971) and they are named as Mekelle dolerite (*Fig 8*). They are black andesine dolerite with ophitic texture and usually occur as sills and dykes intruding the Adigrat Sandstone, Antalo Limestone and Agula Shale formations in the Mekelle Outlier. They also form small stocks intruding crystalline basement and sedimentary rocks in the escarpment (EIGS, 1996). In the Mekelle Outlier, these dolerite bodies, in general, occur in a broad, NE-trending belt of 40 km wide and 100 km long. Such a lineament appears to follow the structural grain of Neoproterozoic basement and probably represent high-level expressions of deeper crustal structures (Kuster et al., 2005).

4.1.1.1.4. Cenozoic Sediments

In the TRB , the Quaternary era is represented by a great variety of loose unconsoldiated sediments. The main deposits are alluvial and colluvial. The alluvial deposits are of two types: those spread out in alluvial plains and lake basins and those strips along rivers and streams. Alluvial plains are filled up grabens and large stretches of flat land in the river valleys and along the western lowlands. These are troughs in the lowlands where during the pluvial period streams deposited large amounts of sediments carried down from the highlands. The thin strips of alluvium along rivers occur everywhere, both in the highlands and the lowlands. In the alluvial plains, alternating layers of fine and coarse sediments are characteristic and in many cases the alluvial deposits have moderate to high permeability. Particularly, those plains in the western lowlands around Humera (*Fig 8)* have relatively thick sediment deposits with coarse grain sizes of moderate to high permeability and productivity (IAEA, 2011).

A large part of Quaternary deposits in the western lowlands is covered by colluvium. The colluvium is associated with rock pediment originated mainly from the basaltic plateau in the east. In several parts of the plain, it passes into black cotton soils. Less than 20% of the area in the TRB is covered with Quaternary deposits and most of these sediments are thin, at least not thick enough to compose a good aquifer.

4.1.1.2. Geological Structures in the TRB

The different rocks in the basin are affected by tectonic activities at different periods in the geologic time. This is reflected by the presence of different sets of faults and folding.

4.1.1.2.1. Structures in the Mekelle and Werii Areas

The older (Neoproterozoic) structures (such as the Negash, Chehmit, Tsedia and Mai Kinetal synclinoria foliations) and the younger, Neotectonic structures (such as the Chelekot, Mekelle and Wukro faults and lineaments) are some of the prominent geological structures found in the Werii sub-basin and Mekelle Outlier (Beyth, 1971, 1972; Mulugeta Alene, 1998; Nata Tadesse, 2003; Tesfamichael Gebreyohannes et al., 2009). The interplay of all these geological structures makes the area more complex and unique.

The Neoproterozoic Basement rocks in the TRB in general have been subjected to lower greenschist facies metamorphism, and at least two phases of ductile deformation. The most prominent ductile structures are the older NNE-trending pervasive regional foliations and tight minor folds and the younger major synclinoria (Beyth, 1971, 1972; Mulugeta Alene, 1998). The synclinoria are open and upright with NNE axial trend and contain slate and metacarbonate sequences in the Tambien Group. In addition to the pervasive cleavage, the Tambien Group rocks display sedimentary features such as bedding, graded bedding, cross-bedding, mud cracks, channel-fill structures and ripple marks in the slates and metacarbonates. In between the synclinoria, there are metavolcanic and metavolcanoclastic units of the Tsaliet Group forming anticlinoria that show deformation fabric varying from massive to fracture- and phyllitic-cleavages (Beyth, 1971; Mulugeta Alene, 1998). The foliations and minor folds are considered to have developed prior to the formation of such large open folds which did not produce significant cleavage and believed to be associated with E-W directed shortening during the end-phase collision between East and West Gonwana in the Arabian-Nubian Shield (Mulugeta Alene, 1998; Mulugeta Alene and Sacchi, 2000). There are also Precambrian and younger normal and strike-slip faults within or bounding the main synclinoria.

The Mekelle Outlier is structurally bounded and dissected by a set of WNW striking normal faults, probably originating from pre-flood basalt extension (*Fig 10*). Some 100m of vertical displacements have occurred along these faults. A set of NNE-SSW directed lineaments also occur in the median part of the area, but has not lead to visible displacements (Kuster et al., 2005). These faults and lineaments are Late Cretaceous and early Tertiary structures developed in the area particularly in the sedimentary succession. The WNW striking normal faults are pre-rift structures aligned obliquely with the N-S trending marginal faults of the rift forming four major blocks (*Fig 10*): the Amba-Aradam block between the Fucea and Chelekot faults, Mekelle block between the Chelekot and Mekelle faults, the Agula-Wukro block between the Mekelle and Wukro faults, and the Negash block is north of Wukro fault. The geometry of these faults shows that the maximum vertical displacement is at the midway of the faults, and that there is no significant dropdown at the fault terminus. Other features associated with the fault structures are the drag folds found at the base of the fault scarp. These are concave upward folds formed as a result of opposite vertical movement of the hanging- and foot-wall blocks *(Fig 10)*. These structures are responsible for the development of local basins along the faults.

Another group of faults is the N-S to NNE-SSW trending faults associated with the rifting phase (*Fig 11*), and are confined to the eastern part of the Mekelle Outlier. The sedimentary strata are generally flat-lying or slightly tilted eastward (Kuster et al., 2005). The eastern boundary is the great escarpment of the Ethiopian Rift, whereas to the west (Abi Adi region) there is no precise limit because the stratigraphic closure of the sedimentary succession overlying the basement is partly dismembered by the recent erosion and progressively reduced by the angular unconformity with the overlying Amba Aradam Formation (Bossellini et al., 1997).

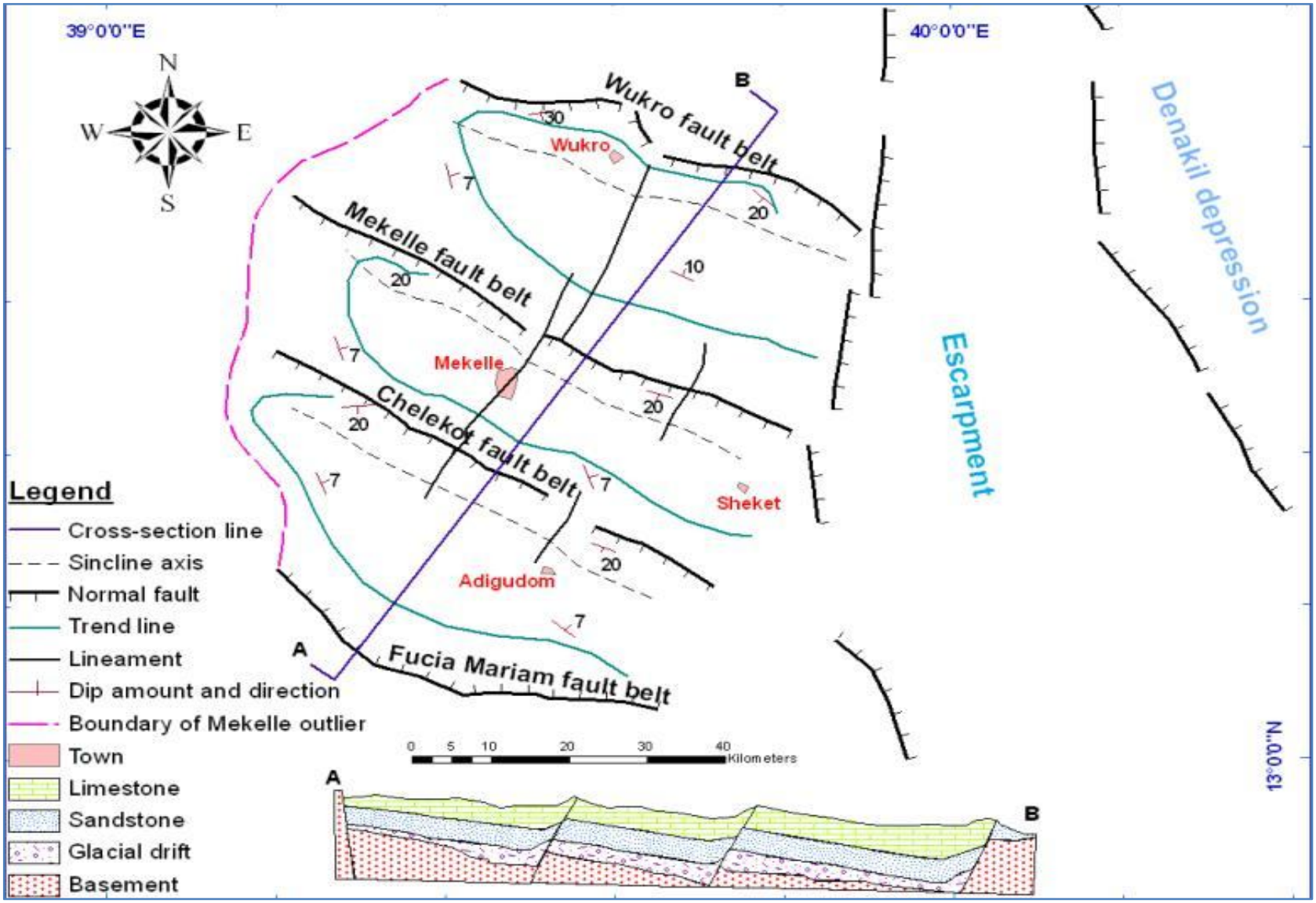

Fig 10 *Structural sketch map, Mekelle Outlier (Modified from Beyth, 1972)*

4.1.1.2.2. Structures in the Upper Tekeze sub-basin

The boundaries of the Upper Tekeze sub-basin are formed by prominent regional tectonic structures. In the east, it is bounded by rift margin faults; in the west by the Chilga-Gondar sub-rift of the Lake Tana structure; and in the south by the Debretabor sub-graben of the Lake Tana rift (*Fig 7*). In its central part it is cut by a prominent NNW-SSE running Tsirare fault system (*Fig 11*). The Tsirare fault dissects the Upper Tekeze into two and passes just east of the Abune Yoseph massive pile, while the spring with the highest discharge of 50-60 litre/second (Sanka spring near Woldia town) recorded in the area emerges on the southern extension of this fault. Within its bounds the Upper Tekeze is characterized by presence of several dyke swarms, fractures, faults and slump structures. A major curved shape valley also dissects the Simen massif (Mount Ras Dashen) which is thought to be the result of regional slump (Seifu Kebede, 2013). A number of NW-SE running faults are also observed in the Sekota area. In general, the faults are responsible for block rotation, lateral disruption of lithologies, and emergence of springs in the area (FWWDSE, 2007).

4.1.1.3. Regional Groundwater hydrology in the TRB

All the rock types of Precambrian, Mesozoic, and Tertiary age in the basin are affected by several episodes of deformation and intrusion. The quaternary sedimentary deposits in the area play a role in favoring groundwater recharge and sometimes serve as shallow (subsurface) aquifers in intermountain valleys and lowlands. In general, the TRB has a complex hydrogeological setting and requires a lot of scientific researches inorder to fully understand the system. Figure 12 shows the simplified hydrogeological map of the basin (extracted from the hydrogeological map of Ethiopia at the scale of 1:2,000,000).

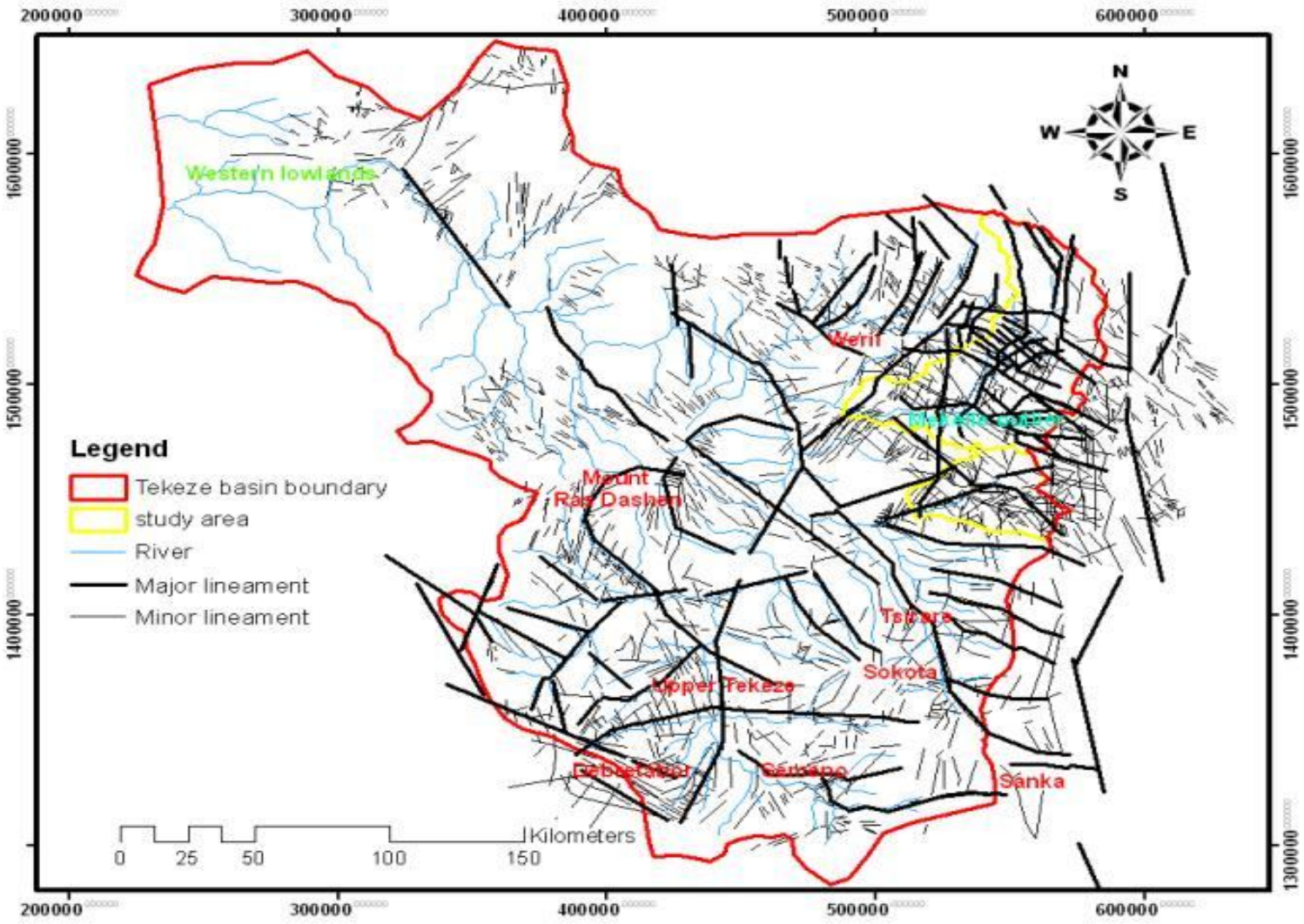

Fig 11 *Lineament map of the Tekeze River Basin*

Three major aquifer classes were identified based on the mode of origin and rock types. These are 1) Extensive aquifers with intergranular permeability (unconsolidated sediments: alluvium, eluvium, colluvium, lacustrine sediments), 2) Extensively fractured and weathered volcanics (basalts, rhyolites, trachytes and ignimbrites) and 3) Extensively fractured and/or karastified sedimentary rock aquifers. The northwestern highlands of Ethiopia have relatively lower fracturing and many interbedded clay layers and they, therefore, are classified as low productive aquifers with well yields varying from 0.45 to 9.9 lt/sec (Tesfaye Chernet 1988). But in the highlands of Gonder and Mekelle, many wells with yields more than 20 lt/sec are recently reported (Andarge Yitbarek, 2002; Samuel Yihdego, 2003; FWWDSE, 2007; DH-consult, 2010).

Correlation of apparent resistivity and well yield from the north-western highlands of Ethiopia revealed aquifers with different thickness and productivity in the Trap Series volcanics (Seifu Kebede, 2004). This is related to the variation in the degree of weathering and presence of interbedded paleosoils and river gravel. In contrast to this, the productivity in the basement hard rocks is almost exclusively related to the presence of faults and Tertiary and Quaternary sediments that overlay the basement.

4.1.1.4. Regional aquifers in the TRB

A wide range of patchy previous hydrogeological studies within the TRB are reviewed. Pertinent data from different sources, pumping test data, well lithological logs and geophysical survey results are employed to classify the aquifers and their hydraulic characteristics including groundwater recharge and discharge conditions in different parts of the basin. The result revealed that all kinds of aquifers exist (confined including artesian, semi-confined and unconfined). The most dominant aquifers are of unconfined and semi-confined types forming the

shallow and most used aquifers in all kinds of rocks and physiographic regions.

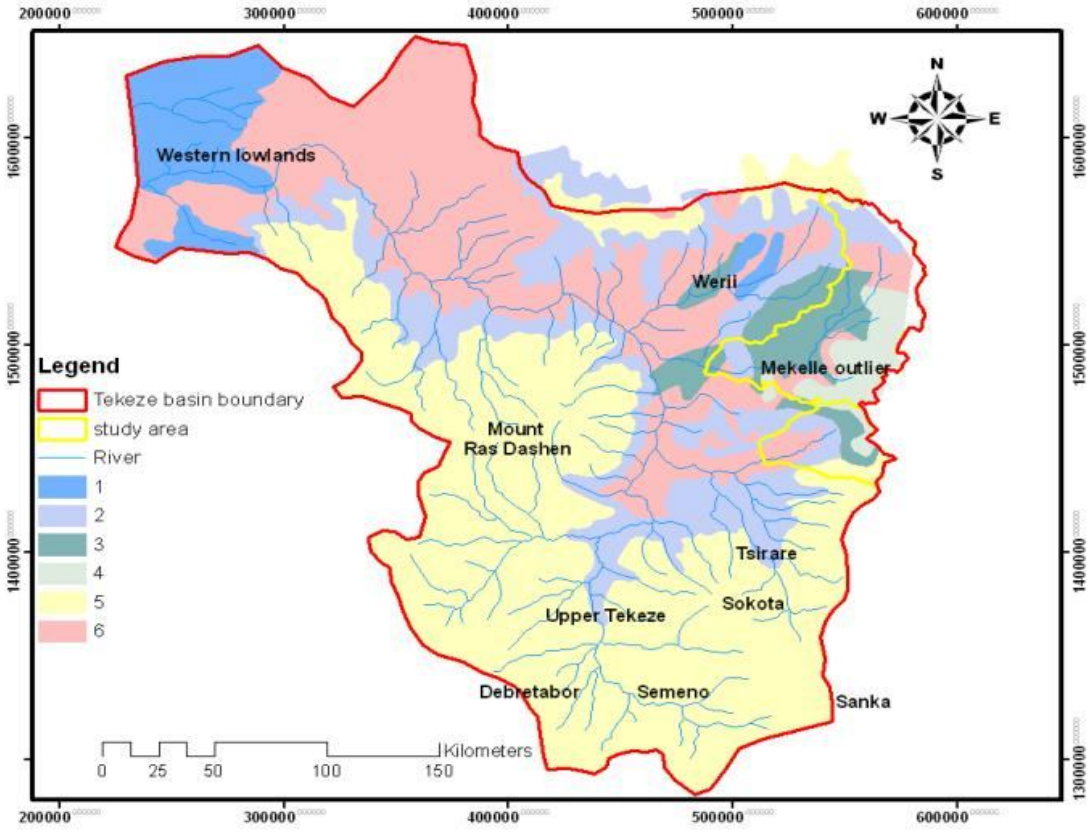

Fig 12 *Simplified aquifer class map of the TRB and its surroundings to the west and south (Modified from Tesfaye Chernet, 1988). Number on the legend represent aquifer classes: 1 = Mainly shallow unconfined aquifers in the Quaternary sediments; 2, 3 and 4 = Aquifers in the Mesozoic sedimentary rocks mainly existing along river valleys, 5 = diverse productive aquifers in the volcanics; 6 = Shallow less productive aquifers in the basement rocks.*

In the TRB, even if Adigrat Sandstone outcrops in the northern, north-eastern and north-western parts of the Mekelle Outlier, it is mostly overlain by thick piles of the Antalo Limestone, the

Agula shale and in some localities the Amba Aradem Sandstone. Thick masses of the flood basalt also overlay the Mesozoic sediments in most part of the southern half of TRB.

Due to their extension and continuity and lithological characteristics, the only sedimentary rocks, Adigrat sandstone and Antalo limestone, can represent regional aquifer in the TRB. Even though the Enticho/Tekeze sandstone, the Agula shale and volcanic rocks sometimes cover considerable areas, their incision by erosion, their own lithological heterogeneity, and their discontinuity makes difficult to consider them as regional hydrogeological units. Their behaviour can be assimilated to separate hydrogeological units, independent from each other because of the presence of poorly fissured areas and deep valley entrenchments. Whereas, the Amba Aradem sandstone forms isolated mountain ridges surrounded with steep cliffs which only bears localized groundwater and mostly serves as recharging zone to the underlying rock units (Seifu Kebede, 2013).

Semi-regional aquifers can be found in the fractured and weathered volcanics that form elevated plateaus and alluvio-colluvial sediments filling intermountain depressions, river valleys and lowland planes. Alluvial deposits dominated by volcano-clastics and river gravels and paleaosoils are present within the Trap series basic volcanics and in interbedded loose pyroclastic materials and reworked agglomerates or breccias within the mafic and acidic lava flows (Tesfaye Chernet, 1993; Tenalem Ayenew et al., 2007; Seifu Kebede, 2013).

Thick pyroclastic deposits, buried paleo-valleys and volcanic rocks within structural discontinuities in the highlands are known to provide one of the best aquifers in the country (Tesfaye Chernet, 1993; EIGS, 1993). Due to the presence of different interbedded layers of river gravels and paleosoils, the north-western highland volcanics of the country form multi-layer

aquifers. Good examples of multilayer aquifers in the highlands of Ethiopia are those located around Dessie, Mekelle, Ambo and Addis Ababa areas with yields as high as 40 lt/sec (Molla Demelie et al., 2008).

In the Upper Tekeze sub-basin, the volcanic rocks particularly the Ashange basalts are important aquifers. These rocks, which form the western and eastern highlands of the sub-basin, bear considerable amount of secondary porosities that result from the effects of extensive weathering, jointing, faulting and fracturing. Emergence of springs of significant discharge at the rift escarpment from the Ashange basalts suggests the productivity of these aquifer systems. Field evidence suggests that most of these springs emerge at the contact between the Ashange sequences and the underlying Mesozoic sediment. At the contacts these Mesozoic sedimentary rocks are mostly highly indurated and thermally compacted (Seifu Kebede, 2013).

In the Precambrian basement and intrusive rocks, which cover significant portion of the north-central and western TRB *(Fig 8)*, a complicated hydrogeological environment is evident owing to the geological histories the rocks have passed. The absence of uniform permeable sediments extending over large areas implicates that extensive aquifers are unlikely to exist. Instead, exploitable groundwater occurrence is limited to isolated areas where the groundwater is localized in depressions, isolated grabens and along large fracture zones. Weathering and fracturing have created significant secondary porosity and permeability which is highly variable. As a result, the storage and transmission of the groundwater in these rocks is limited and restricted to the weathered zones, joints, fractures, shear zones, faults and other discontinuities. Weathering and fracturing are generally more intense at the surface (8 - 36 m) but become rarer with depth (Tenalem Ayenew, 2009).

Synclines and anticlines are common in many parts of the crystalline terrains. Anticlines do not usually provide potential areas for groundwater storage. However, in the TRB folding is accompanied by fracturing of rocks and these fractures have positive effects on the occurrence and movement of groundwater. Particularly along an anticline, the crest undergoes higher tensional stresses and hence develops open tensile fractures, which may constitute better sites for groundwater development. The schistosity and foliation planes are inlets for infiltration of water.

With regard to the Quaternary deposits in the western lowlands of the TRB around Humera, a well drilling report at the center of Humera town revealed that the black cotton soil extended to a depth of 4m. Below the clay, sand and gravel were encountered. At a depth of 42m the drilling stopped because granite had been reached. Some other drilling reports indicate that the drilling of several boreholes had to be stopped because granite was encountered at shallower depth and the wells remain dry. Many other productive wells near Humera are drilled into the Mesozoic sandstone, weathered basalt and the alluvium. The groundwater table in this area dips away from the Tekeze River, indicating that the (influent) river recharges the groundwater. This appears to be the only recharge of the weathered and/or fractured rocks underlying the black cotton soils, because these soils are with low infiltration rates and low permeability. This means that, near Humera, pumped groundwater represents induced-recharge from the Tekeze River (MWR, 1998).

The aquifer hydraulic parameters and yield also vary widely in the TRB (Table 2). The data in table 3 were summarized from measurements taken in boreholes, hand dug wells and springs. The mean depth of the boreholes was 65 m and the maximum depth was 186 m. For the hand dug wells the mean depth was 9.5 m and it ranges between 2 m and 36 m.

Based on the geological origin, springs in the TRB can be classified into joint, contact (of two different lithologies), fault, depression and strata types (MWR, 1998). The depression type springs are mostly found in alluvial deposits, tuff layers, Precambrian rocks and the Antalo Limestone; while the joint and strata type springs are dominant in the basalts. On the basis of the geomorphologic location of the springs, they can also be classified into valley bottom, hillside, flat area, slope-break and river bank types. Most flat area springs are located in alluvial deposits, mainly near streams; while hillside type and slope break type springs are abundant in the basalt formations.

Table 2 Summary of some hydrodynamic characteristics of the various geological series in the TRB (Source: MWR, 1998)

Formation	Yield (l/s)			Specific Capacity (l/s/m)				Transmissivity (m^2/day)		
	average	max	min	count	average	max	min	average	Max	Min
Quaternary alluvium	3.6	6	0.5	5	4.6	10.8	0.06	482	1005	12
Ashange basalt	1.8	5	0.2	6	0.033	0.065	0.01	16	32	1
Amba-Aiba basalt	2.6	6.2	0.3	14	0.33	0.74	0.05	20	40	6
Welega basalt				5	1.16	11.43	0.9			
Agula Shale	2.4	5	0.6	2	0.23	0.45	0.01	20	20	20
Agula Shale & Antalo Limestone	0.9	1.5	0.3							
Antalo Limestone				4	1.26	2.63	0.22	76	146	7
Antallo limestone & dolerite	3.1	7	0.3					125	140	110
Tertiary dolerite	3.6	6	0.5	6	1.8	3	0.24	178	351	8
AmbaAradem Sandstone	2.2	6	0.2	3	1.53	4.54	0.02			
Enticho Sandstone	2.7	5.5	0.4	5	0.21	0.7	0.01	35	123	1
Adigrat Sandstone	2.8	6.9	0.2	9	0.25	0.92	0.01	229	261	196
Edaga-arbi glacials	0.7	1	0.5							
Precambrian metamorphic	1.6	8	0.1	11	0.18	0.36	0.03	20	57	3
Alluvial & Ashange basalt	0.7	1.4	0.1	2	0.03	0.06	0.01			

Groundwater is shallow in the TRB (MWR, 1998). Its depth varies from 1 m along streams to around 66 m in some localities near Humera. The most common depth to the static water level in the north-eastern part of the basin is about 12 m, while depths in the plateau planes from Adwa through Endasilassie to Gonder are less (around 4 m). Well yields in the basin range from 0.1 to 10 l/s. The mean value is about 2.6 l/s. High yields were observed in the Tertiary dolerites (average 3.6 l/s) and the Antalo Limestone (3.2 l/s). Lower yields were measured in the various basalt types (less than 2.6 l/s) and Precambrian metamorphic rocks (1.6 l/s). Specific well capacities vary from 0.0033 to 14 l/s/m, with a median value of 0.21 l/s/m. The Quaternary alluvium has the largest mean specific well capacity of 4.1 l/s/m followed by the Tertiary dolerite, the Antalo Limestone and the Adigrat Sandstone. Just as in the case of well yields, the Precambrian rocks and the Ashange rocks showed the lowest values of specific discharge (0.03 l/s/m).

Specific well capacity decreases with increasing depth. The Quaternary alluvium has the highest mean transmissivity value, 482 m^2/day, followed by the Adigrat sandstone (229 m^2/day), the Tertiary dolerite (178 m^2/day) and the Antalo Limestone (76 m^2/day). Again, the Precambrian rocks (20 m^2/day) and the basalts (16-20 m^2/day) revealed the lowest transmissivity. In general, it can be observed that there is good agreement between the different parameters (yield, specific well capacity and transmissivity). Thus, from the hydraulic properties point of view, the best aquifers in the basin are the Quaternary alluvium, the Tertiary dolerite and the Antalo Limestone formations. The least promising are the Precambrian basement rocks (MWR, 1998). But the data presented in these previous works are based on measurements from shallow wells and springs data. A lot of data from recently drilled deep wells in different geologic formations of the area have indications that further data can be found to modify the conclusions in the previous works.

4.1.1.5. Regional Groundwater flow pattern in the TRB

The groundwater flow in the TRB is an intricate interaction of recharge and discharge under local and regional groundwater flow systems. The groundwater level records are patchy to reconstruct the local and intermediate (sub-regional) flow systems and the groundwater and surface-water interactions. However, from the distribution of springs, seepage zones, shallow wells and the existing geological and geomorphological maps, a qualitative description of groundwater flow system of the basin can be made.

In many places since the wells are screened across various intervals, the water level recorded does not necessarily accurately represent the piezometric surface in particular aquifers within the multi-aquifer geological profile, mainly in the volcanic plateau (IWMI, 2009). For the sake of this discussion the water level is referred to as the groundwater surface rather than the potentiometric surface as it is recognized that under different recharge and discharge conditions in shallow and deeper aquifer intervals, the potentiometric surface of individual aquifers may vary vertically.

In the TRB the groundwater contour maps are often subdued replica of the topographic contours. In other words, the regional groundwater flows generally sub-parallel to the surface water flow direction at regional and sub-regional scale (MWR, 1998; Tesfamichael Gebreyohannes, 2009; Tenalem Ayenew, 2009; DH Consult, 2010). Preferential groundwater flow is also apparent parallel to the axes of large folds and major fault zones.

The abundance of springs at different elevations, and the overall relation of groundwater level with topography, particularly in steep landscapes, suggests that the shallow groundwater flows in local flow systems is controlled by ground elevation. However, the thickness and lateral extent

of the aquifers indicates that deeper, regional flow systems operate mainly in the volcanic and sedimentary rocks. Most of the Precambrian rocks have shallow aquifers. In these aquifers depth to groundwater level is not more than a few tens of meters (EIGS, 1996; Tesfamichael Gebreyohannes, 2009; DH-consult, 2010).

In general, the regional groundwater flow in the TRB is to the west, with southward flows in the north and northward flows in the southern part of the basin (MWR, 1998; FWWDSE, 2009; DH Consult, 2010). This general flow pattern indicates that most intermountain depressions and lowlands are discharge areas characterized by a number of springs and seepage zones. In these discharge areas depth to groundwater is very shallow (MWR, 1998; Tesfamichael Gebreyohannes, 2009; DH-consult, 2010).

4.2. Local Geology

A wide range of lithologic units and tectonic structures of Neoproterozoic to Quaternary in age characterizes the study area (Arkin et al., 1971; Kazmin, 1979; Merla et al., 1979; EIGS, 1993, 1996; Bosellini et al., 1997; Mulugeta Alene et al., 2006; Garland, 1980; Worash Getaneh, 2002; Kuster et al., 2005; Tesfamichael Gebreyohannes et al., 2009).

The Precambrian basement (metavolcanic and metasedimentary rocks) is exposed to the surface in the northern highland plateaus around Atsbi and Negash, and in the southwest around Agibe and Yechila (*Fig 13*). In the northern part they are found at the same elevation with that of the adjacent Paleozoic-Mesozoic sedimentary rock formations because of the normal faults of the Wukro fault belt.

The Negash Geosynclinal Fold and associated plutonic intrusion, the Wukro, Mekelle, Chelekot and Fucea Mariam fault belts, and the dolerite sills and dykes around Mekelle town are some among the megascopic geological structures in the area (*Fig 13*).

More than 60% of the study area is covered with sedimentary rocks. These Mesozoic sedimentary rocks, belonging to marine and continental facies (from top to bottom: Amba Aradem Sandstone, Agula Shale, Antalo Limestone and Adigrat Sandstone) and the underlying inter-fingered Paleozoic glacial sediments (Edaga Arbi Tillites and Enticho Sandstone) form the Mekelle sedimentary outlier. It is surrounded to the north, northeast and west by the basement rocks and to the south by the Tertiary flood basalts (*Fig 13, Fig 14a, b, c*). In the east it is truncated by the normal faults of the Afar rift margin, resulting to intermountain graben and horst structures until the crystalline rocks appear again close to the center of the rift.

Continuous joint sets of diverse orientations are also common in all rock formations of the study area. Isolated thin covers (2m to 30 m) of residual and alluvio-colluvial soil deposits that result from the quaternary weathering and erosion processes are observed on flood plains in the plateau, and at bottoms of narrow river gorges.

The data of joint set orientations measured on different rock formations in the field has been plotted in rose diagrams. Like the major faults and lineaments (*Fig 15*), the dominant orientations of joint sets are also NNE and WNW (*Fig 16*). The joints in the older rocks (Basement, Adigrat Sandstone and Paleozoic sediments) trend more dominantly in the WNW direction parallel to the major Mesozoic extensional faults of the study area which indicates that they have older genesis related to the break-up of the Afro-Arabian plate (age) (opening of the Red Sea Rift and Gulf of Aden).

Similarly, the dominant WNW orientation of the dykes measured in the country rocks of all ages has indicated that the magma which feed these dykes has mainly used these older deep seated faults and then emplaced the sills mainly through the contact plane between the upper Antalo and Agula Formations.

Whereas the NNE orientation of the other joint set is dominantly found in almost all rocks formations of the area including the youngest Cretaceous flood basalts. Cross cutting relationship shows that they are the youngest (*Fig 16*). They are therefore genetically related to the extensional rifting of the East African Rift system (Afar Rift). These two major joint orientations are nearly orthogonal to each other.

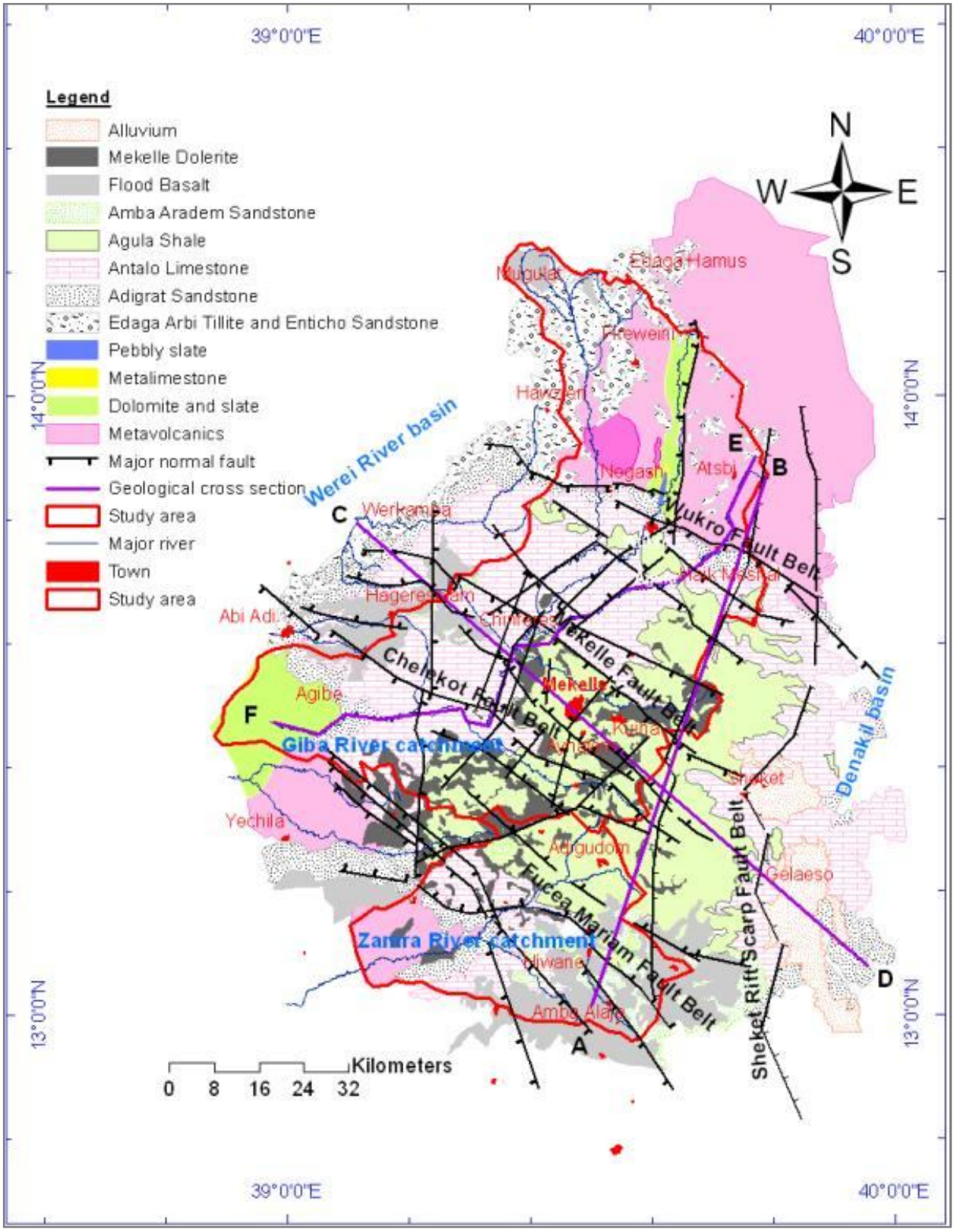

Fig 13 *Geological map of the study area*

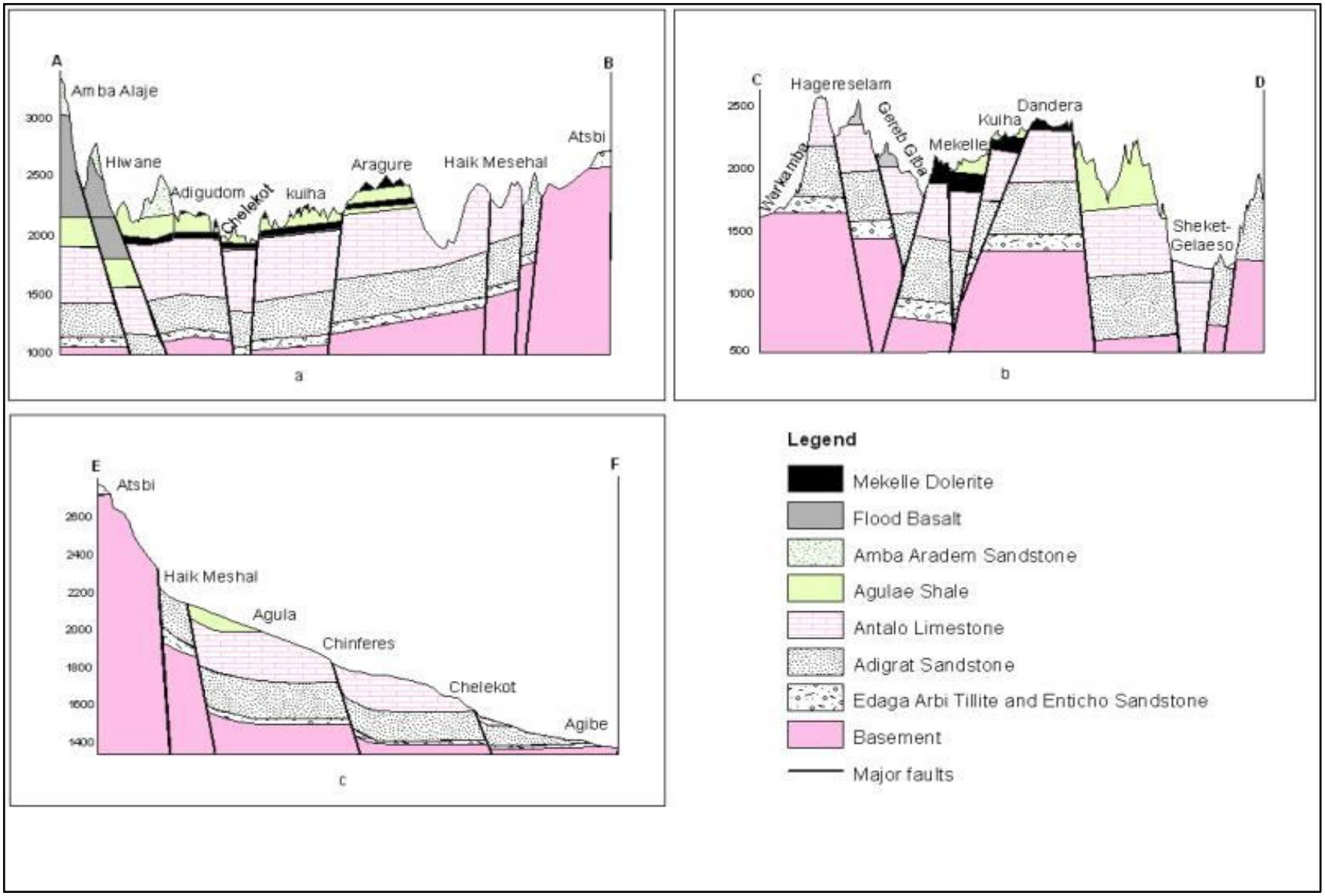

Fig 14 *Geological cross sections along selected lines A-B (a), C-D (b), E-F (c) in Fig 12*

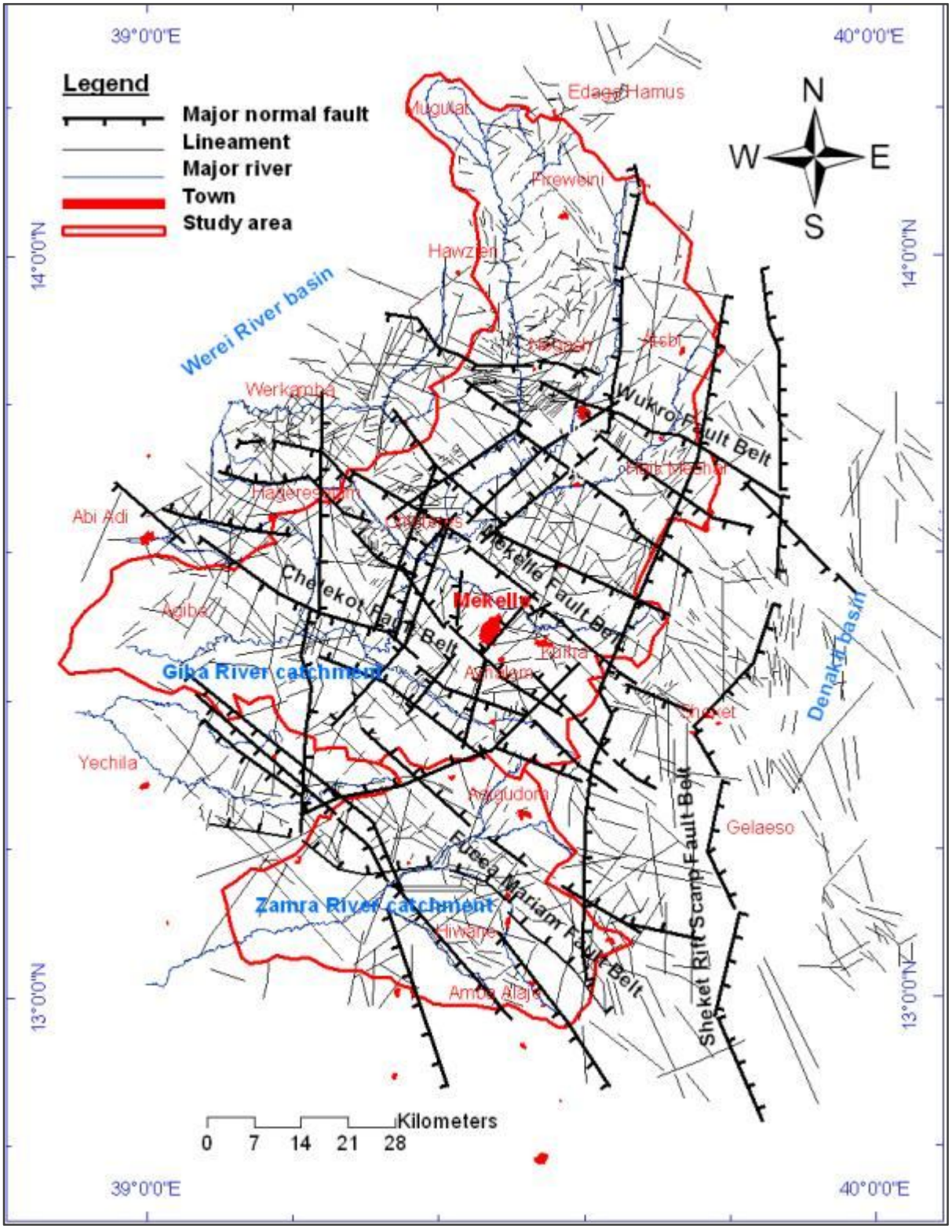

Fig 15 *Major faults and lineaments traced from satellite images*

From measurements of bedding thickness and joint spacing on limestones around Messebo and Abreha WeAtsbeha, it has been observed that they have positive linear relationship (*Fig 17*). Thicker beds of limestone and marl have widely spaced joints and therefore less fracture intensity. This indicates that thicker beds have more strength and therefore are proportionally less fractured than the thiner beds when exposed to a similar stress field.

The average values of measured joint spacing and fracture density in different rock formations of the area have been summarized in table 4. The Adigrat Sandstone Formation is characterized by wider joint spacing and least fracture intensity while the highest values are recorded in the Paleozoic sediments and the Metavolcanics as they are older and hence affected by most of tectonic events that occurred in the area. The Antalo limestone has relatively higher fracture density than the Agula Shale and the Dolerite.

The wide ranges of joint spacing and fracture density in each lithologic formation are attributed to the location of measurement points with respect to fault and shear zones. Closer Joint spacing and higher fracture intensity are found close to the major tectonic structures.

Joint aperture within the dolerite, Adigrat Sandstone, Paleozoic sediments and Neoproterozoic basement rocks is dominantly tight, hardly exceeding 1mm even when measured on the surface. Whereas in the Agulae shale and Antalo limestone it varies widely (tight to 20 cm) depending on their location with respect to the major faults (their closeness to the major structures and/or located either on the foot-wall or hanging-wall) and extent of rock weathering, erosion and other gravitational process. On gently dipping hanging sedimentary blocks, the joint opening ranges from 0.5 cm to 25 cm. But as going away from the fault surface, the block get to be foot-block for the subsequent major fault where sedimentary beds become nearly horizontal and stable and joint openings are tight having dominantly less than 5 mm joint aperture.

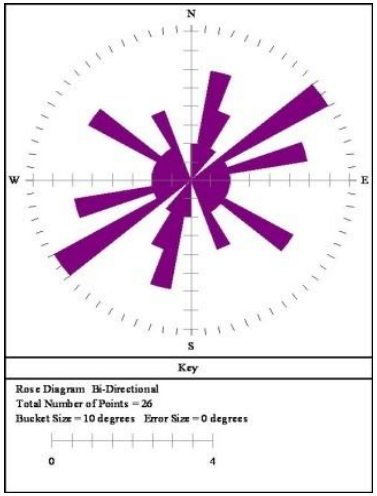

Dolerite

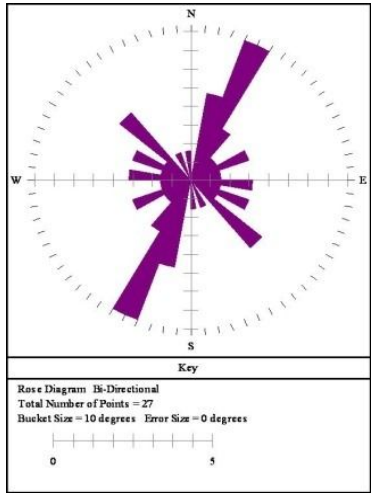

Agula Shale

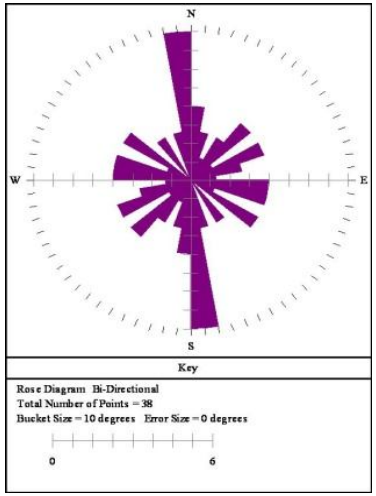

Antalo Limestone

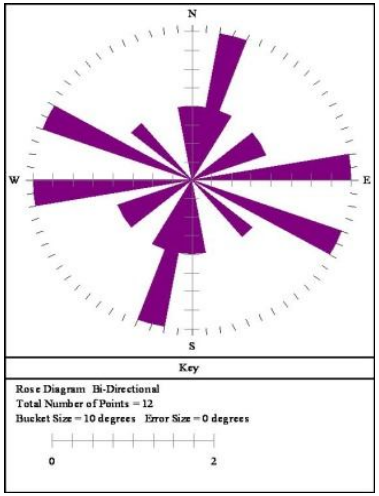

Adigrat Sandstone

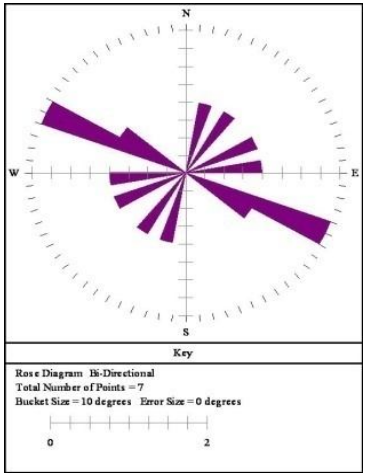

Paleozoic

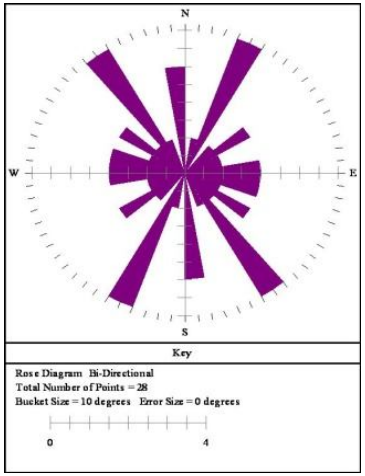

Basement

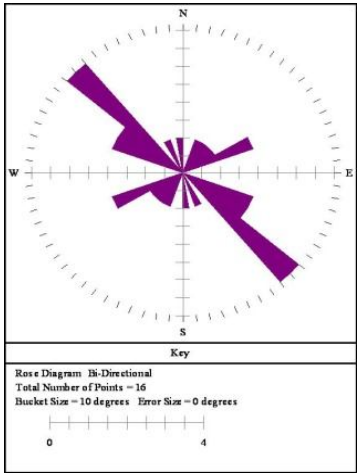

Dykes

Fig 16 *Rose diagrams of joints measured in different rock formations*

Table 3 Data of joint spacing versus bed thickness in limestones

Joint spacing (cm)	Bed thickness (cm)
6.6	2.25
7.8	3.36
40	10
95	40
250	100
170	65
109	50
275	120

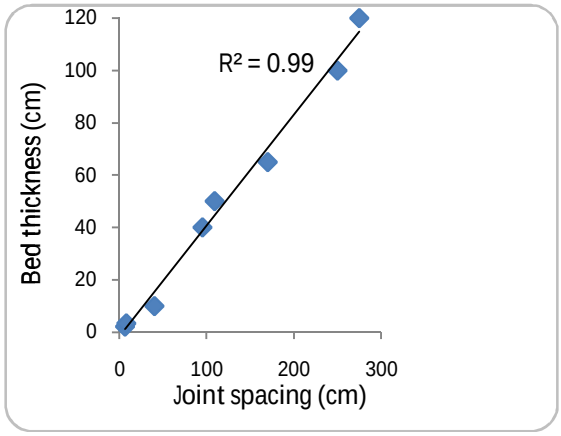

Fig 17 *Cross plot of bed thickness versus joint spacing in limestones around Messebo and Abreha Weatsbeha*

Table 4 Summary table of joint spacing joint density in different rock formations

Formation name	Range of joint spacing (cm)	Average Joint spacing (cm)	Range of joint density (m/m^2)	Average joint density (m/m^2)
Agula Shale	8 - 340	74.5	0.8 – 8.8	4.3
Antalo limestone	5 - 280	78	1 – 28.6	6.2
Dolerite	1 - 300	79	1.8 - 10	4.6
Adigrat sandstone	35 - 400	218.5	0.6 – 1.6	1
Paleozoic sediments	3 - 50	13.6	14.7 - 20	17.3
Metasediments	15 - 120	55.2	2.7 – 7.7	4.6
Metavolcanics	2 - 300	61.5	1.8 – 85.7	15.8

The joints in the basement rocks, Paleozoic sediments and the Agula and Antalo formations are dominantly continuous laterally as long as they are within the same lithology. But there are slight shifts and/or deviation in orientation of the younger (NNE oriented) joints due to interruptions of

their propagation by the pre-existing WNW joints. In the vertical direction joints are observed to change their intensity when there is change in lithology. Joints in the Adigrat Sandstone and dolerite are usually discontinuous and more complex except when they are close to fault zones where the joints are usually parallel to the faults and relatively continuous over longer distances.

In localities close to fault zones the fracture openings are generally devoid of any infillings because of their wider openings which favors fast drainage of infiltrating water washing out the soil residuals which may accumulate during the dry seasons. This case has exceptions within the Agula Shale formation in which case clay sediments washed out from the intercalating shale units filled-out the joints within limestone and marl beds. In more stable localities (away from fault zones) joints in sandstones and dolerites are also usually filled with quartz or calcite precipitates while in the Agula and Antalo formations they are filled with silt clay soils to very shallow depths (< 5 m) below the surface.

5. Hydrogeology of the study area

5.1. Hydrostratigraphy

5.1.1. Neoproterozoic basement rocks

The Neoproterozoic Basement rocks in the study area constitute low grade metavolcanics, metagraywackes, slates, schists, carbonates and plutonic rocks. They belong to the Arabian-Nubian Shield (ANS) that developed during the East African Orogeny and possess tectonic fabric as well as lower greenshist facies metamorphism. Neoproterozoic penetrative NNE-trending sub-vertical ductile planar fabrics are associated with the NNE-trending upright tight

folds like in the Negash synclinorium (Arkin et al., 1971, Beyth, 1972, Garland, 1980, Mulugeta Alene, 1998, Mulugeta Alene et al., 2000, 2006).

These rocks are affected by sets of fractures/joints prominently oriented in the WNW and NNE directions; the first being associated to the NE-SW Mesozoic extension (brake-up of the Afro-Arabian plate) along the Red Sea and the second to the nearly E-W Cenozoic extension of the East African Rift. There are also sub-horizontal joints that form as result of exhumation of overburden. Joints are closely spaced in the slates, shists and phylites than in the metabasalts, metabrecias, limestones and dolomites. All the joints and fractures are dilational with open apertures ranging from less than a millimeter to 2 millimeters. Joint apertures are more open close to the ground-surface and get tight at increased depths.

In these basement and intrusive rocks, which cover the north eastern and western parts of the study area (*Fig 13*), a complicated hydrogeological environment and a complex groundwater regime, is evident owing to the geological histories the rocks have passed. Most of the rocks have low primary porosity and permeability. However, weathering and fracturing have created significant secondary porosity and permeability which is highly variable both spatially and with depth. The absence of uniform permeable sediments extending over large areas implicates that extensive aquifers are unlikely to exist. Instead, exploitable groundwater occurrence is limited to large fracture zones and associated depressions and grabens. Weathering and fracturing are generally more intense at shallow depths but become rarer with depth. The thickness of the fractured zones ranges from 12-60m. Therefore, the storage and transmission of the groundwater in these rocks is limited and restricted to the shallow weathered zones, joints, fractures, shear zones, faults, contact zones with intrusive rocks and other discontinuities (*Figs 18, 19, 20*).

Fig 18 Inclined widely spaced non-systematic joint in the metavolcanic rocks (564749 E, 1533964 N) around Negash.

Fig 19 Sub-horizontal and sub-vertical closely spaced systematic joint sets in the slaty rocks (561952 E, 1537751 N) (a) and phylitic rocks (564388 E, 1537965 N) (b) around Negash.

Fig 20 *Sheared slates and phyllites around Sheweate Higum near to Yechila*

5.1.2. Paleozoic Sedimentary rocks: Edaga Arbi Tillites and Enticho sandstone

The Paleozoic sediments are essentially constituted of Edaga Arbi glacial Tillite and Enticho Sandstone (Beyth, 1972). They have measured thickness of 150-180m and found exposed in the western and northern margins of the Mekelle Outlier. The Edaga Arbi Tillite consists of poorly sorted, unstratified, and poorly consolidated sediments (*Fig 21*), forming small conical hills or irregular slopes below the cliffs of the overlying Adigrat Sandstone Formation (*Fig 22*).

Groundwater occurence and flow in the Edaga Arbi tillite is very localised to the thin (<15m) upper weathered and fractured zone in localities of slightly depressed landform along stream channels and occasionally as perched aquifers in more permeable horizones at depth that pinches out at short distances. Joints and fractures are discontineous both laterally and vertically due to high variation in lithilogical composition and hence strength.

The poorly sorted and unstratified nature of this unit results in only local accumulation and slow rate of groundwater flow and recharge. Springs from this unit has less discharges hardly exceeding 2 lit/sec. Hand dug wells and shallow tube wells (8-70m depth) have seasonaly fluctuating discharges. During the rainy months they discharge as high as 3-8 lit/sec but they may even dry out at the mid or late months of the dry season.

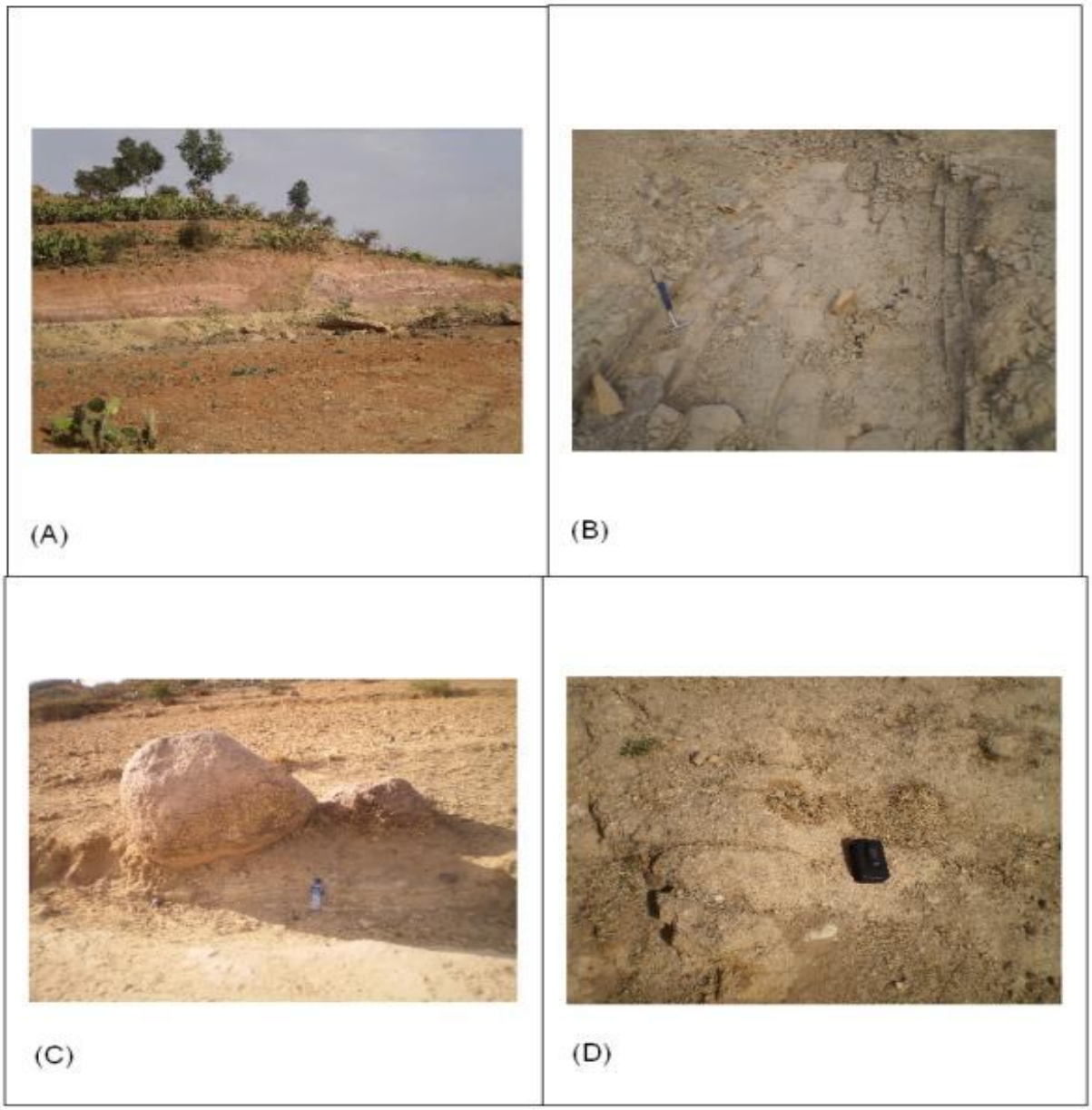

Fig 21 Sample pictures taken from the Paleozoic glacial sediments around Hawzien and Edaga Hamus. Lose varigated shally-tillite/ 560363 E, 156363 N (a), compacted marly-tillite with joints/ 552960 E, 1549038 N (b), granitic boulder inclusions within fine-grained matrix/ 549962 E, 1553889 N (c), conglomeratic sandstone/ 549004 E, 1532486 N (d)

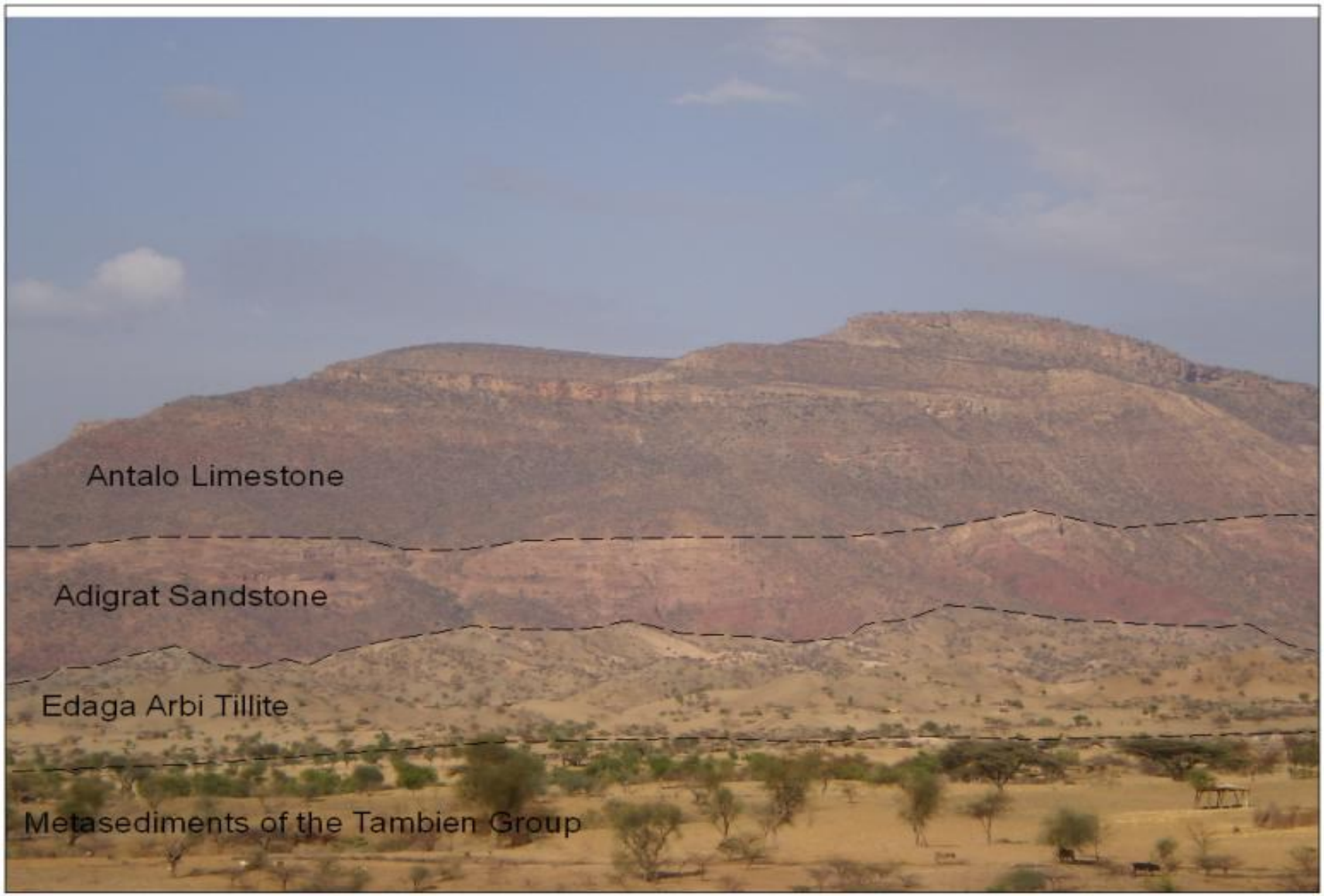

Fig 22 *Morphology of the lithologic contacts between the different rock formations in study area (Shweate Higum near to Yechila)*

The Enticho Sandstone which is the lower most sedimentary unit generally forms dome-shaped hills and flat-topped plateaus unconformably overlying the basement rocks around Edagahamus and Atsbi towns (*Figs 23and 24*). Its thickness reaches up to 100 meters. It is exposed and covers large area in the northern part of the study area. This sandstone unit is characterized in the lower part by white, medium to coarse grained sandstone, coarsely cross-bedded with silty beds and some ferruginous layers. On its upper part, it exhibits calcareous sandstone, with lenses of polymicritic conglomerates, pebbles and large granite boulders.

This unit is more permeable and it has relatively extended aquifers that intercalate with aquicludes (silt beds). Joints and fractures are contineous eventhough they are mostly filled with silica and calcite precipitates. But in places where it is exposed to the surface, it is found discontinued by faults and recent weathering and erosion. Therefore, it ussualy forms Mesa strusctures that stand here and there. There are points of higher discharge (2-5 lit/sec) and perennial contact/fault springs at the feet of these Mesa structures (*Fig 24c*). Tube wells (35-90m depth) drilled into this fomation has discharges of 3-7 lit/sec. But its storage capacity is low because of high permebility nature of the course and well sorted sediments and therefore mainly serves as temporary groundwater storage with less residence time and as a recharge zone to the undelying highly fractured basement rocks. It is also noted that the Enticho sandstone is some times found interfinged with Tillite beds resulting in perched aquifers.

Fig 23 *Morphology of the lithologic contacts between the Enticho Sandstone and basement rocks on the surface of the Afar Rift escarpment, east of Edaga Hamus*

Fig 24 *Exposures of the Enticho Sandstone around Edaga Hamus with a weathered surface (a), with intercalated beds of siltstone and sandstone (b), with contact spring (c), intruded with dolerite dyke oriented in the NE direction (d)*

5.1.3. Mesozoic sedimentary rocks

Overlying the Paleozoic rocks is a sequence of Mesozoic sedimentary formations (*Figs 14, 22, 27*). In the Mesozoic era, the Jurassic transgression came from southeast, reaching its maximum limit in western Ethiopia and Eritrea during the Kimmeridgian. This transgression deposited a sandy formation (Adigrat Sadstone), followed by neritic sediments composed mainly of thick

limestone and marl intercalations (Antalo Limestone). A regression towards the southeast began at the end of limestone deposition (Portlandian) giving rise to the Agula Shale formation and then a nearshore "Upper Sandstone" facies (Amba Aradam formation) accumulated above the Adigrat and Antalo/Agula formations (Danielli, 1943) (*Fig 27*).

The Adigrat Sandstone and the Ambaradam Sandstone are fluviatile in origin and the Ambaradam sandstone is separated from the underlying units by an angular unconformity (Bossellini et al., 1997).

5.1.4. Adigrat Sandstone formation

The Adigrat Sandstone in the study area is mostly massive and thickly bedded (*Fig 25c*) with frequently observed cross-bedding. It is white or grey to red, fine- to medium-grained and well sorted (*Fig 25*). It has conglomerate layers of varying thicknesses (especially toward the base). It generally shows intercalations of silt-shale layers, highly ferrugenized laterite beds, and particularly towards the upper part exhibit layers of carbonate rocks. The sandstone is not well cemented. The volume of cement (which is dominated by silica with subordinate amount of kaolin, calcite and hematite) is small compared to the volume of clastic grains (Worash Getaneh, 2002). It is unfossiliferous except for some silicified wood. In general, the Adigrat Sandsone formation is highly matured and reworked sandstone. It has a maximum thickness of about 700 m in the study area around Abi Adi (Beyth, 1972), but even more thicknesses have been measured towards the eastern margins of the Mekelle outlier in the Denakil basin (Hutchinson and Engels, 1970). In many places the Adigrat Sandstone uncomfortably overlies the Palaeozoic continental sediments (*Fig 22*), but in some places, it directly overlies the basement rocks.

Fig 25 *Hill of Adigrat Sandstone near Megab (Hawzien) (a), closer look into exposure of the Adigrat Sandstone (jointed gravely-sandstone) near Agibe (b), hill side exposure of jointed sandstone near AbrihaWeAtsbiha (c), water supply borehole drilled in to the Adigrat Sandstone in Wukro (d)*

Double porosity (both intergranular and fracture porosity) is characteristic of the Adigrat sandstone formation (*Fig 25b*). It hosts regional aquifers of mostly confined type. The confinement is due to the inter-beds of the less permeable siltstones and mudstones between the sandstone aquifers. Most deep wells (>100m) drilled into this sandstone formation are found to be artesian or the water level rises close to the surface. Many deep wells (350-600m) drilled around the Mekelle city with the intension to penetrate into the Adigrat Sandstone aquifers were not successful because of the thick pile of the Antallo supersequence.

But other deep wells drilled around Wukro and Chinferes, where the sandstone is found on the surface due to the regional faults of the area, show high productivity with discharge rates of up to 60 lit/sec and insignificant draw-downs during pumping tests. There are also high discharge (>30 lit/sec) springs at the western margins of this sandstone formation around Agibe and Abi Adi. In the vicinities of Yechila and Samre towns (south west of the study area) this formation gets thinner and sometimes forms isolated hills because of denudation by erosion.

5.1.5. Antalo supersequence: Antalo Limestone formation and Agula Shale formation

The Antalo Limestone is largely constituted of limestones, marls (*Fig 26, 27*) and even sandstone especially towards its base. The upper marly part of the carbonate succession is named as Agula Shale which includes some shale but mostly marlstone, coquinoid limestone, quartz sandstone and gypsum. The boundary between Antalo and Agula formations is transitional and completely arbitrary.

Both the Antalo Limestone and Agula Shale (Antalo Supersequence) thickens gradually east-ward and acquires more and more basal characteristic. At Sheket (halfway to the Afar Rift escarpment, these Antalo carbonates are more than 700 m thick (the base is not exposed) and consist of black limestone, locally with chert layers, alternating with laminated marlstone (Bossellini et al., 1997) (*Fig 26b*). Antalo thicknesses of 1000 m have been measured in several places along the Afar rift escarpment, but its maximum known thickness of 1420 m is in the Denakil Alps (Eagels, 1966; Hutchinson and Engels, 1970).

Within the Antalo Supersequence groundwater flow is generally restricted to fractures, dissolution cavities (*Fig 28*) and along bedding planes in thinly bedded horizons. The intensity of

fracturing is higher within the marl units than in the limestone beds while the fracture openings are wider within the limestone beds. Therefore, flow rates of the groundwater vary accordingly.

Fig 26 Hill side exposures of Antalo Limestone near Agula town (a) and near Shiket (b), river side exposure of thinly bedded limestone in the lower section of the Antalo Limestone near Hareko village (c), river side exposure of jointed thickly bedded limestone near Agula town (d)

When water passes though the wider fractures within limestone units to the marl units, its vertical flow is hindered because of the more tight fractures within the marl and hence hydrostatic pressure builds at the contacts between the limestone and marl units. This results to the accumulation and horizontal flow of groundwater along these contact zones. Many springs within the Antalo and Agula formations are observed to emerge at the contacts between limestone and marl or shale. Superficial Solution cavities within limestone are also common in

Fig 27 *Hill side exposure of the major rock formations in the study area (slightly east of Hagereselam)*

these contact zones. The development of deep and interconnected karsts in the limestones of the Mekelle outlier is sometimes hindered by the frequent intercalations of marl and shale beds. In areas where the potential of dissolution is low, mechanical erosion dominates giving rise to cliffs instead of karst (Singhal and Gupta, 2010) as in the case of the study area where narrow valleys bordered by steep cliffs of intercalated limestone-marl-shale is not uncomment.

The deeper aquifers in the Antalo limestone formation are confined type and artesian wells that penetrate into these aquifers are encountered (*Fig 29*). The extents of the aquifers in this formation are also semi-regional. In localities where the marl beds are brought closer to the surface, as a result of faulting and subsequent erosion of overlying material, the fractures are observed to be locally widened because of pressure relief. In such cases the marl units also serve as important aquifers although they are mostly aquicludes at depth. Except close to faults and along axes of associated drag folds, the intensity of fracturing within these carbonate sequence decreases with depth and become tight below 200m.

At the transitional contact zones between the Antallo Limestone formation and the Agula Shale formation, thin layering of sedimentary beds result to increased amount of primary porosity along bedding planes (*Fig 30*). In localities that are close to stream valley and fault zone, this transitional intercalation unit is observed to accommodate significant amount of shallow groundwater. Many productive hand-dug-wells and shallow boreholes are encountered in such localities around the Mekelle town.

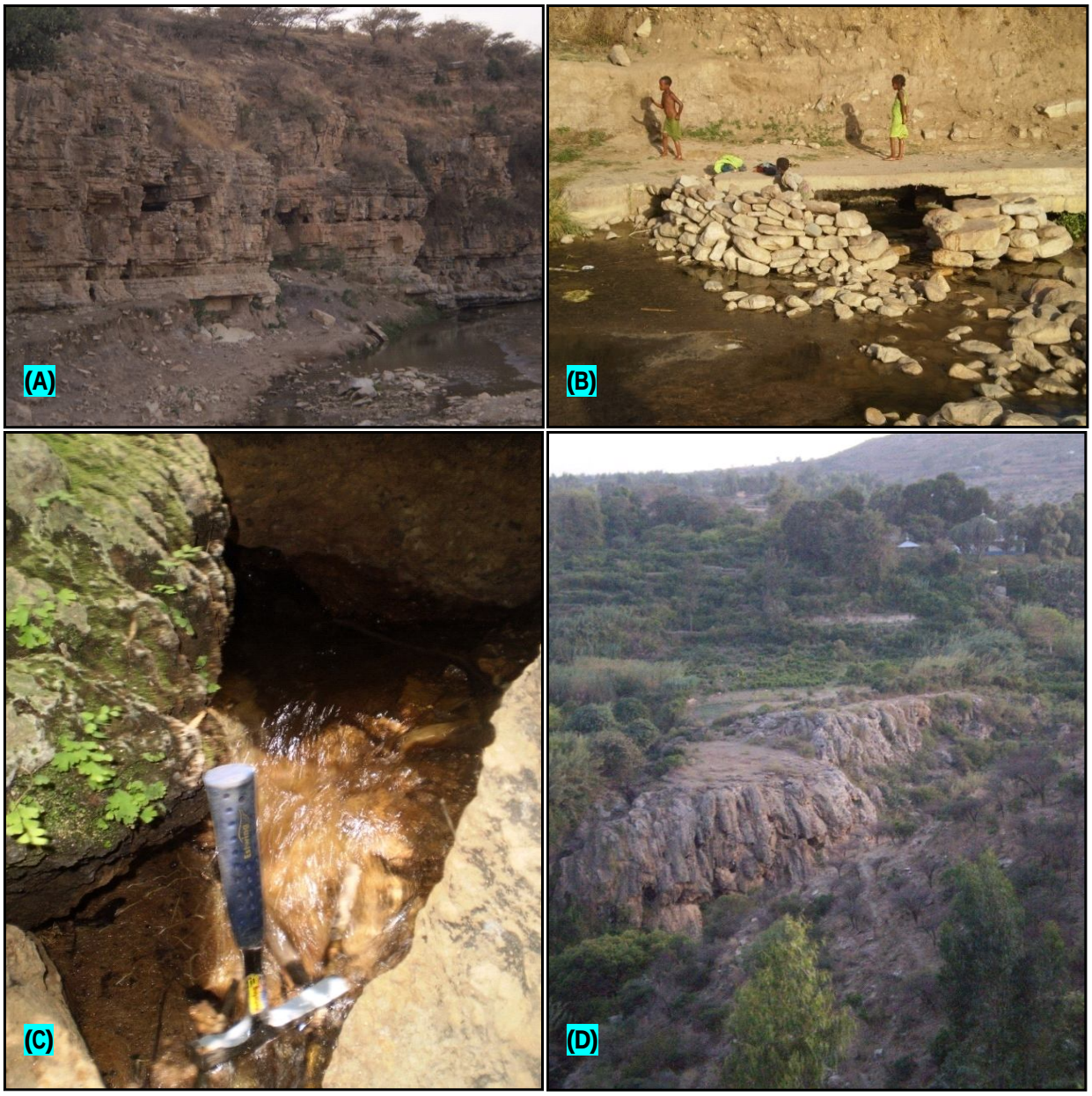

Fig 28 *Dissolution cavities along bedding planes on a river side exposure (~5 Km east of Agula town) (a), high discharge springs through dissolution cavities (~5 Km east of Agula town) (b) and at EndabaHadera (c), travertine deposit and high discharge springs along dissolution cavities (~10 Km west of Mekelle town) (d). Such features are frequently observed within the Antalo formation in the study area*

Fig 29 *Artesian deep wells in the Chelekot valley (650m deep) (a) and near Agula town (350m deep) (b)*

The upper most part of this Mesozoic sedimentary sequence (Agula Shale Formation) is characterized by thick shale beds intercalated with thin horizons of limestone, marl and gypsum (*Fig 31*). Even though this formation is also affected by diverse sets of joints, its dominantly clayey composition results to swelling of rock blocks when saturated by infiltrating water. This minimizes their secondary permeability. On outcrops of this rock formation, the fractures within the limestone intercalations are also observed to be filled with clay materials that are washed away from the shale beds. Therefore, although significant amount of moisture is found in these shale beds and their intercalated limestone and marl, the flow rate of groundwater is so slow that they should be considered as aquiclides. The shale dominated units are therefore be considered as recharging horizons to the underlying limestone and marl units of the Antalo Formation even though recharge rates can also be low.

Fig 30 *Intercalations of thinly bedded limestone marl, and shale (within the Agula Shale Formation) where frequent encounters of productive hand dug wells and shallow boreholes are observed (Photos taken from close vicinities to Mekelle town (d))*

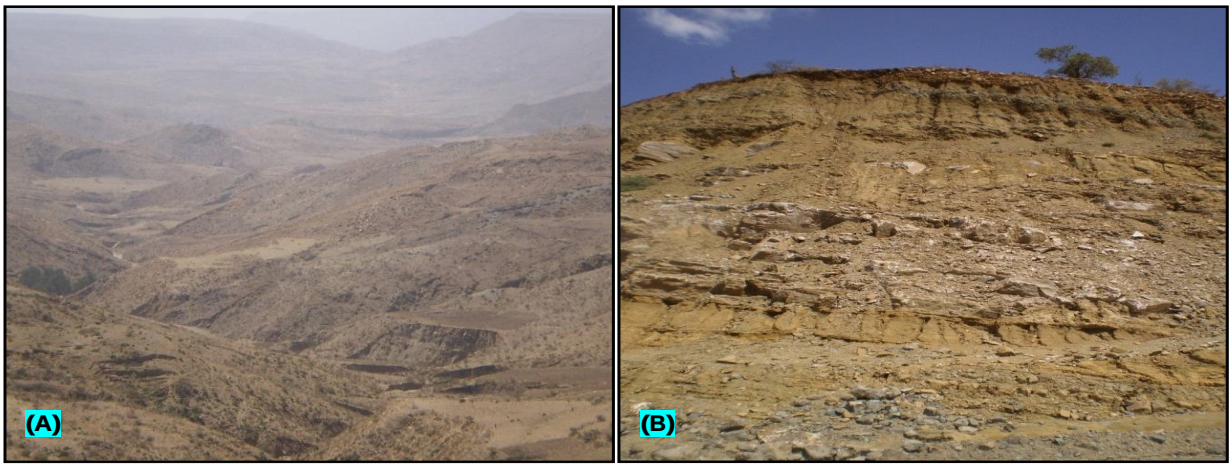

Fig 31 *Morphology of Agula Shale when dominated by thick shale units around Adigudom town (a), outcrop of gypsum unit sandwiched between shale beds within Agula Shale 15 km east of kuiha town (b)*

Fig 32 *Highly jointed black limestone in the Agula Shale formation in contact with dolerite sill and natures of contact between dolerite intrusions and country rocks around Mekelle town*

But in the locality around Mekelle town and slightly to its south, the dolerite intrusions has created a backing effect (contact metamorphism) which gives rise to more crystallized and brittle rocks within the Agula Shale Formation (eg, the black limestones). Cooling fractures and joints result to higher levels of secondary porosity and permeability within these rocks. High discharge perennial contact springs and high discharge tube wells are common from such horizons in the Aynalem well field and surroundings.

Ingeneral, the Adigrat sandstone and Antalo limestone are the most productive semi-regional aquifers in the study area. Whereas, the Amba Aradem Sandstone, Agulae shale, Paleozoic sediments and basement rocks are characterised by shallow and local groundwater systems and mostly serve as recharge to the underlying lithologic formations.

5.2. The Major structures and their control on groundwater

5.2.1. Faults and folds

Very old (Neoproterozoic) structures (like the Negash Geosynclinal fold and the foliations in the metamorphic rocks) and the Neotectonic structures (like the Fucea Mariam, Chelekot, Mekelle and Wukro faults and many other lineaments) are some among the major geological structures to be mentioned (*Figs 15, 33*). The interplay of these independently formed structures makes the area structurally more complex and unique.

The Negash Geosynclinal fold which mainly affects the Tembien Group (Metasediments and Metavolcanics) is an over-turned fold with its axis trending roughly N-S and plunging 15^o to 20^o towards south which terminates at the Wukro fault belt (north eastern border of the Mekelle outlier) (*Fig 13, 33*). The inner-core of the fold is constituted by the youngest meta-sediment (diamectites) and the outer core by the interbedded yellowish dolomite and slates. The bedding-

foliation surface interaction follows the general relationship and becomes orthogonal at the hinge zone and parallel at both limbs. Metamorphic structures such as foliations and lineations are prominent in these metamorphic rocks where the foliations are dominantly trending N-S with linear alignments of minerals and grains in the same direction (Beyth et al., 2003).

In this open synformal fold, groundwater flow is more controlled by the dip of strata and plunging of the fold. The older non-foliated metavolcanic rocks in both the western and eastern margins of the fold form hilly landforms. Because of their geomorphologic setting and their hard and compact nature, these rocks mostly act as run-off zones. Groundwater occurrence is restricted along faults, fractures and joints in these rock unit and their contact zones with the apilitic dyke intrusions and granitic plutons. Towards the core of the fold, narrow valleys (elongated in the N-S direction) that are dominated by foliated slates and phylites and covered with thin alluvial sediments are found to be more productive. Most of the productive hand-dug-wells and shallow boreholes in the metamorphic terrains are found along these narrow valleys. In between these valleys, metadolomites and metalimestons form elongated inselbergs (residual hills) oriented in the same direction. Similar to the metavolcanic hills, these inselbergs have negligible groundwater potential due to the small recharge area, steep slopes and low permeability of the rocks.

The basement rocks in the study area are affected by sub-horizontal sheet joints formed by erosional unloading which are dissected by sub-vertical joints. These are sources of secondary porosity and significantly contributing to the occurrence and flow of shallow groundwater in almost all the basement rocks. But these joints are more open and closely spaced near the ground surface and decrease in frequency and aperture with depth.

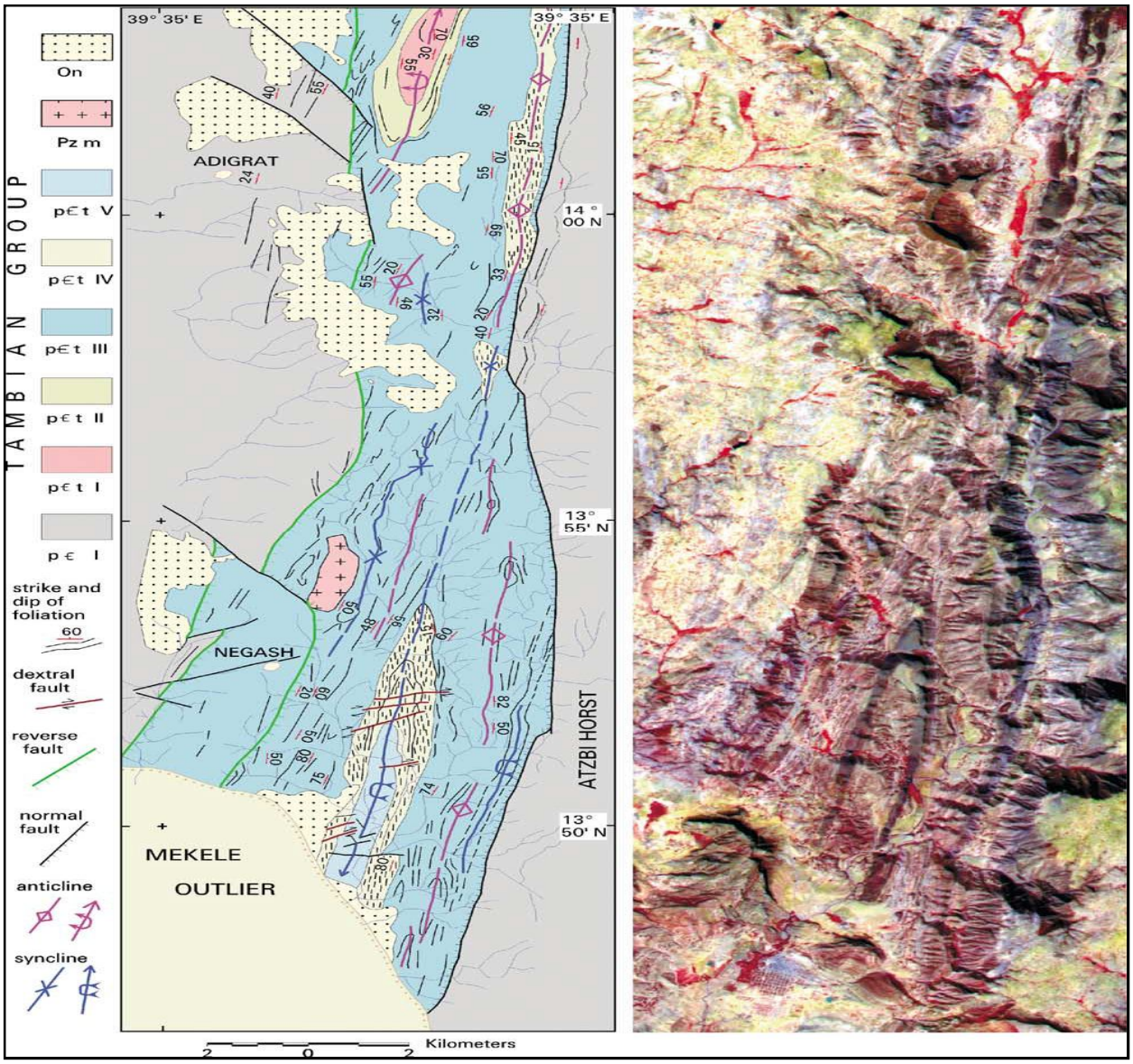

Fig 33 *MOMS-2P spectrometry, Negash Synclinorium: left-geological interpretation (modified after Beyth, 1972). On: Enticho Sandstone; Pz m: Mareb Granite; PCt V: pebbly slate; PCt IV: limestone; PCt III: dolomite and slate; PCt II: slate; PCt I: greywacke; pC I: Tsaliet Metavolcanics; A: strike and dip of foliation; B: dextral fault; C: reverse fault; D: normal fault; E: anticline; F: syncline; right: MOMS-2P data, mosaic of scenes 04 and 05/datatake T081 A, mode B: multi-spectral, acq. date 18 December 1996, bands 4/3/1 = RGB, resampled (Beyth et al., 2003)*

These permeable horizons in the basement rocks are non-extensive and restricted to shallow depths. Their groundwater potential is not comparable with that of the Mesozoic sedimentary rocks in the area. Most of this shallow groundwater in the basement rocks is discharged in the form of springs and seepages. Singhal and Gupta (2010) also stated that although crystalline rocks may extend over large areas and to greater depths, due to structural controls it is unlikely that the flow system extends over long distances.

The Paleozoic-Mesozoic sedimentary rocks in the study area are structurally bounded and dissected by sets of WNW oriented normal faults (Fucea Mariam, Chelekot, Mekelle and Wukro faults), probably originating from pre-flood basalt extensional tectonics. Cross-cutting relationship indicates that they are pre-rift structures aligned obliquely with the NNE directed marginal faults of the Afar Rift (*Fig 15*). Some 100 m of vertical displacements have occurred along these faults. These faults create four major blocks. The Amba-Aradam block is the southernmost block, bounded by the Fucea Mariam fault in the south and the Chelekot fault in the north. Next are the Mekelle, the Agulae-Wukro, and the Negash blocks (*Fig 13*).

The geometry of these normal faults shows that the maximum vertical displacement is at the midway of the faults, and that there is no significant dropdown at the fault terminus in the east and west. The density of other WNW striking lineaments (traced from satellite images) is higher closer to these major fault zones than within the respective hanging and foot blocks (*Fig 15*). Close to the fault surfaces, sedimentary beds on hanging walls are gently dipping away from the fault surfaces. This resulted to the drug folds with axes parallel to the strike of the fault surfaces. These concave upward folds are formed as a result of opposite vertical movement of the hanging and foot blocks.

These folds are responsible for the development of local basins parallel to the fault orientation (Beyth, 1972). The gently dipping and highly fractured parts of the hanging blocks can create preferential recharge and flow of groundwater from east and west towards the Giba River. The encounter of artesian wells along the fold axes both in the Adigrat Sandstone and Antalo Limestone formations can be due to higher hydraulic heads with confined groundwater flow through the tilted bedding planes towards the fold axes. In the inner parts of the blocks away from the major faults, sedimentary strata are nearly flat-lying and undisturbed resulting in lower intensity of fracture.

Karst features in limestones of the Antalo formation are frequently observed close to the major fault zones and along the axes of the drag folds where concentrated groundwater flow occurs along the dense and more open joints and fractures. Highly discharging Perennial springs (like the Michael Tselamo and Mai Ambesa near Mekelle town, Birki Gebriel near Agulae and Endaba Hadera, EndabaNoh and Ruwakisa near Hagereselam, Aini-mai-shugala near Shiket and many other springs aligned along the foot of the Afar rift escarpment) emerge through such dissolution cavities.

In general, the major fault zones in the sedimentary terrain are the main source of localized recharge particularly to the deeper aquifers. The groundwater in the shallow aquifers is discharged in the form of springs and baseflow in the upper steam reaches of the study area where the rock mass is truncated by the major faults and subsequent erosion.

The other group of NNE trending faults and lineaments (*Fig 15*) are associated with the East African rifting phase. These Late Cretaceous and early Tertiary lineaments get denser towards the eastern part of the Mekelle outlier, where the escarpment of the rift predated the outlier

(Beyth, 1972). Kuster et al. (2005) has stated that mostly these faults have not lead to visible displacements. The major ones are observed to have significant displacements (100m to 500m) giving rise to the existence of the Giba River valley.

The regional groundwater flow from the east and west of the Giba River is therefore structurally controlled to converge towards this valley and ultimately flow in the southwest direction. Significant part of this regional flow is discharged to the perennial flow of the Giba River and at the contacts between the Adigrat sandstone and the paleaozoic sediments/basement rock in the Agibe-Yechila low lands.

In the Abi Adi area there is no precise limit of the Mekelle Sedimentary outlier because the stratigraphic closure of the sedimentary succession overlying the basement is partly dismembered by recent erosion and progressively reduced by the angular unconformity with the overlying Amba Aradam Formation (Bossellini et al., 1997). Small proportion of the regional groundwater flow percolates down to recharge the fractured basement aquifers and/or the narrow and thin (<20 m) alluvial aquifers in the lower reaches of the Giba River. The fractured basement rocks possess significantly lower porosity and permeability as compared to the over-laying Adigrat sandstone and the fractures tend to be tighter at shallow depths (at 100-150 m depth).

From field observation, it is evident that towards the Afar Depression step faulting is very common where the hanging blocks are gently/steeply tilted towards the rift scarp fault surfaces forming graben and horst land form. The grabens are elongated parallel to the rift faults (roughly in N-S direction) and filled with thick unconsolidated sediments generated from slope denudation and erosion of the up-thrown blocks.

Very deep ground water circulation is expected in this part of the Mekelle outlier and the grabens are promising groundwater potential zones for future development by drilling deep wells which can penetrate though the unconsolidated sediments and deep into the fractured carbonate sequences. Further east in the Afar Depression where the earth's crust is thin, the deep circulating groundwater can get in contact with hot magma at shallower depths giving rise to the possibility of having significant amount of geothermal energy in the area.

5.2.2. Dolerite sills and dykes

Dykes are vertical or steeply inclined intrusive igneous bodies which cut across the pre-existing rocks (*Fig 34*). They are usually of basic composition and have medium to coarse grain sizes. Dykes vary in thickness from a few decimeters to hundreds of meters, but widths of 1–10 m are most common. In length they may be from a few meters to several kilometers long. As dykes are usually more resistant to erosion than the country rock they stand out prominently as wall-like ridges (Singhal and Gupta, 2010).

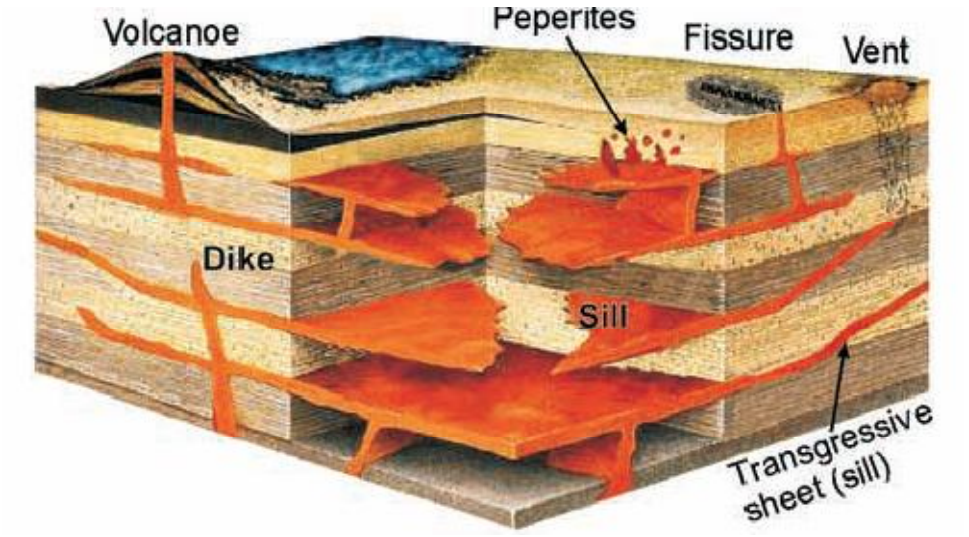

Fig 34 *3D Model of dykes, sills and related volcanic structures (Neumann et al., 2003)*

Sills are nearly horizontal tabular bodies which are commonly concordant and follow the bedding of enclosing sedimentary rocks or the older lava flows (*Fig 34*). Some sills are very thick and extend over large areas (eg. Karoo System of South Africa). Due to their low permeability, except when fractured, sills form perched water bodies (eg. Hawaiian Islands). However, studies in the Palisades sill in Newark Rift Basin, New York show that the main transmissive zones are located within the dolerite-sedimentary rock contact zones characterized by chilled dolerite. This is mainly a result of thermal cracking and fracturing of both formations resulting in higher permeability along the contact zone (Matter et al., 2006).

In the study area, clusters of black andesine dolerite dykes and sills with ophitic texture intrude into the Adigrat, Antalo and Agula Formations (*Figs 13, 14*). The sills intrude mainly the upper part of the Jurassic limestone-shale succession (Agula Shale) and display a generally sub-concordant relationship with the flat-lying sedimentary rocks. Thickness of the sills may reach 50-100 m with a large areal extent of up to 20 km and more along strike. Depending on local erosional morphology, the sills either form steep cliff or flat mountain-tops (Kuster et al., 2005). These dolerites occur in a broad belt around 40 km wide and 100 km long which roughly strikes NE. The belt spatially coincides with NE-SW striking lineaments which cut across the median part of the Mekelle sedimentary basin. These lineaments apparently follow the structural grain of Neoproterozoic basement and probably represent high-level expressions of deeper crustal structures. It is likely that the mafic magmas predominantly used NE to NNE directed basement faults or shear zones as conduits through the crust. However, closer to the surface the magmas also exploited the NW directed normal faults of the Mekelle basin, especially the Mekelle fault which hosts a number of massive gabrodolerites dykes. These dykes may represent feeder zones to the adjacent sills (Kuster et al., 2005). Generally, the geometry and emplacement mechanism

of these Mekelle dolerites is complex and less understood; their roles in controlling the groundwater occurrence and flow are also meagerly studied.

From field observation on rock outcrops and drilling data (drilling rates, strike of groundwater/increase of discharge and rock cuttings), it has been observed that the contact zones between the dolerite intrusions and the host sedimentary rocks are more fractured and zones of faster groundwater flow (*Fig 35*). Sometimes intrusion of dykes and sills may cause fracturing of the adjacent country rock due to thermal effects and differences in the mechanical properties resulting in formation of effective conduits for groundwater flow parallel to the contact (Gudmundsson et al., 2003). In such cases, drilling into the country rock close to the dyke/sill is recommended, e.g., in the Precambrian crystalline basement rocks of South Africa, Western Australia and north-east Brazil (Boehmer and Boonstra, 1987). Similar cases are also common in the Precambrian crystalline basement rocks and Mesozoic sedimentary rocks of Northern Ethiopia.

In cases where the dolerite sills and dykes are thicker (>5 m), wider fractures and therefore permeable horizons are restricted to the outer parts of the sills and dykes near the contacts with the country rocks. This can be the effect of fast cooling. Many intermittent and semi-perennial springs with discharges ranging 0.2-3 L/s emerge from these contact zones.

In the inner parts of the dolerite sills and dykes; the fractures get very tight and less interconnected, drilling rates get slower and even cases where drilling bits are eaten by the friction with these massive dolerites are encountered in the Aynalem well field.

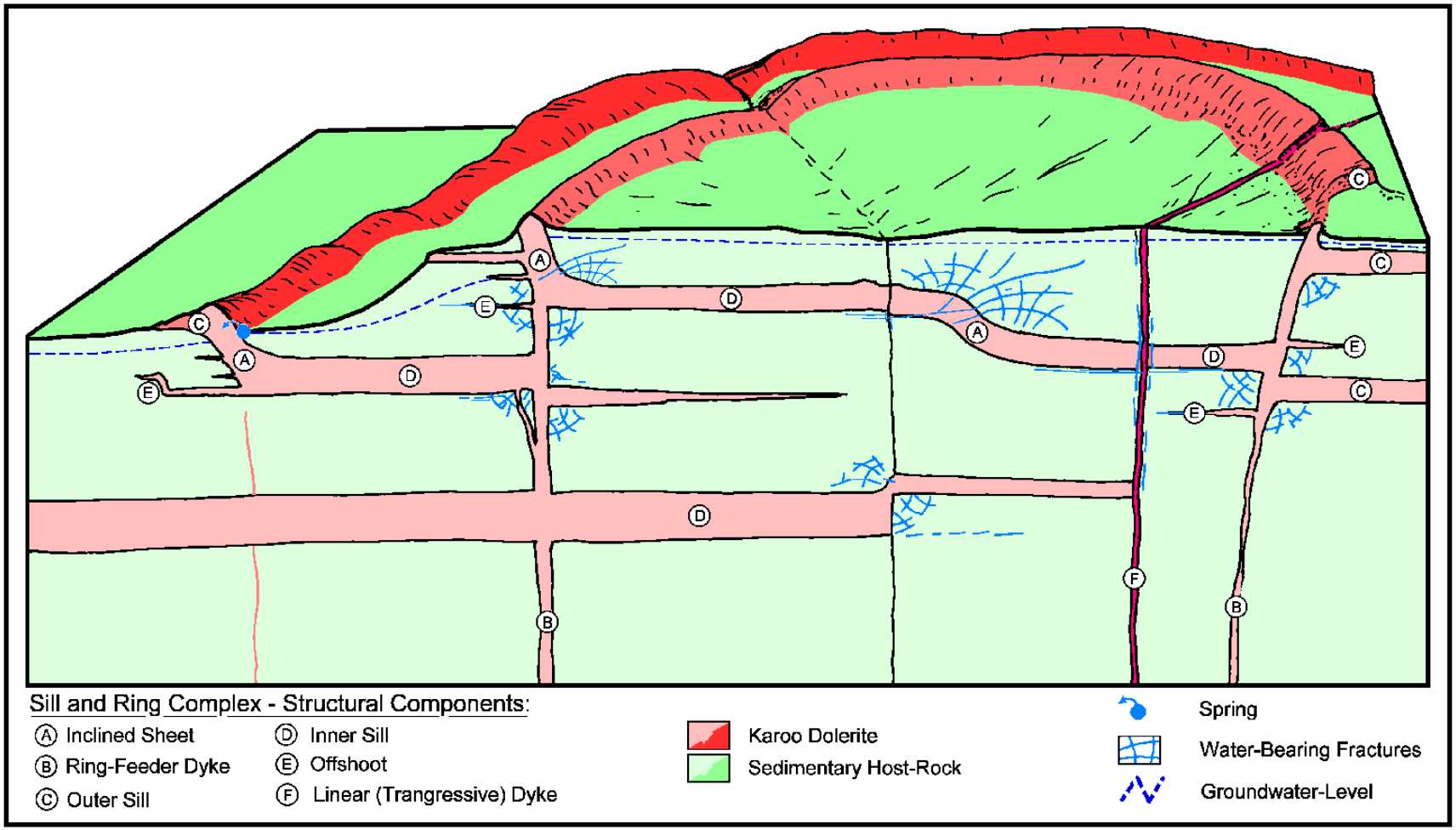

Fig 35 *Hydro-Morphotectonic Model of a Ring Complex (Chevalier et al, 2001 in SRK Consulting, 2012).*

In the localities that are away from the younger NNE trending faults and lineaments the dolerite sills dominantly serve as barriers to the downward/vertical flow of groundwater creating perched groundwater aquifers on the fractured and weathered upper part of the dolerites and overlying fractured and/or weathered sedimentary rocks. Massive and unweathered dykes form barriers for lateral movement of water, thereby confining surface and groundwater. The basalt flows in Hawaiian Islands which are highly permeable are isolated by cross-cutting igneous dykes, which are groundwater dams. The groundwater is trapped at a high elevation behind these natural underground dams (Fetter, 1994).

Pumping tests in dyke areas from Botswana indicate that dykes that are thicker than 10 m serve as groundwater barriers, but those of smaller width are permeable as they develop hydraulic continuity with the country rock through cooling joints and fractures (Bromley et al., 1994). In the Witwatersrand goldfields area of South Africa, a series of north-south trending dykes between 6 and 60 m in thickness that intrude volcanic and sedimentary rocks have created a series of isolated aquifer compartments. Recharge to the compartments occurs from rainfall while discharge occurs through springs located at the downstream contact of the dolomite and the intrusive dykes. In south-western Australia, dolerite dykes impede the lateral flow of groundwater, forcing it to the surface where evaporation can cause salinization (Engel et al., 1989 in Cook, 2003)

On the other hand, fractured dykes and sills may form good aquifers. One of the dykes in the Palaghat Gap (western coast of India) extends for a strike length of about 14 km and is highly fractured, forming a potential source of groundwater. The discharge from some of the wells in this dyke is of the order of 240–840 m^3/d (Kukillaya et al., 1992). Closer to the younger fault

zones in the study area, both the dolerite intrusive bodies and the surrounding country rocks are seen highly fractured with a probable faster recharge and interconnection of groundwater between the upper and lower sedimentary aquifers.

5.3. Aquifer hydraulic characteristics

One of the most fundamental parameters in characterizing aquifer heterogeneities, estimating groundwater flow dynamics and parameterizing groundwater flow models is the hydraulic property of rocks. However, measurement of hydraulic parameters (such as Transmissivity (T), and hydraulic conductivity (K)) is one of the most difficult tasks in hydrogeological studies as it requires drilling into aquifers with full penetration, proper screening of the aquifers with provision of observation wells, proper well development, conducting pumping test with the appropriate pump for the test and accurate measurement of well yield, drawdown and well recovery. Simpilification of aquifer dimensions and heterogeneity and boundary conditions can introduce a lot of errors into the estimates of hydraulic parameters. Selection of appropriate pumping test data interpretation method, most of which are basically formulated for interpretations in porous media aquifers, is also another challenge in getting acceptable estimates particularly for fractured hard rock terrains similar to the study area of this PhD research work.

The study area lacks enough and accurate data on hydraulic properties of aquifers. Most of the limited available data concentrates around the Mekelle town where relatively more detailed hydrogeological investigations were done to solve the water supply problem of the town. As the boreholes drilled for the investigations are at the same time intended to be production wells, they penetrate into multilayer aquifers and hence only cumulative values of the hydraulic parameters are acquired. These values provide vague information about the aquifers because other required

supplementary data about the wells (such as: borehole location, lithologic log) are mostly difficult to find. But there is an opportunity that such rough data can give some clue about the overall hydrogeology with certain degree of uncertainty particularly when integrated with results from other study techniques such as geological, geophysical, tracer and hydrochemical techniques. Therefore the collected secondary data is presented in annex 4 and some preliminary conclusions from previous works are summarized here. In this research work, these limited data (boreholes' yield, springs' yield and T) are used to see patterns and spatial distribution of the aquifer hydraulic parameters and the results are integrated with the findings from the hydrochemistry and isotope hydrology approach in the preceeding chapters.

According to FWWDSE (2007), the aquifer in the lower part of the Agula Shale (~54 m thick) which is found on top of the dolerite sill in the Aynalem well field has transmissivity ranging between 100 and 4750 m^2/day and for the upper part of the Antalo Limestone (~200 m thick) found below the dolerite sill, it ranges between 100 and 3500 m^2/day. Whereas, significantly lower values that range between 1.02 and 5.5 m^2/day are reported in this study for the dolerite sill. DH-consult (2010) has estimated an average transmissivity of 412 m^2/day for the lower section of the Agulae Shale. Pumping test analysis of two recently drilled wells into the Upper part of the Antalo Limestone (350 m and 375 m deep) gives rise to similar transmissivity value of 432 m^2/day. A nearly equal transmissivity (421 m^2/day) is estimated for the Adigrat Sandstone from a well drilled (180 m) into the formation at Chinferes.

The basement rocks, glacial deposits and dolerites in the study area are characterized by shallow and localized aquifers mostly associated with faults and shear zones. Boreholes drilled into these rock formations have well yields mostly less than 5 L/s. The upper part of the Mesozoic

sedimentary sequence (the whole Agula Shale and the upper part of Antalo Limestone) is dominated with shale and marl units although gypsum and thin beds of marl and limestone are also minor constituents found as intercalation. It is mostly intruded by dolerite sills and to a lesser extent dolerite dykes. Although it is affected by intense joints, the groundwater occurrence and flow in this upper part of the sedimentary section is limited due to clay dominated lithology. Wells and springs have low discharge hardly exceeding 2 L/s. But at the contact zones with the dolerite intrusions, boreholes that discharge 12-40 L/s are common (*Fig 36*). Whereas the Adigrat Sandstone and the lower part of Antalo Limestone are characterized by extensive/semi-regional aquifers with boreholes' yield mostly ranging between 10 L/s and 60 L/s.

Intensity of fracturing and disturbance of rock mass are higher close to the major faults of the area where joints, fractures, dissolution cavities and bedding planes are observed to be more open for groundwater accumulation and flow. Localized groundwater recharge occurs along the highly fractured and dipping sedimentary beds (drag folds) adjacent to these major faults. This creates confined aquifers and artesian conditions along the axes of the drag folds because of higher hydraulic heads in the dipping beds and the confining units (shale and marl intercalation within the sedimentary sequence).

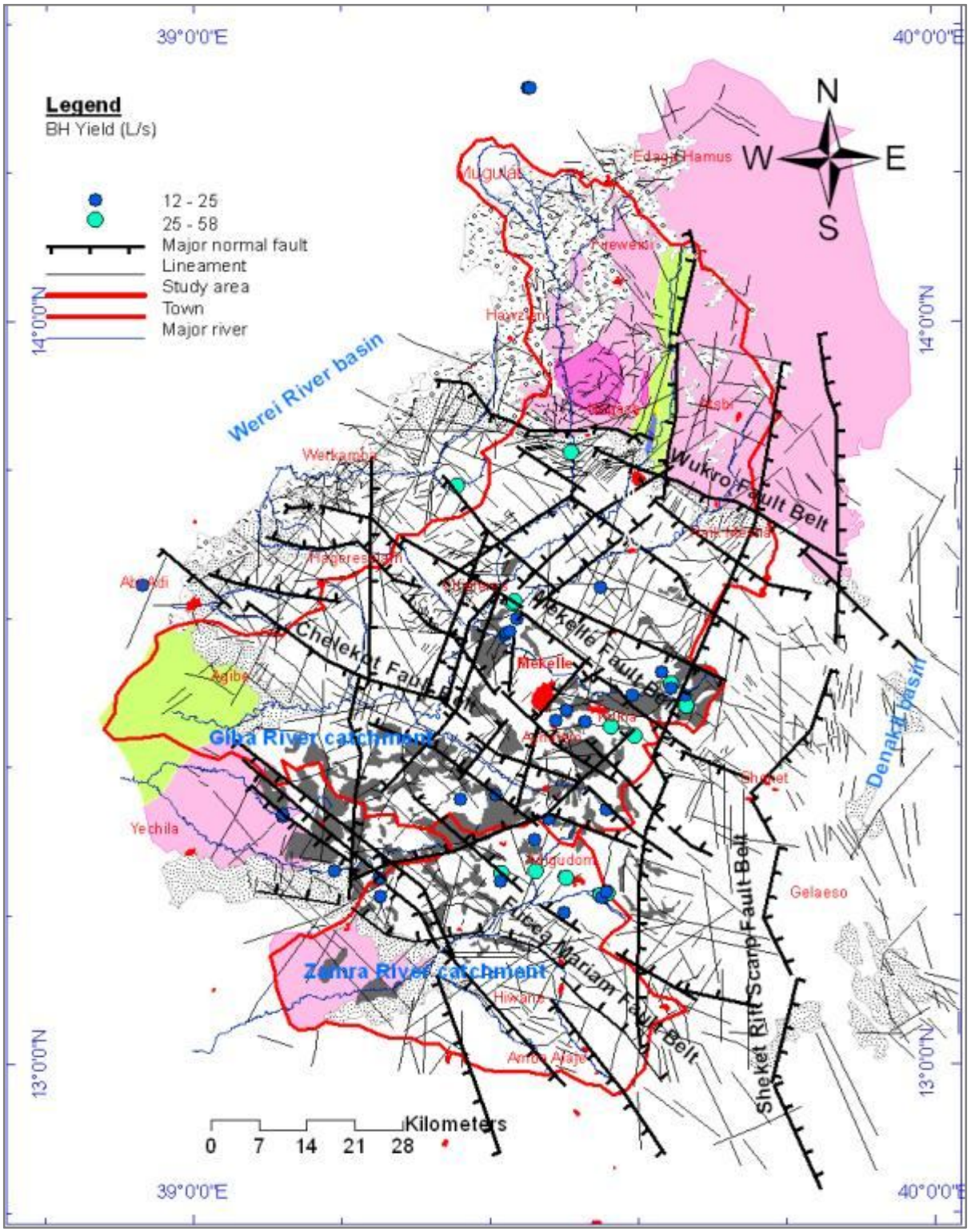

Fig 36 *Distribution of high yield boreholes on the geological map of the study area (Note: the white shaded area is covered with Agula Shale and Antalo Limestone formation)*

Most of the high yield boreholes and the perennial and high discharge springs are found close to the major faults and lineaments of the area and at the contacts between the Mesozoic sedimentary rocks and the Mekelle dolerite (*Fig 36 and 37*). A similar pattern of higher boreholes' yield parallel to the major faults and lineaments is also observed on the shaded contour map of the boreholes' yield (*Fig 38*). Based on limited data of transmissivity of aquifers, there is a clue that higher transmissivity values are more frequent close to the major faults of the area (*Fig 39*).

But there are also cases where adjacent deep wells (< 1.5 Km apart) drilled into the Adigrat Sandstone and Agula/Antalo formation on opposite sides of faults close to the Wukro and Mekelle fault belts show significantly differing hydraulic properties (table 5). These faults brought the Adigrat Sandstone and Agula Shale to be found adjacent to each other on the surface particularly around Abrehaweatsbeha and Chinferes localities. And the wells drilled into the Adigrat formation are characterized by higher well yields (>50 L/s) and transmissivity values (around 400 m^2/day) while those on the Agula Shale indicate much lower well yields (< 3 L/s) and transmissivity values (< 3 m^2/day) regardless of their close location to the major faults of the area (table 5).

Table 5 Hydraulic properties of adjacent deep wells drilled in to different lithologies on opposite sides of faults (clear rows are on Adigrat Sandstone while shaded ones on Agula Shale)

Borehole code	**X**	**Y**	**Depth (m)**	**SWL (m)**	**Yield (L/s)**	**T (m^2/day)**
CHF BH2	546783	1505537	254	6.74	58.1	421
CHF BH3	546978	1505955	180	10.72	33.6	390
CHF BH-2	546113	1505533	180	Dry	-	-
MO-TW23	555157	1428161	202	Artesian	> 50	
MO-TW11	555135	1526855	350	3	3	< 3

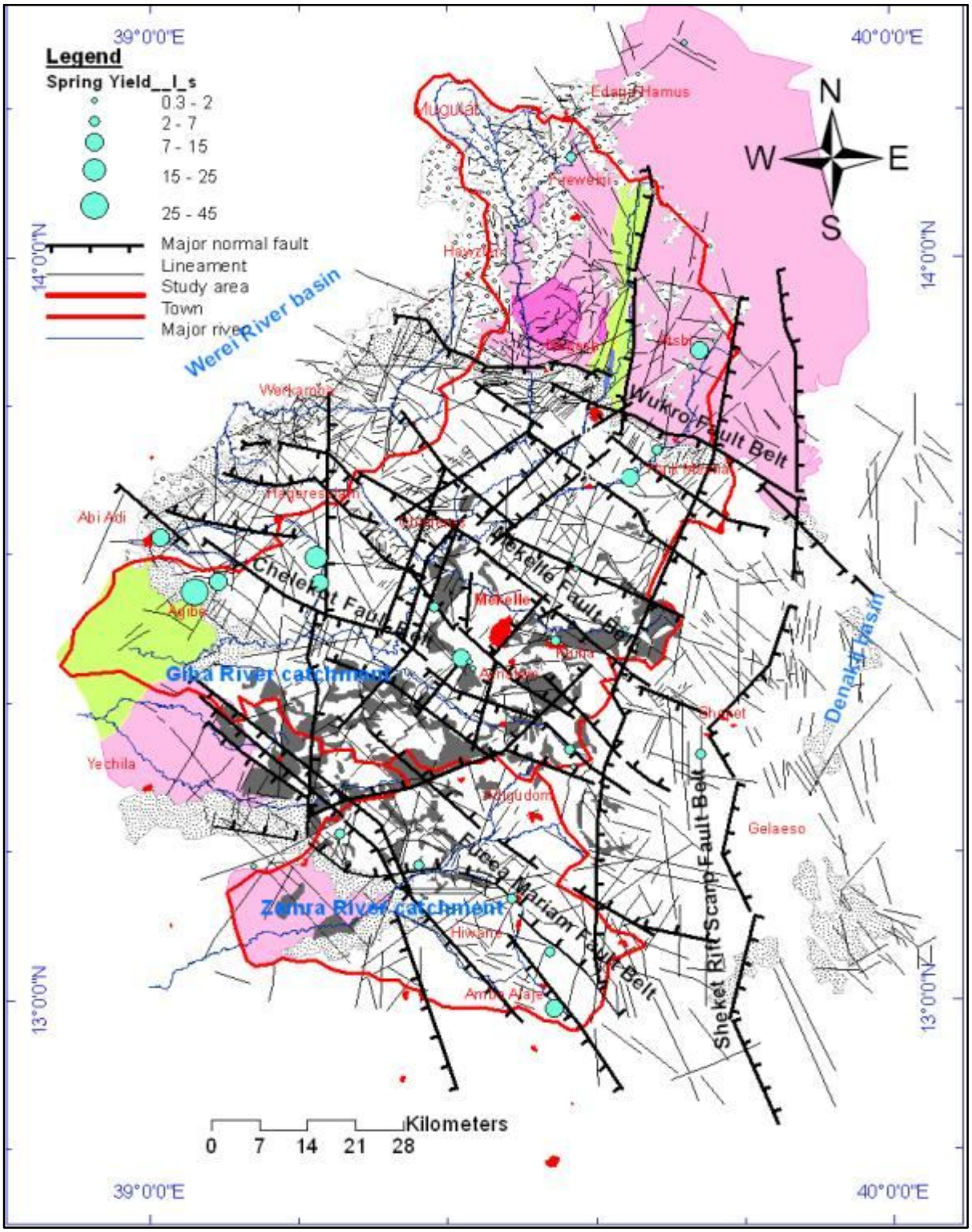

Fig 37 *Distribution of perennial and high discharge springs with respect to major geologic structures in the study area*

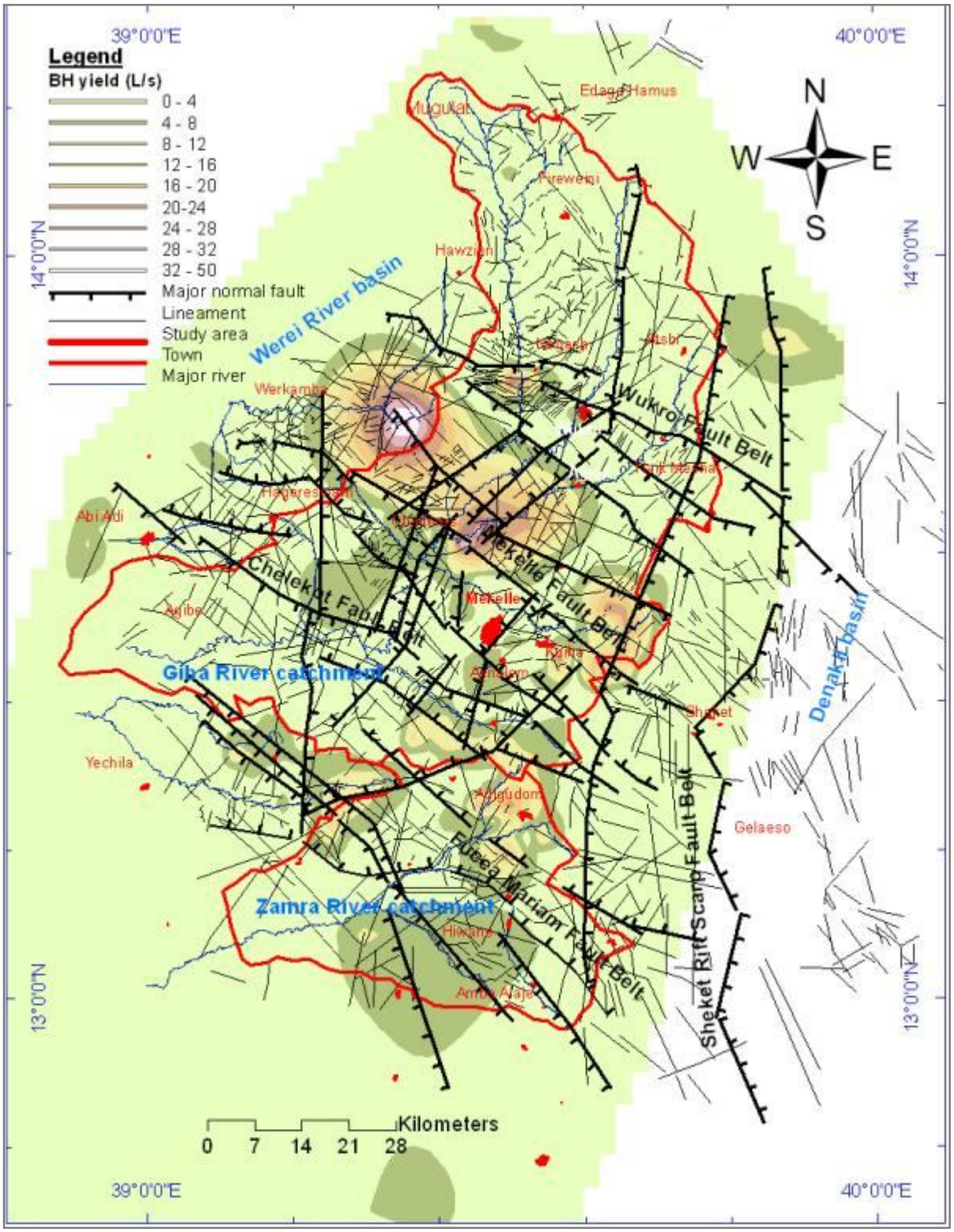

Fig 38 *Shaded contour map of boreholes' yield in the study area (Note: Yield values are in L/s)*

6. Hydrochemistry and isotope hydrology

6.1. Isotopic composition of water samples compared with the Addis Ababa LMWL and the GMWL

From the scatter plot of $\delta^{18}O$ and $\delta^{2}H$ of the water samples collected in this study (*Fig 39*), it is observed that most of the groundwater samples lie close to the Addis Ababa LMWL indicating that local precipitation is the major source of recharge to the aquifers of the area. Sight shifting of some of the groundwater samples towards the left (ellipses 'A' and 'B' of *Fig 39*) is mainly attributed to their location at higher altitudes, and hence the combined influence of the altitude effect and the difference in isotopic composition of its local air mass from that of Addis Ababa.

Owing to the cold and humid summer weather of the relatively elevated localities in the study area, a depleted and high d-excess air mass is expected below the cloud base. Whereas, Addis Ababa is located close to the Lakes Region of the Ethiopian Rift Valley, and hence the isotopic exchange of rain droplets with the relatively enriched vapor from these continental water bodies can result to a relatively enriched precipitation and groundwater recharge. These differences in isotopic composition of local air-masses may often lead to much more complex relationships at the local level between $\delta^{2}H$ and δ18O than suggested for the regional or continental scale by the global "Meteoric Water Line" equation (Hoefs, 2009). Samples in ellipse 'A' are relatively at higher altitude than those in ellipse B resulting to more depletion of samples in ellipse 'A'.

The distance effect can also have a slight impact, as the area is located far from the moisture source to the summer precipitation in this region as compared to Addis Ababa. The moisture comes both from the Indian and Atlantic oceans when the Inter Tropical Convergence Zone (ITCZ) lies north of Ethiopia. Seifu Kebede at al. (2005) have also indicated that the major

source of recharge to the Ethiopian groundwaters is the summer rainfall and the distance and altitude effects are prominent factors in depleting the precipitation in the northern highlands of Ethiopia.

A similar leftward shift of samples SP18, SP19 and SP20 as the others in ellipse 'B' while they are relatively in lower altitudes indicates the presence of fast groundwater flow along open fractures and dissolution cavities in limestones from the Hagereselam highlands towards the sampling points. The mouth of these springs also display accumulations of travertine deposits and the springs also emerge from highly fractured limestone terrains with observable dissolution cavities. Shifting of the samples in ellipses 'C' and 'D' of Fig 40 parallel to the x-axis is related to their location in low elevations and hence shows the importance of local precipitation that has undergone isotopic exchange with the hot and dry air mass under the cloud base which should be heavily enriched.

The regression line for the river water samples has produced a shallower slope than both the LMWL and the GMWL. This line is considered as a surface evaporation line ($\delta^2H = 4.47\delta^{18}O + 6.42$; $R^2 = 0.8$) (*Fig 39*). Four river samples (R3, R6, R9 and R13) that are relatively depleted than the other river samples (*Fig 39* and *Fig 12a*) indicate that they have effluent sections around the respective sampling points. The shift of some groundwater samples towards the enriched river samples values (polygon 'E' in *Fig 39*) signifies the influence of local recharge from nearby surface waters (microdams and rivers).

Some case studies in the previous works have indicated similar observations in other parts of the study area, by comparing hydrochemical parameters (Tesfamichae Gebreyohannes, 2009) and water level fluctuation measurements in groundwater versus nearby surface water bodies

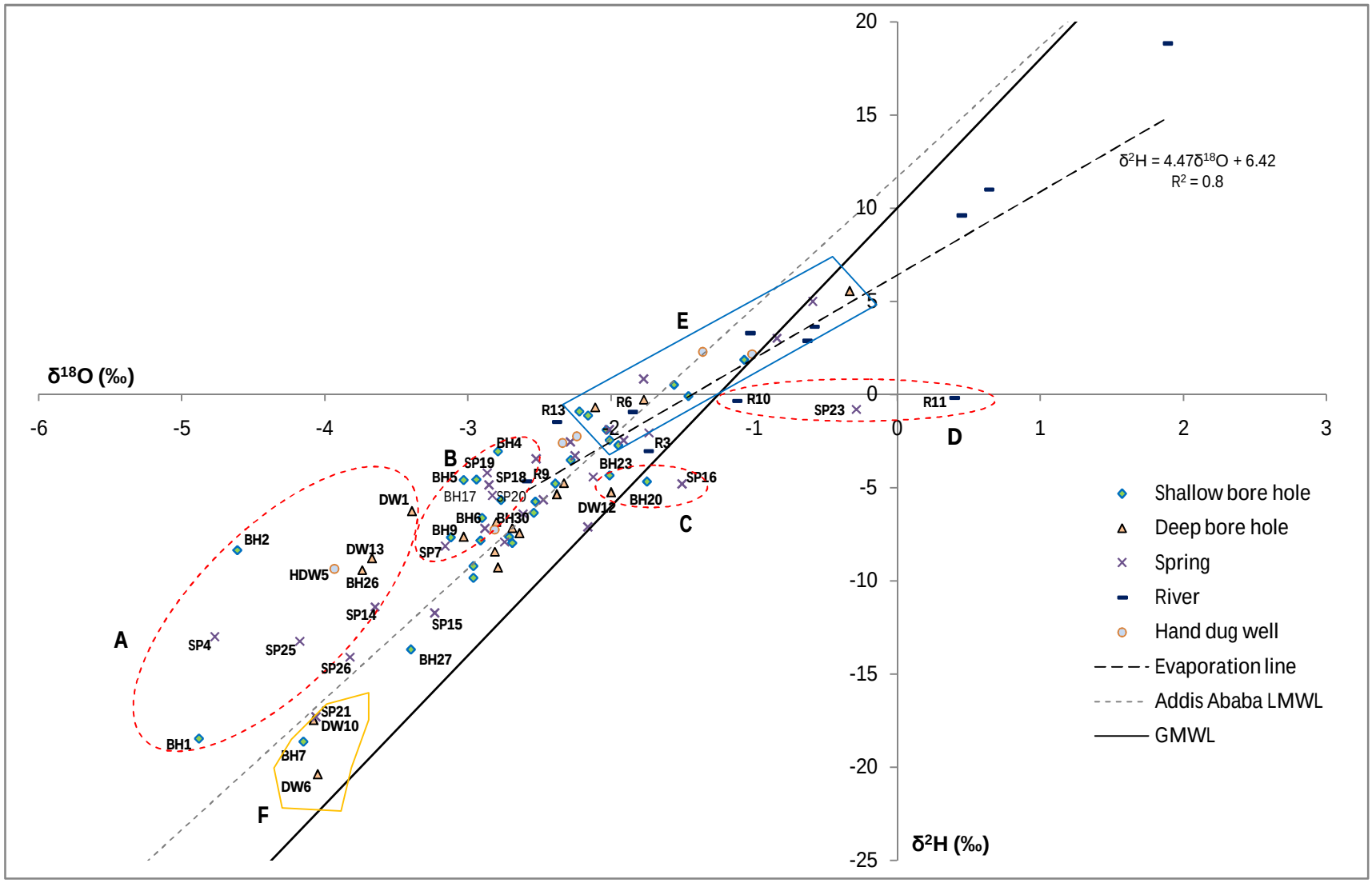

Fig 39 *Scatter plot of $\delta^{18}O$ versus $\delta^{2}H$ of the winter water samples with the Addis Ababa LMWL and the GMWL*

(FWWDSE, 2007; Teklay Zereay, 2007; Tesfamichael Gebreyohannes, 2009), and observation of recharge conditions during well pumping tests (Abdelwassie Hussein, 2000). In polygon F of Fig 41, the samples SP21 and DW6, which are collected from the Adigrat Sandstone Formation in the groundwater discharge areas, indicate deep groundwater circulation.

The samples DW10 (taken from the Edaga Arbi Tillite) and BH7 (taken from the Agula Shale) have uniquely depleted isotopic signatures and higher EC as compared to other nearby groundwater samples (*Fig 12a* and Annex 1) indicating perched (isolated) aquifers. In the Edaga Arbi Tillite and Agula Shale Formations, lenses (layers) of shale that hinder circulation of groundwater, are not uncommon (Beyth and Shachnai, 1970; Tesfaye Chernet and Eshete Gebretsadik, 1982; FWWDSE, 2007; DH-consult, 2010). The samples in this polygon can have relatively longer residence times.

6.2. Spatial distribution of $\delta^{18}O$

From the relationship of $\delta^{18}O$ and altitude for shallow groundwater samples in the study area (*Fig 40*), it is observed that they are inversely related and the regression line on the plot indicates a depletion rate of -0.51 ‰/100 m for the $\delta^{18}O$ as one goes from the western lowlands towards the highland areas (altitude effect), which is within the range -0.2 to -0.6 ‰/100 m obtained from other mountainous tropical regions of the world (Rozanski and Araguas-Araguas 1995). On the other hand, Seifu Kebede and Travi (2012) have estimated a depletion rate of -0.1 ‰ /100 m for the Blue Nile basin (altitude effect) and a similar rate for the Afar depression towards the north western highlands of Ethiopia (pseudo-altitude effect). The 'pseudo-altitude effect' occurs due to evaporative enrichment of raindrops during the fall beneath the cloud base which is larger at low altitudes where the cloud base is typically high above the ground level. Such an effect is

observed clearly in intermountain valleys and on the leeside of a mountain range (Moser and Stichler, 1971).

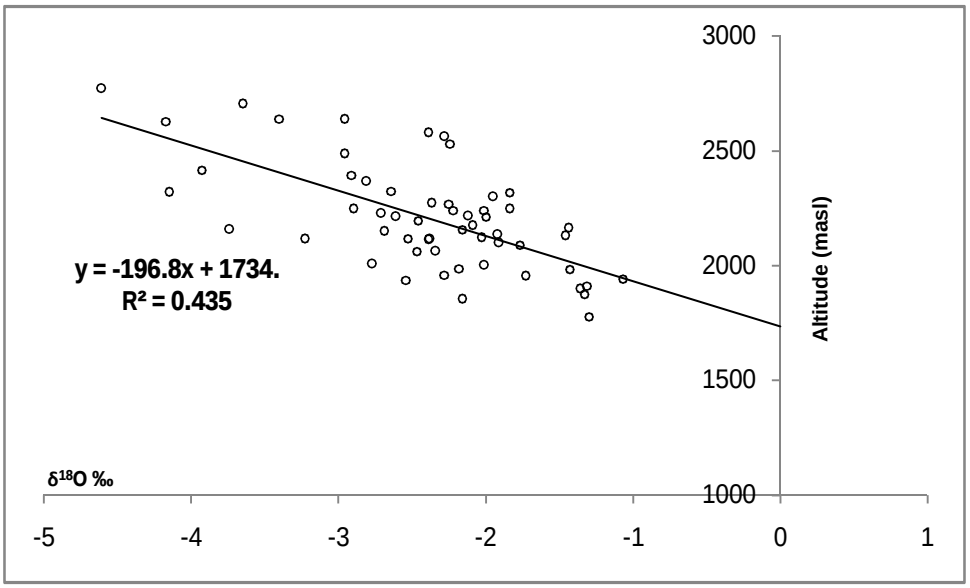

Fig 40 *Scatter plot of $\delta^{18}O$ versus altitude for shallow groundwater samples of the study area*

Therefore, the depletion in $\delta^{18}O$ of the shallow groundwater in the highland plateau of the study area (polygon 'A' in *Fig 41*) is due to recharge from already depleted precipitation reaching these elevated grounds due to the 'altitude effect' and less residence time. But the enrichment of shallow groundwater in the intermediate and lower elevations (polygon 'B' in *Fig 41*) of the study area can be interpreted as due to four reasons: (1) recharge from already enriched local rainfall, (2) evaporation prior to recharge of the surface runoff, (3) percolation of evaporated shallow groundwater to deeper aquifers which discharge in the western lowland area, and (4) evaporation from the shallow groundwater in these discharge area. Further study on isotopic composition of rain water in different elevations of the study area can help to verify which of these reasons can be the major factor.

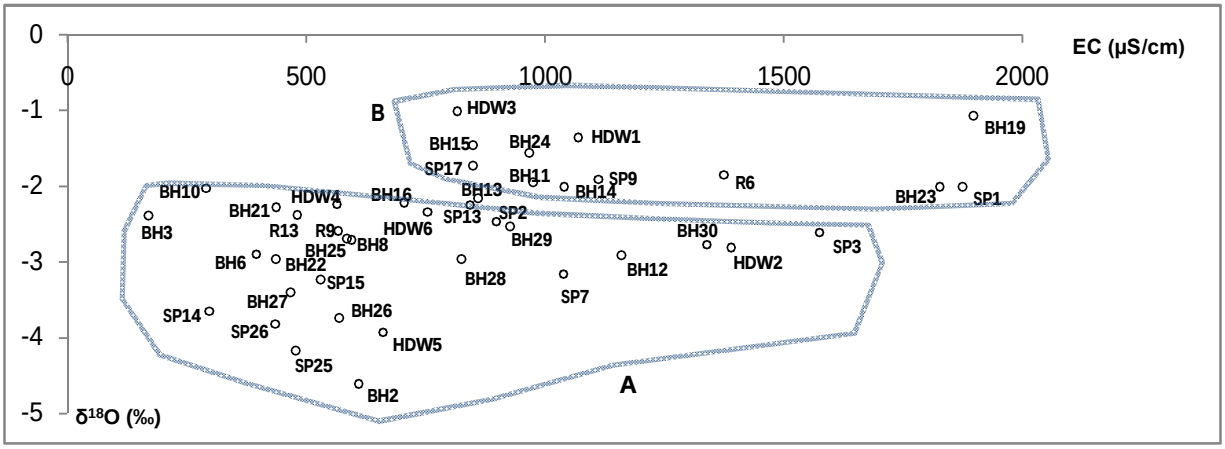

Fig 41 *Scatter plot of $\delta^{18}O$ versus EC for shallow groundwater samples of the study area*

For the progressive enrichment of river water as moving towards the western lowlands (*Fig 42*), it is due to continuous evaporation as the surface water flows downstream and further evaporation of the shallow groundwater that feeds the base flow in the discharge areas in the lower parts of the Giba and Zamra rivers and their tributaries (*Fig 13* and evaporation line in *Fig 39*).

Shallow groundwater samples (BH1 and SP4) collected at the foot of the Afar Rift escarpment have similarly depleted $\delta^{18}O$ values (-4.88 ‰ and -4.77 ‰) as those of the highland groundwater (*Fig 43* and *Fig 12a*), while their EC values are quite higher (1560 µS/cm and 1395 µS/cm) than measured in the highland groundwater (<700 µS/cm) around Edagahamus and Atsbi (*Fig 12a*). This result shows that there is deep groundwater circulation with longer residence time towards the Afar Depression through the deep seated faults of the rift escarpment. Further study and additional data is needed to fully understand how this deep groundwater flow system operates and its residence time.

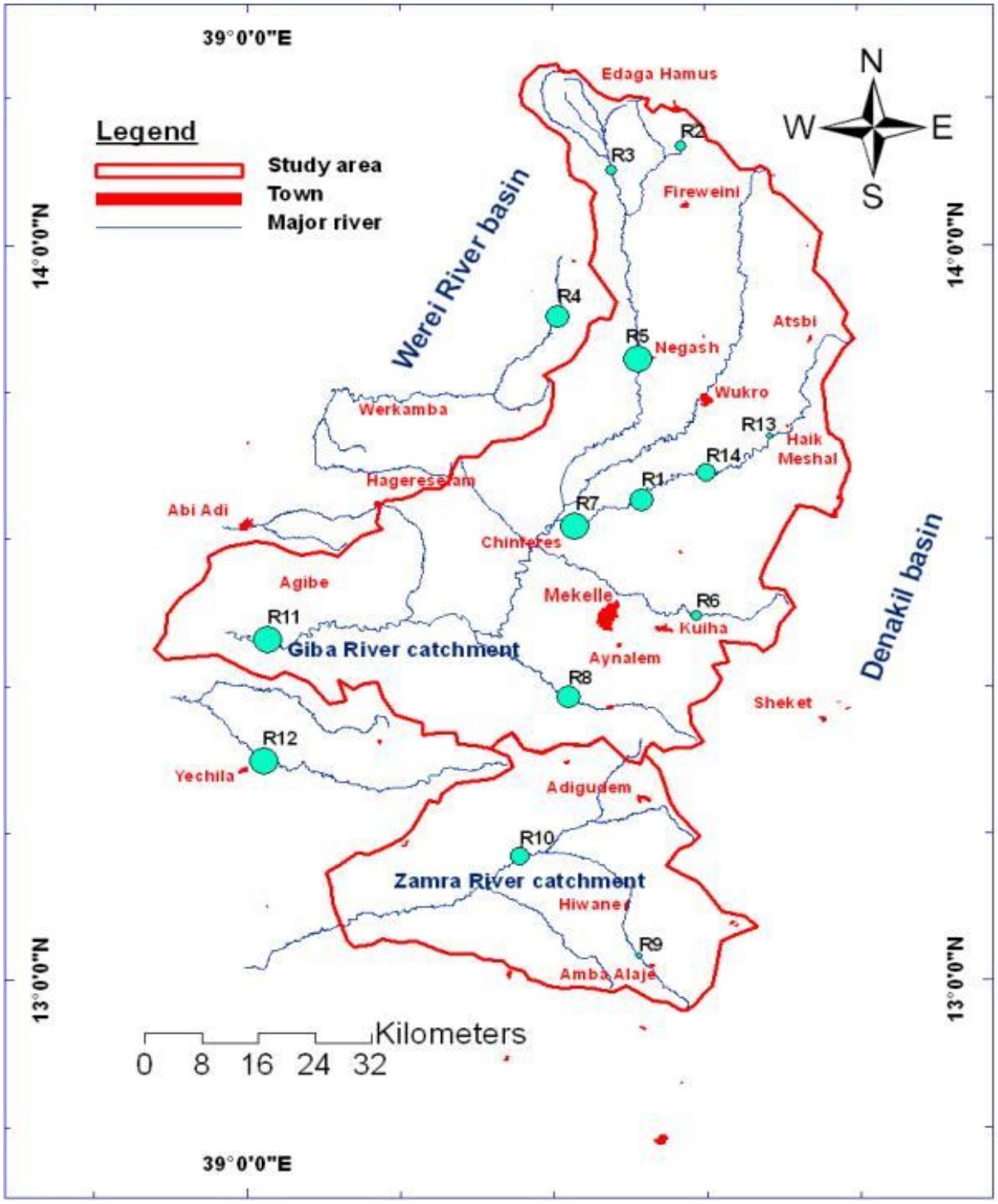

Fig 42 *Variability of $\delta^{18}O$ values in river samples from upstream to downstream areas (Note: Bigger circles show higher $\delta^{18}O$ values and progressively smaller circles represent progressively smaller $\delta^{18}O$ values)*

On the western side of the highland plateau (in the lower Giba river catchment), two groundwater samples (SP21 and DW6) collected from the Adigrat Sandstone also have depleted $\delta^{18}O$ (-4.06 ‰ and -4.05 ‰) and similar lower EC (287 µS/cm and 947 µS/cm) as those of the groundwater samples collected from the basement rocks and sandstones around Edagahamus and Atsbi highlands (*Fig 43* and *Fig 12a*). The area in between these localities is covered with a thick (>1000 m) shale-marl-limestone rock sequence of the Agula and Antalo formations (*Fig 13* and *Fig 14*) in which the average groundwater EC is 1306 µS/cm. This indicates that there is a deep groundwater flow mainly through the fractured sandstone formation with minimal leakage from the overlying more soluble rocks probably because of the aquicludes (mudstones and marls) at the base of the Antalo Limestone. This deep groundwater flows in the southwest direction parallel to the surface water flow of the Giba River. Clues of multi-layer aquifer systems with contrasting groundwater quality were also found in some of the pervious works based on categorization of lithologic formations into hydrostratigraphic units (Chernet and Eshete, 1982; Gebreyohannes 2009), borehole geophysical logging (FWWDSE, 2007; DH-consult, 2010) and monitoring of groundwater level and yield of wells with different depth in the Aynalem well-field (FWWDSE, 2007).

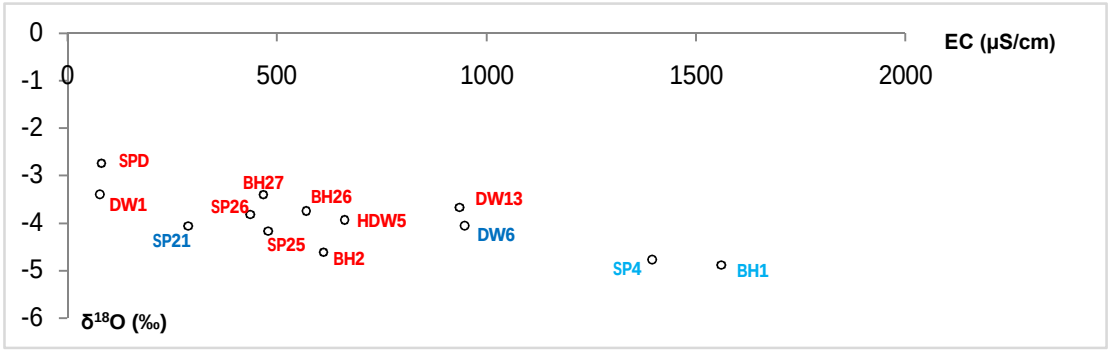

Fig 43 *Scatter plot of $\delta^{18}O$ versus EC for groundwater samples BH1, SP4, SP21, DW6 and groundwater samples at the highlands of Edagahamus and Atsbi*

6.3. Variability of $\delta^{18}O$ and $\delta^{2}H$ with depth

Water samples taken from close proximity rivers, shallow wells (35-70m depth) and deep wells (350-650m depth) in four localities were also analyzed for stable isotopes ($\delta^{18}O$ and $\delta^{2}H$) to identify similarity or difference of the groundwater flow paths at different depths. The deep wells from which samples "A", "B" and "C" were collected are artesian wells. The result on Fig 44 indicates that there is a clear segregation of stable isotope compositions with depth in all the areas.

The groundwater samples from the deeper sources (A "DW6", B "DW16", C "DW9") show relatively depleted isotopic compositions as compared to their respective shallow groundwater samples (a "BH13", b "BH30", c "BH18", d "BH31"). The surface water samples (a' "R7", b' "R14", c' "R8") show high enrichment of both $\delta^{18}O$ and $\delta^{2}H$. These differing isotopic signatures reveal that there is very limited interaction between the surface water and the groundwater of the localities and that there exist shallow and intermediate groundwater flow systems with slow rates of leakage between them. There is also an observation from borehole resistivity logs that the shallow groundwater in the Mekelle Outlier is generally of low salinity with increasing trend of total dissolved solids (TDS) values with increase in drilling depth until once again turns to lower values after the depth of 200 m, which indicates multi-layer groundwater flows and salinity stratification with minimum mixing (FWWDSE, 2007; DH-consult, 2010).

The case is clearer at locality "A" (*Fig 44*) where the groundwater samples are from different lithologic formations in the stratigraphic column (Adigrat Sandstone and Antalo shale-marl-limestone intercalation sequence) indicating clear shallow and deeper groundwater circulations.

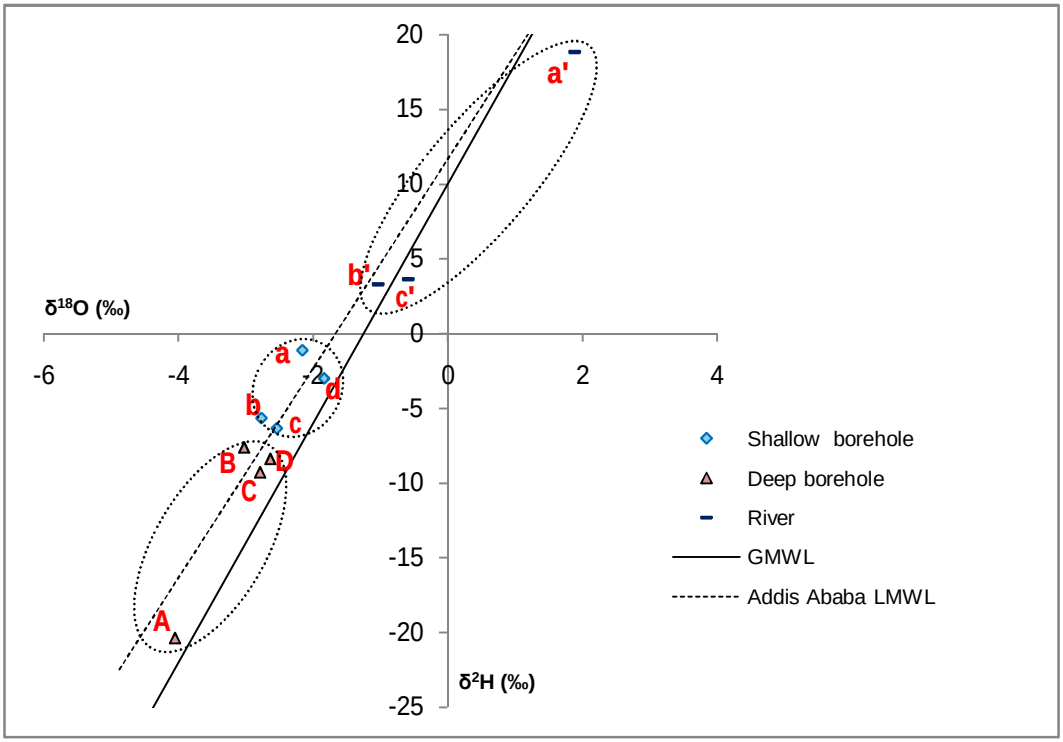

Fig 44 *$\delta^{18}O$ versus $\delta^{2}H$ plot of water samples collected at different depths respectively located within close proximity (A,a,a' = Chinferes, B,b,b' = Agula, C,c,c' = Chelekot, D,d = Kuiha)*

The enrichment of the river samples at these localities shows that the river water travels longer distances at the surface where it is fully exposed to evaporation and has little replenishment from the groundwater baseflow in close vicinities. This result may further indicate that the shallow aquifers at the plateau mostly discharge their water to the rivers within the plateau itself (i.e. only after a short residence time in the aquifers) and/or at the mouths of the deep river gorges cutting into the plateau areas.

Based on the relationship between a water table map and the topographic contours and using particle tracking path lines, it is observed that this shallow groundwater system is recharged from precipitation in the highland plateaus and it discharges through springs and baseflow to rivers and wetlands that are found along the major valleys in the Giba basin (FWWDSE, 2007;

Tesfamichael Gebreyohannes, 2009; DH-consult, 2010). The remaining part of infiltrated water may percolate down to recharge the deeper aquifers through fractures and joints. For this last interpretation, additional evidence can be the similarity in EC of the shallow and deep groundwater within the Agula Shale Formation and the upper units of the Antalo Formation respectively (refer section 6.4).

6.4. Local meteoric water line of the study area

Historical measurements of the stable isotopes in precipitation is lacking in the study area. Although LMWL of an area should be best constructed based on such long-term data in precipitation, there is an observation that deep groundwaters show no seasonal variation in δ^2H and $\delta^{18}O$-values and have an isotopic composition close to amount-weighted mean annual precipitation values (Hoefs, 2009). Based on this, the LMWL of the Mekelle Plateau and its close surroundings is constructed by using the stable isotope data acquired from deep groundwater that is collected from the study area in the dry season in order to minimize the influence of the most recent summer precipitation which constitute much of the pumped water from the wells during summer (refer section 6.3.5) and may dominate in the isotopic signature. Accordingly, the regression line on Fig 45 with the equation $\delta^2H = 6*\delta^{18}O + 9.8$ ($R^2 = 0.8$) is proposed to be a proxy to the LMWL of the study area.

This LMWL of the area has a slightly smaller slope as compared to that of Addis Ababa. This smaller slope results from the shift of most of the samples to the left of the Addis Ababa meteoric water line. As discussed in section 6.3.1, this shifting is considered to be resulting from the combination of altitude effect, differences in the isotopic composition of their local air-masses and the distant location of the area (as compared to Addis Ababa) from the moisture

sources to the summer precipitation that recharges the groundwater of the study area (distance effect).

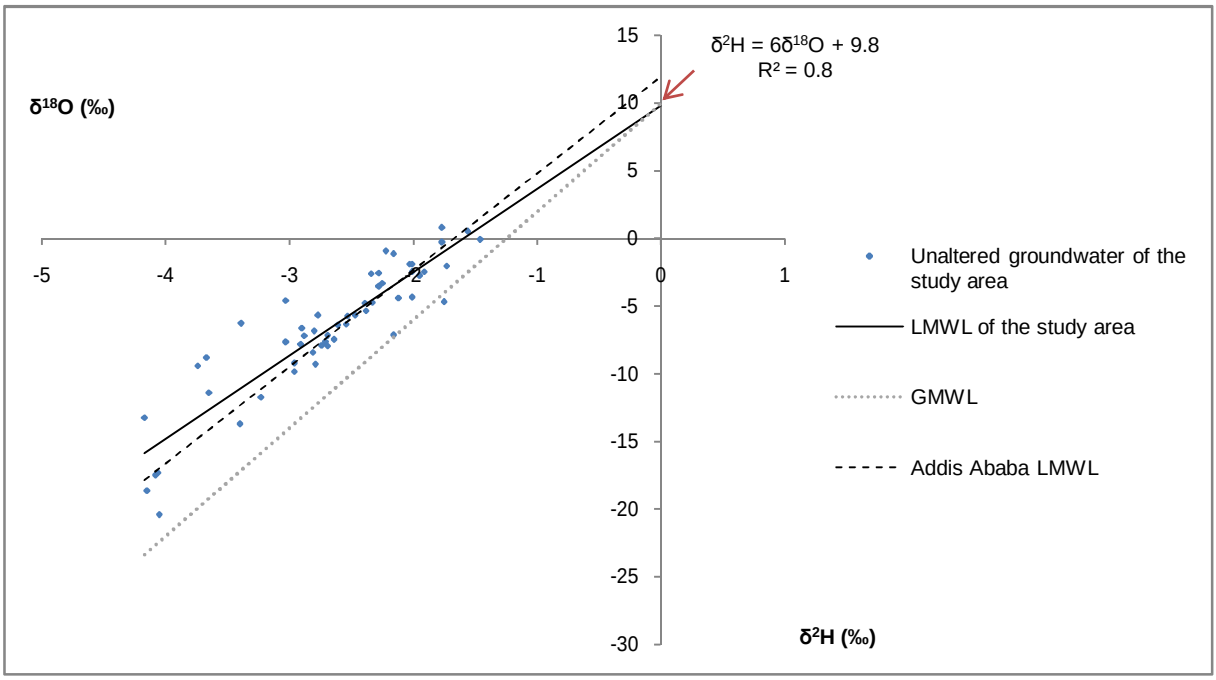

Fig 45 *Local meteoric water line of the study area developed from $\delta^{18}O$ versus $\delta^{2}H$ plot of groundwater samples collected in the winter season, plotted with the GMWL and the Addis Ababa LMWL*

6.5. Isotopic signatures of groundwater samples collected in different seasons

When the groundwater samples collected in two different seasons (rainy and dry) from vicinities to the Mekelle town (around 20 Km radius) are plotted in the $\delta^{18}O$ - $\delta^{2}H$ bivariate plot, the regression line of the summer samples is shifted to the right of (are relatively enriched as compared to) the winter samples (*Fig 46*).

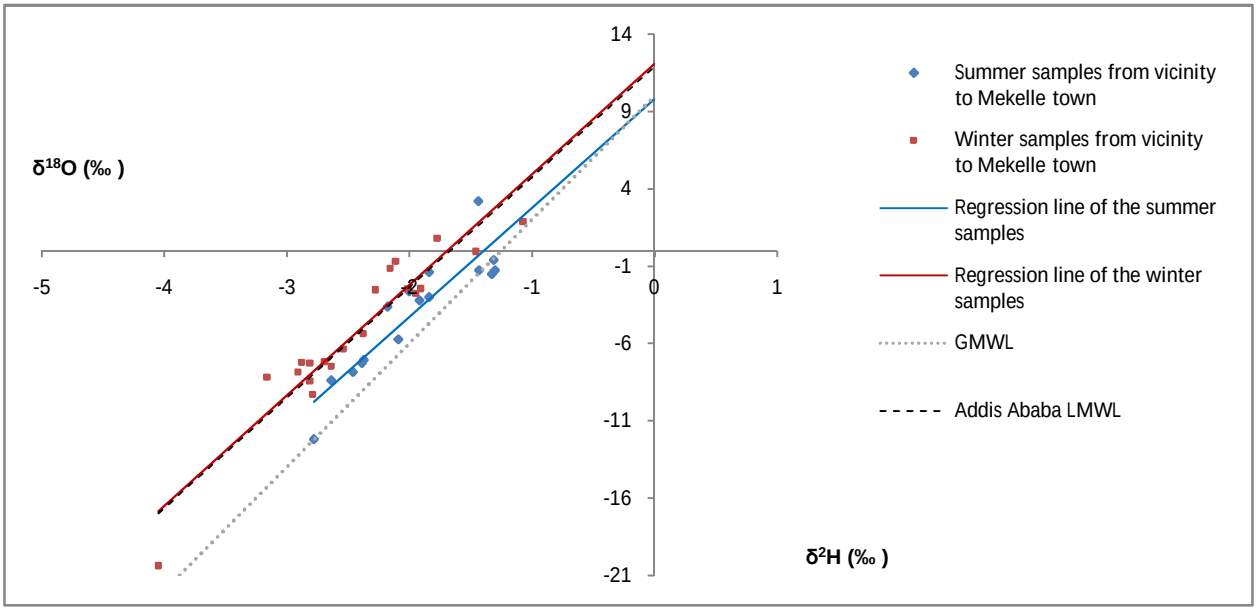

Fig 46 *Scatter plot of $\delta^{18}O$ versus $\delta^{2}H$ of summer and winter groundwater samples from vicinities to Mekelle town with the GMWL and the Addis Ababa LMWL*

This shifting indicates that during summer (rainy season) there exists a shallow subsurface sheet flow in the upper highly weathered and fractured horizon of the aquifers, which is close to the surface and there is the effect of evaporation. This interflow (throughflow) contributes to the pumping from wells during the summer. But it is mostly discharged in the form of baseflow to the intermittent springs and rivers in the upper parts of the catchments. Small part of it percolates down to recharge the aquifers in the successively downstream reaches of the study area.

During the dry season pumping is mainly from the deeper aquifers. The recharge to these deeper aquifers comes from fast infiltration and percolation of the depleted rainfall in the highland areas along the major fault zones. An observation of salinity stratification in which lower TDS values are observed in deeper limestone aquifers in the Aynalem area is attributed to the interpretation that the main recharge of this deeper groundwater is from the lower (limestone dominated) units of the Antalo Formation that outcrop in the upstream reaches of the adjacent Illala and Chelekot

catchments, through the deep seated fractures of the Mekelle and Chelekot Fault Belts (FWWDSE, 2007). It should also be noted that the regression line of the dry season groundwater samples collected from around Mekelle town fits with the LMWL of Addis Ababa, showing the meteoric origin of the deep groundwater in this area.

As the area is characterized by semi-arid climate, groundwater level fluctuations can be significantly high during extended periods of drought and when there is over pumping from wells. Therefore, efficient water resources management practices such as frequent monitoring of groundwater levels, massive implementation of groundwater recharging structures and conjunctive use of surface water and groundwater are highly recommendable in the area.

6.6. Indications from tritium data

Activity of tritium has been measured in 35 systematically selected water samples (Annex 1) that are collected from deep wells, shallow wells, springs and rivers at different locations within the study area. The tritium activity values narrowly range between 1.73 TU and 3.66 TU (σ = o.5 TU). The lowest and highest tritium activities were measured in SP21 (high discharge spring emerging from the Adigrat Sandstone in the western lowland) and SP18 (high discharge spring emerging from karstified limestone at the lower part of the Antalo Limestone) respectively (*Fig 12*).

According to Clark and Fritz (1997), waters with tritium concentration from about 0.8 to 4 TU may represent a mixture of water that contains components of recharge from before and after 1952 (<0.8 TU represent recharge prior to 1952; 5 to 15 TU indicate recharge after 1987; 16 to 30 TU is indicative of recharge since 1953; >30 TU show probably of recharge in the 1960s or 1970s; >50 TU show predominantly recharge in the 1960s). Hence, the range observed in the

study area (1.73 to 3.66 TU) indicates components of pre- and post-1952 recharge. Having this and the background geological and geomorphologic knowledge of the study area, we can at least say that the lowest tritium activity in SP21 shows a deep circulation of relatively older groundwater (pre-1952) within the Adigrat Sandstone. And the highest tritium concentration in SP18 indicates more proportion of post-1952 recharged groundwater that flows from the Hagereselam Highlands towards the discharge area around the sampling point, along interconnected dissolution cavities within the limestones of the area. In these karstic limestones, fast flow of groundwater can be evident from recharge to discharge areas.

Most of the deep well samples (DW1, DW4, DW9, DW14 and DW16) display higher tritium activities (>3 TU) which shows that they are pumped from aquifers with more proportion of young groundwater. These deep wells are mostly located close to major fracture zones and hence acquire their groundwater recharge from recent precipitation which percolates fast along interconnected fractures. Generally, the probability of encountering very old (tritium depleted) groundwater in the study area is unlikely. Relatively older groundwater can be expected only towards the Afar depression (east of the study area), where the Mesozoic sedimentary rocks are relatively thick and extensive and the deep seated faults of the Afar rift can lead the groundwater into very deep positions, where flow rate can be slower.

As it is recommended by Newman et al. (2010), the ages of such young groundwaters in the study area can be more precisely determined by using a suit of tracers such as tritium, noble gasses (including tritium/^{3}He dating and ^{39}Ar), chlorofluorocarbons (CFCs), and sulphur hexafluoride (SF_6). Measurement of ^{14}C can also be required for groundwaters from the central part of the Denakil Depression. Future sample collection strategy for this dating purpose should consider sampling from wells screened only in target aquifers, from systematically selected

springs, river points based on expected groundwater flow directions and from rainfalls in different altitudes along selected transects.

6.7. Indications from dissolved ions concentration distribution

Five groundwater groups have been identified from the EC – altitude – lithology scatter plot (*Fig 47*). A similar pattern of categories is also identified from a preliminary Hierarchical Cluster Analysis (HCA) based on major ions chemistry (Li^+, Na^+, K^+, Mg^{2+}, Ca^{2+}, HCO_3^-, SO_4^{2-}, F^-, Cl^-, NO_3^-), EC and altitude of the water samples collected in this study (*Fig 48*). The groundwater samples from the highland areas of Atsbi, Hawzien, AmbaAlaje and HagereSelam lay within the low EC-high altitude range (Group I in *Fig 47*). Most samples in Sub-Group 4 (SG4) and SG5 of the HCA lay in this group and they are characterized by low concentration of all the major ions. They were collected mainly from basalt, sandstone, tillite (sand dominated), dolerite and metavolcanic rock aquifers. This low EC (76 to 705 µS/cm) nature arises from their location within the recharge area (low residence time) and the low solubility aquifer composition. The samples in Group II (SG3 of the HCA) have an EC values range (99 to 719 µS/cm) and low concentrations of all the major ions similar to Group I, but they are found at lower altitudes. They are collected from highly fractured sandstone and limestone aquifers at lower altitudes around Wukro and Abi Adi, indicating fast groundwater flow.

Groundwater samples of Groups III and IV are located at similar altitude ranges (1695 to 2487 masl). Most samples in SG7 and SG8 of the HCA lay in Group III, and that of SG2 and SG6 lay in Group IV. They are dominantly from the Agula and upper Antalo formations and from dolerite. Some of the samples are collected from metasediments and clay dominated tillite aquifers. The difference in EC arises from the fact that the aquifers from which Group III (795 to 1390 µS/cm) samples collected are characterized by localized and shallow groundwater flow

systems adjacent to fracture zones, and hence probably lesser residence time. But they have relatively higher concentrations of Na^{+}, Ca^{2+}, Cl^{-} and SO_4^{2-} as compared to groups I and II, which is mainly related to the difference in solubility of their respective aquifer lithologies. Tesfamichael Gebreyohannes (2009) has also reported a similar variation of hydrochemical properties of the shallow groundwater with lithology in the Giba basin. Group IV samples are collected from locations where the groundwater recharge areas are extensively covered with thick shale and marl dominated units, and patchy gypsum layers are exposed in some outcrops and in lithologic logs. In these rock units, groundwater movement is slow, which jointly with the presence of soluble minerals enhance rock-water chemical interaction giving rise to the highest EC range (1575 to 2714 µS/cm) and concentrations of Na^{+}, Mg^{2+}, Ca^{2+}, Cl^{-} and SO_4^{2-}. The residence time of most samples in this Group IV must be different from Group III.

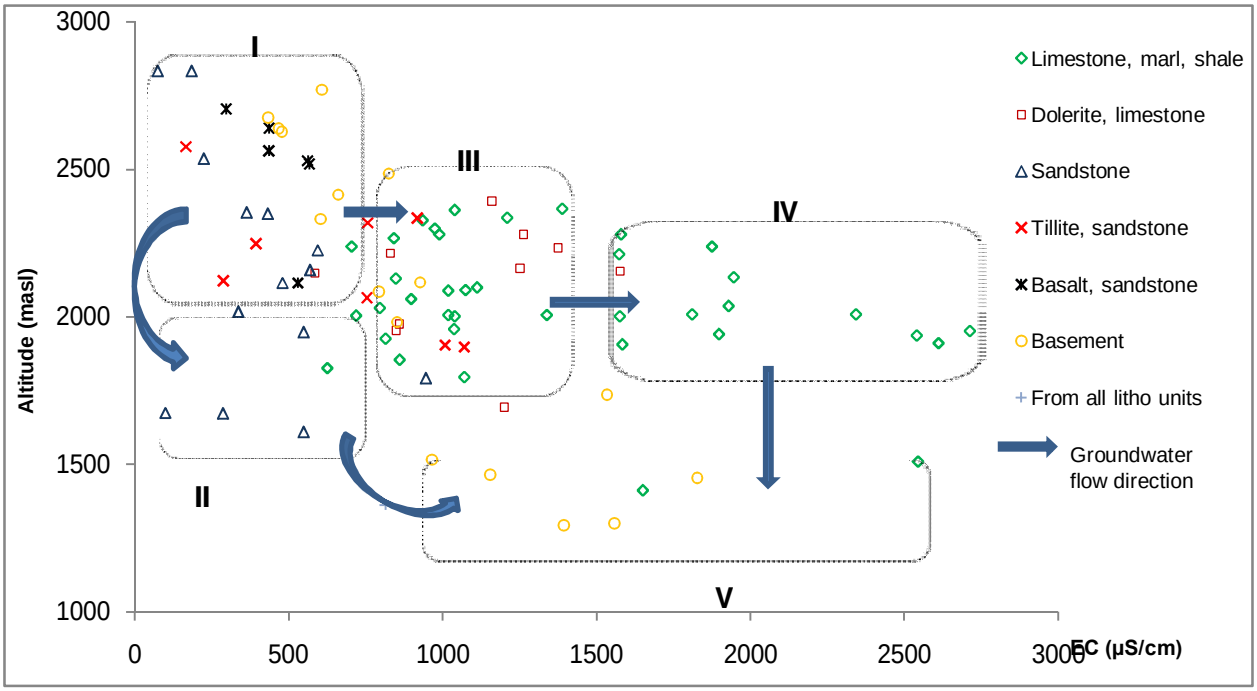

Fig 47 *Grouping of the groundwater based on the scatter plot of electrical conductivity of water samples from different lithological formations versus altitude*

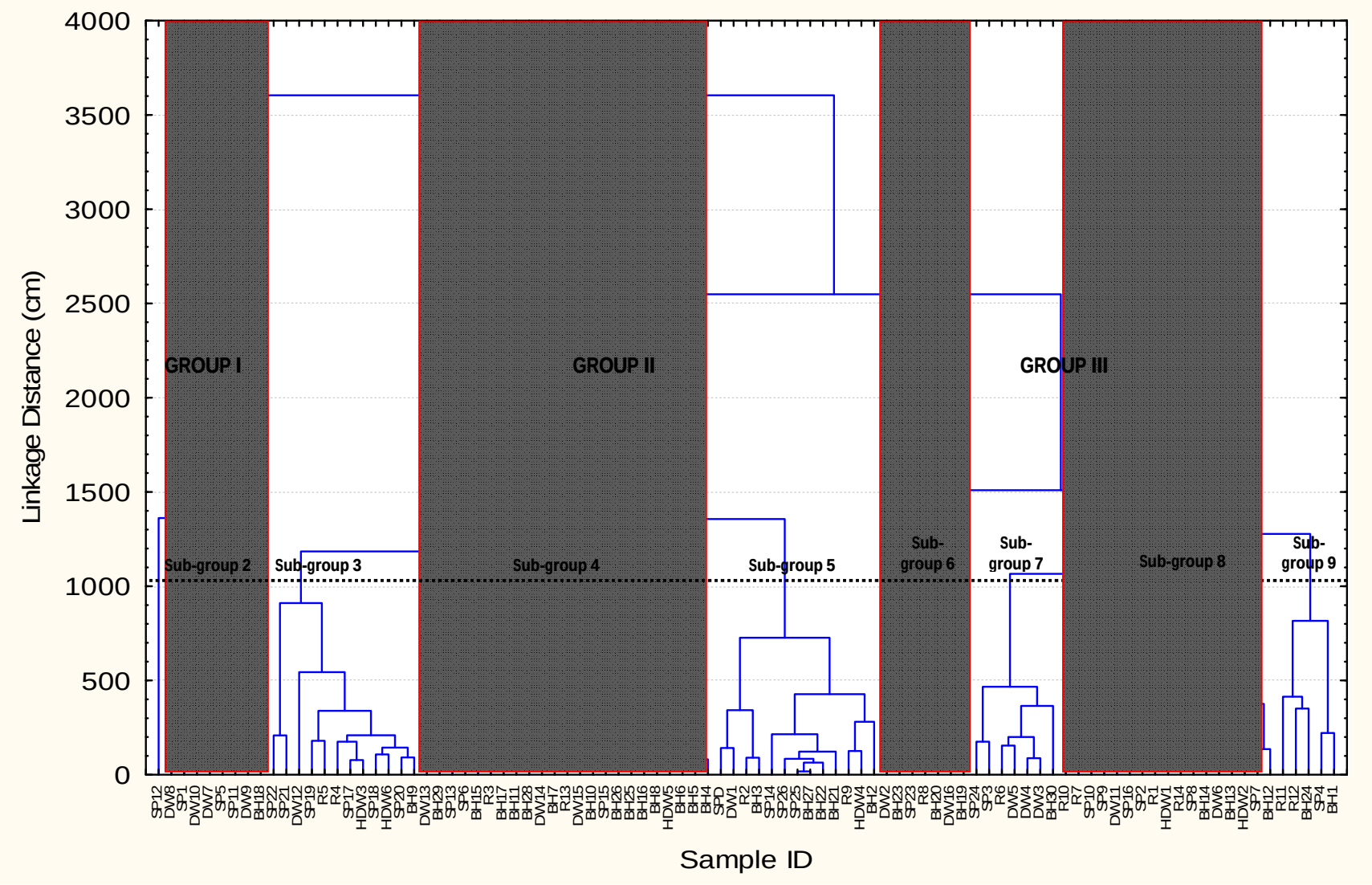

Fig 48 *Categorization of the winter water samples resulting from a preliminary HCA based on major ions chemistry, EC and altitude*

Table 6 Mean EC, mean major ions chemistry and major water types of the groundwater sub-groups from the HCA (unit for major ions concentration is mg/L)

Sub-group	Water type	EC (µS/cm)	Li^+	Na^+	K^+	Mg^{2+}	Ca^{2+}	F^-	Cl^-	NO_3^-	SO_4^{2-}	HCO_3^-
1	Ca-Mg-Na-SO_4	3121	0.20	257	9	207	358	0	308	61	1670	543
2	Ca-SO_4	2403	0.04	83	5	73	479	1	80	9	1547	319
3	Ca-Mg-HCO_3	641	0.00	29	2	23	80	1	24	21	38	377
4.1	Ca-Mg-HCO_3	860	0.00	37	2	32	102	1	38	26	96	451
4.2	Ca-Mg-HCO_3	495	0.00	18	2	17	67	0	17	14	29	280
5	Ca-Mg-HCO_3	380	0.00	16	1	18	54	0	12	11	23	249
6	Ca-SO_4-HCO_3	1697	0.07	63	3	61	310	1	73	14	950	357
7	Ca-SO_4-HCO_3	1370	0.01	42	3	41	256	1	36	9	648	395
8	Ca-Mg-HCO_3-SO_4	1047	0.01	41	3	34	158	1	43	34	294	397
9	Ca-Mg-Na-HCO_3-SO_4	1179	0.00	90	3	53	122	1	82	84	234	411

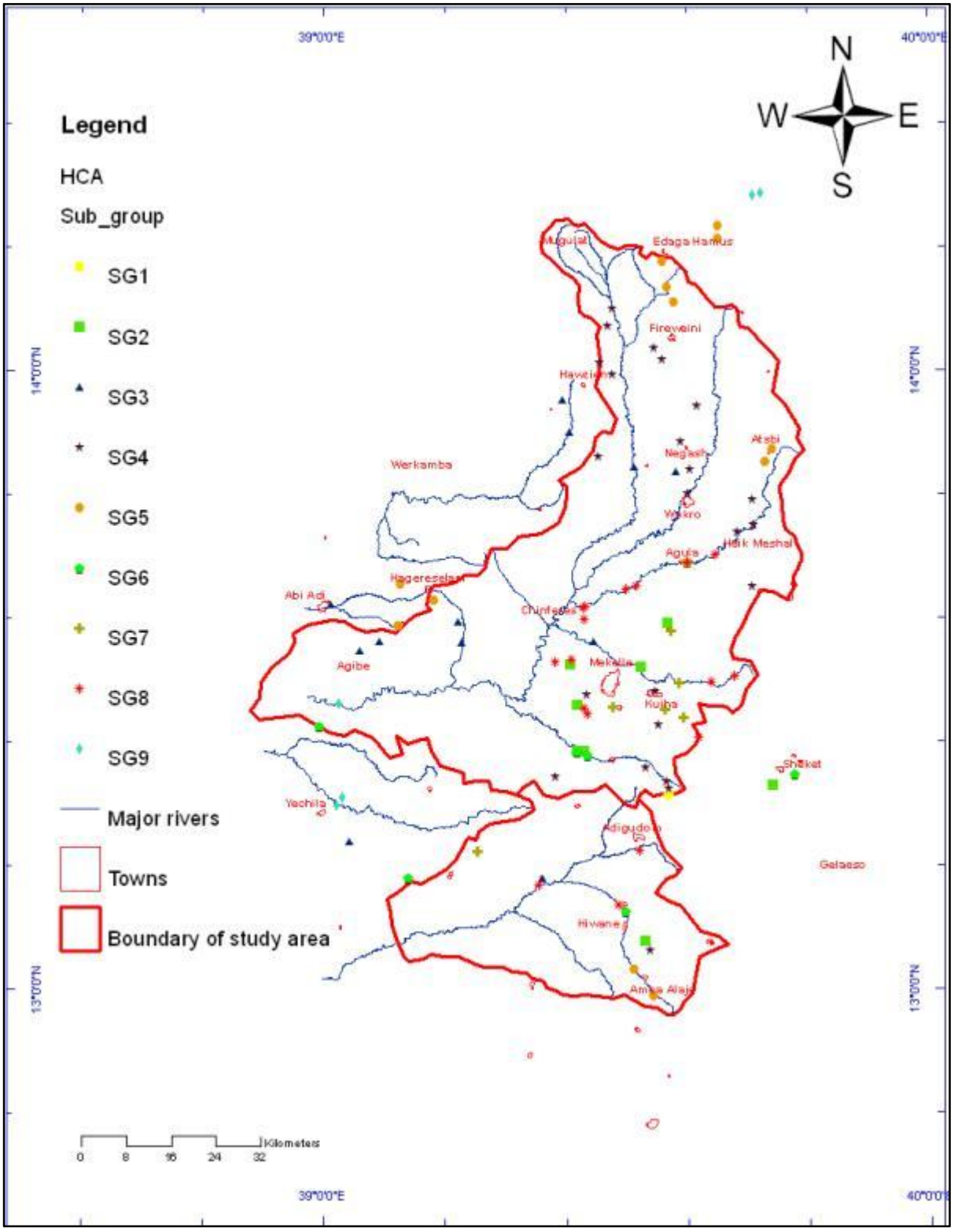

Fig 49 *Spatial distribution of the groundwater sub-groups from the HCA*

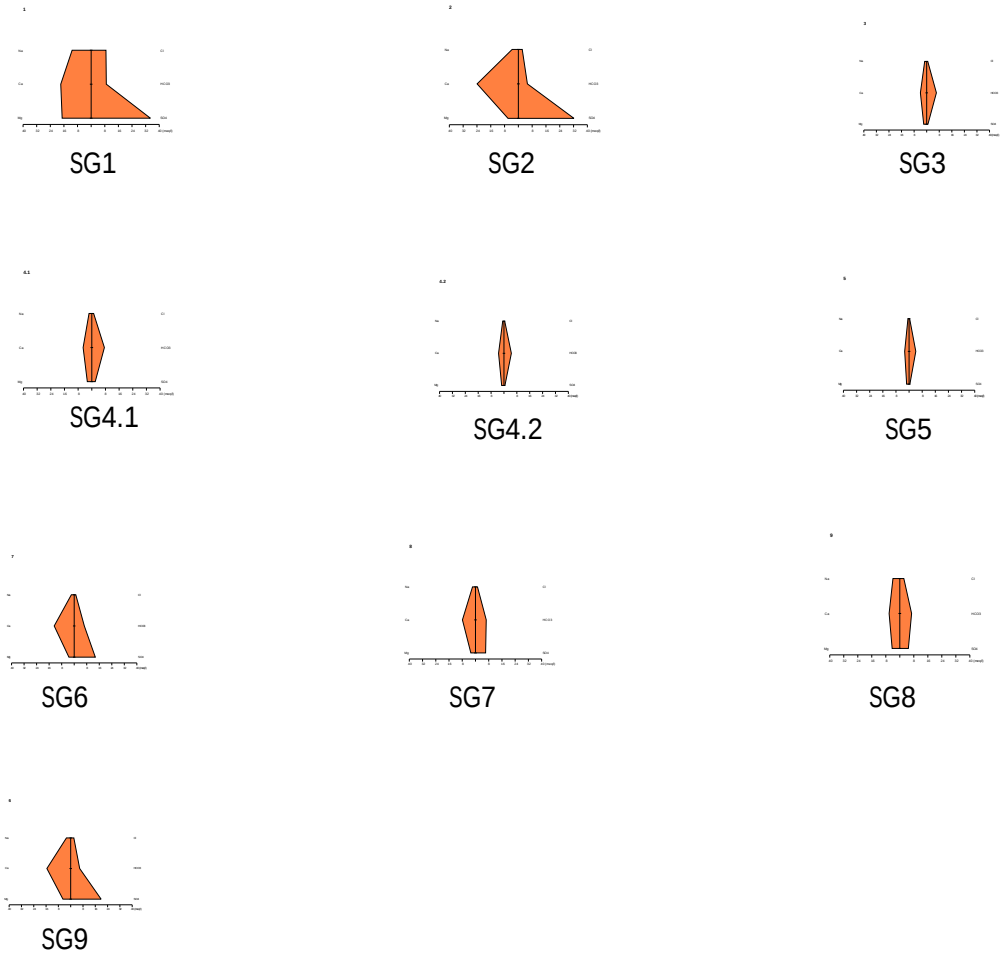

Fig 50 *Stiff diagram of groundwater sub-groups from the HCA*

The water samples of Group V (SG9 of the HCA) are collected from the lowland areas (below 1500 masl) towards the west and east of the study area. They are characterized by high concentrations of Na^{+}, Mg^{2+} and Cl^{-}. The EC values of the groundwater samples within this group are between 967µS/cm and 2546 µS/cm and increases towards the center of the Afar depression, where salt mining and potash deposits are evident. This indicates that deep groundwater circulation and higher residence time of groundwater is expected towards the center of the Denakil basin.

7. Indications from static water level data

The static water level data from spring locations and some measured wells were compiled mainly from pre-existing information (Ministry of Water Resources, 1998; DH-consult 2010; Tigray Water Works Enterprise, 2013) and a groundwater level map is produced (*Fig 51*). The springs that are found at different elevation levels emerge from different lithologic formations in the stratigraphy. The d-excess distribution map in the area (*Fig 53*), which shows high d-excess in the highland and progressively lower d-excess towards the lowland areas, is also presented in this section for comparison. From both maps (*Fig 51, 52 and 53*), it can be observed that the regional groundwater flow have similar pattern as the flow of the major rivers in the study area and the groundwater divide more or less coincides with the surface water divide between the Tekeze River basin and the Denakil basin. Here, it should be noted that the interpretations from the geological, environmental isotopes and electrical conductivity data in the above sections of this paper have similar indications.

8. Groundwater flow systems

The lithostratigraphic, geomorphologic, isotopic and hydrochemical settings observed have indicated that three groundwater flow systems (shallow/local, intermediate and deep/semi-regional) can exist in the study area. The shallow groundwater flow is mainly localized to the highland plateau areas and its water table is a subdued replica of the surface topography. The shallow groundwater system is generally characterized by lower concentrations of dissolved ions (except in perched conditions and encountered lenses of gypsum in the Agulae shale and Edaga Arbi Tillites), depletion in heavy isotopes and higher d-excess. The Neoproterozoic basement terrains, Paleozoic glacial sediments, dolerites, basaltic highlands and the Agula Shale Formation

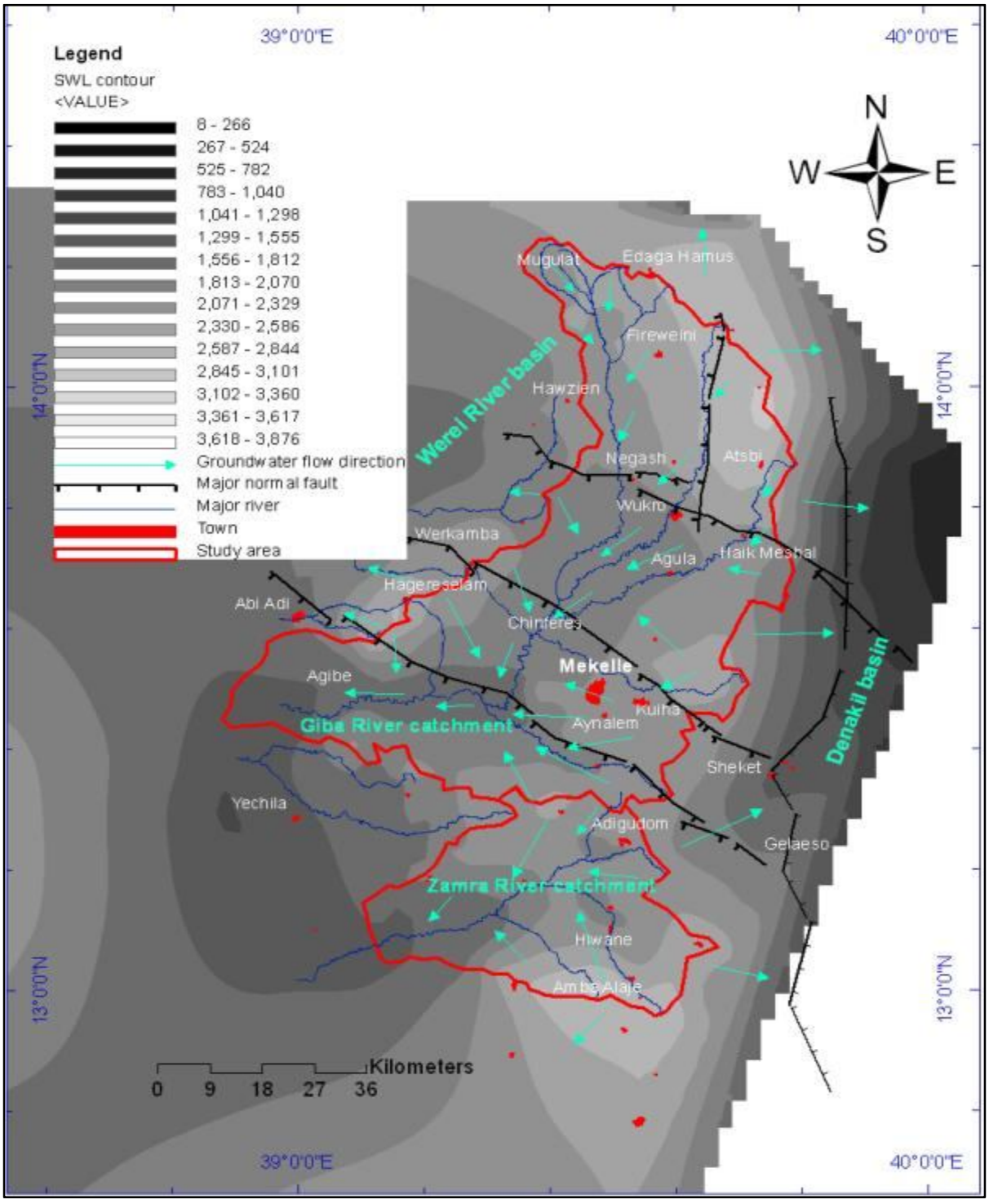

Fig 51 *Groundwater level map and groundwater flow directions based on spring positions and static water levels (SWL) in wells (Note: SWL values are in masl and they decrease from light gray regions towards the dark gray regions)*

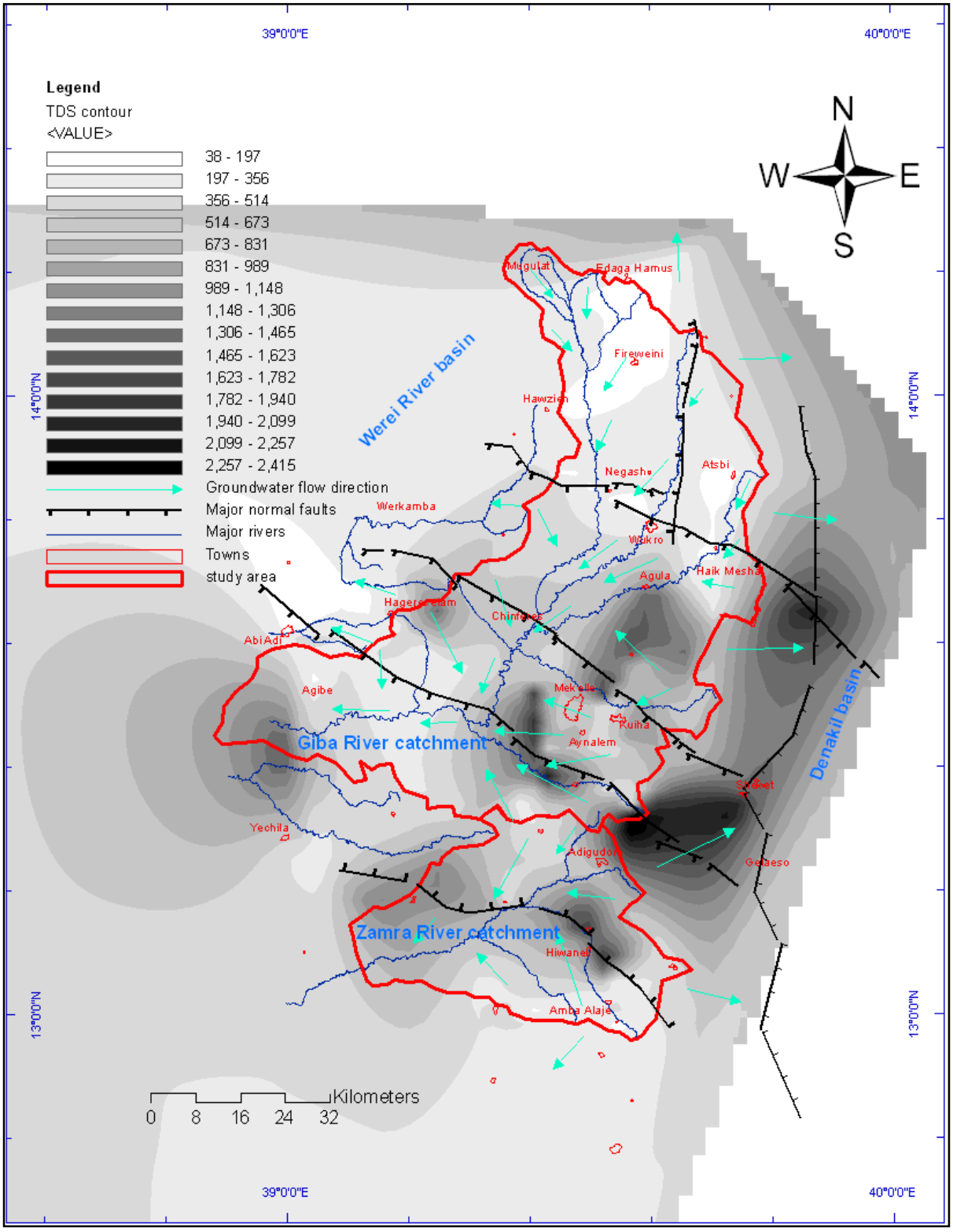

Fig 52 *Shaded total dissolved solids distribution map*

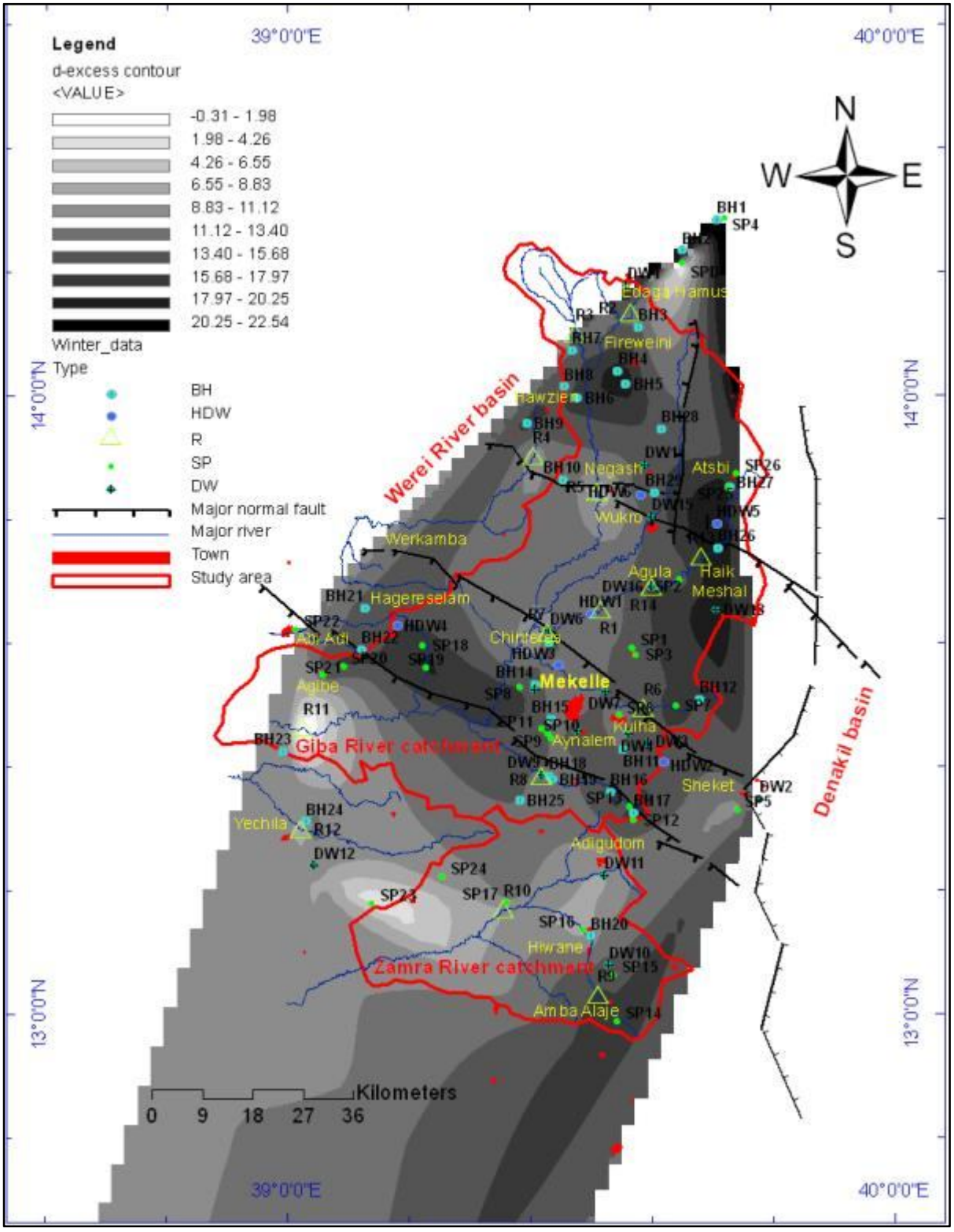

Fig 53 *Shaded Contour map of d-excess in the study area*

are mainly characterized by localized groundwater flow systems and unconfined aquifer conditions. Significant part of the groundwater in these formations is discharged to rivers (in the form of baseflow) and contact springs within the highland plateau and its margins with the narrow valleys that truncate the plateau.

The intermediate and deep groundwater flow is strongly influenced by the lithostratigraphy and major faults in the area rather than by the surface geomorphology. The intermediate groundwater flow in the Upper part of Antalo Limestone Formation has relatively higher dissolved ions concentration, relatively enriched in heavy isotopes and lower d-excess. This flow system is partly discharged to the rivers/springs in the western lowland reaches of the major rivers, where the upper part of this formation is truncated by erosion.

The deeper semi-regional aquifers are identified within the lower Antalo Limestone and the Adigrat Sandstone Formation. As these aquifers are covered (in most parts of the study area) with a thick pile of the upper stratigraphic formations, only few and scattered isotopic and hydrochemical data from areas where they are brought to the surface due to faulting and erosion gave important clues about the existence of this deep groundwater circulation. The geometry of these deep aquifers shown on the geological map and cross-sections also indicate about the lithostratigraphic and structural controls on this deep groundwater flow system.

Generally, the groundwater within these aquifers flows in the SSW direction under confined conditions. This deeper groundwater gets localized recharged through the deep seated fractures adjacent to the major faults in the highland plateaus and discharges mainly in the form of high discharge springs and baseflow in the western lowland sections of the Giba and Faucia Mariam rivers, and finally joins the Tekeze River. Only a small proportion of it percolates down to the

fractured Paleozoic glacial sediments and the fractured upper part of the basement rocks. These lower most rock formations have much lower permeability. However, it is recommendable here that further study and additional data on these deep aquifers is still necessary in order to cross check the interpretations forwarded by this study and/or to get more supportive information.

9. Conclusion

In this research work, the previous geological and hydrogeological knowledge of the area has been reviewed and new information from the field, satellite images, well lithologic logs and geophysical data are employed to modify previous geological maps and construct new geological cross-sections. These data are interactively used with the isotopic signatures ($\delta^{18}O$, $\delta^{2}H$ and tritium), patterns of dissolved-ion concentrations and groundwater-level data to (1) identify recharge and discharge areas and the groundwater divide between the Tekeze and Denakil basins, (2) see the groundwater/surface-water interactions and (3) conceptualize the overall groundwater flow system in the study area.

More than 60% of the study area is covered with sedimentary rocks. These Mesozoic sedimentary rocks, belonging to marine and continental facies (from top to bottom: Amba Aradem Sandstone, Agula Shale, Antalo Limestone and Adigrat Sandstone) and the underlying inter-fingered Paleozoic glacial sediments (Edaga Arbi Tillites and Enticho Sandstone) form the Mekelle sedimentary outlier. It is surrounded to the north, northeast and west by the basement rocks and to the south by the Tertiary flood basalts. In the east it is truncated by the normal faults of the Afar rift margin, resulting to intermountain graben and horst structures until the crystalline rocks appear again close to the center of the rift. The Negash Geosynclinal Fold and associated plutonic intrusion; the Wukro, Mekelle, Chelekot and Fucea Mariam fault belts; and the dolerite

sills and dykes around Mekelle town are some among the megascopic geological structures in the area.

The dominant orientations of joint sets are NNE and WNW. The joints in the older rocks (Basement, Adigrat Sandstone and Paleozoic sediments) trend more dominantly in the WNW direction parallel to the major Mesozoic extensional faults of the study area which indicates that they have older genesis related to the break-up of the Afro-Arabian plate (age) (opening of the Red Sea Rift and Gulf of Aden). Whereas the NNE orientation of the other joint set is dominantly found in almost all rocks formations of the area including the youngest Cretaceous flood basalts. Cross cutting relationship shows that they are the youngest. They are therefore genetically related to the extensional rifting of the East African Rift system (Afar Rift). These two major joint orientations are nearly orthogonal to each other.

Intensity of fracturing and disturbance of rock mass are higher close to the major faults of the area where joints, fractures, dissolution cavities and bedding planes are observed to be more open for groundwater accumulation and flow. Localized groundwater recharge occurs along the highly fractured and dipping sedimentary beds (drag folds) adjacent to these major faults. This creates confined aquifers and artesian conditions along the axes of the drag folds because of higher hydraulic heads in the dipping beds and the confining units (shale and marl intercalation within the sedimentary sequence).

The basement rocks, glacial deposits and dolerites in the study area are characterized by shallow and localized aquifers mostly associated with faults and shear zones. Boreholes drilled into these rock formations have well yields mostly less than 5 L/s. In the basement rocks, weathering and

fracturing are generally more intense at shallow depths but become rarer with depth. The thickness of the fractured zones ranges from 12-60m.

The poorly sorted and unstratified nature of the Edaga Arbi tillite results in only local accumulation and slow rate of groundwater flow and recharge. Springs from this unit has less discharges hardly exceeding 2 lit/sec. Hand dug wells and shallow tube wells (8-70m depth) have seasonaly fluctuating discharges. During the rainy months they discharge as high as 3-8 lit/sec but they may even dry out at the mid or late months of the dry season.

The Enticho Sandstone ussualy forms Mesa strusctures that stand here and there in the northern part of the study area. There are points of higher discharge (2-5 lit/sec) and perennial contact/fault springs at the feet of these Mesa structures. Tube wells (35-90m depth) drilled into this fomation has discharges of 3-7 lit/sec. But its storage capacity is low because of high permebility nature of the course and well sorted sediments and therefore mainly serves as temporary groundwater storage with less residence time and as a recharge zone to the undelying fractured basement rocks. It is also noted that the Enticho sandstone is some times found interfinged with Tillite beds resulting in perched aquifers.

The upper part of the Mesozoic sedimentary sequence (the whole Agula Shale and the upper part of Antalo Limestone) is dominated with shale and marl units although gypsum and thin beds of marl and limestone are also minor constituents found as intercalation. It is mostly intruded by dolerite sills and to a lesser extent dolerite dykes. Although it is affected by intense joints, the groundwater occurrence and flow in this upper part of the sedimentary section is limited due to clay dominated lithology. Wells and springs have low discharge hardly exceeding 2 L/s. But at the contact zones with the dolerite intrusions, boreholes that discharge 12-40 L/s are common.

Whereas the Adigrat Sandstone and the lower part of Antalo Limestone are characterized by extensive/semi-regional aquifers with boreholes' yield ranging 10-60 L/s.

Most of the higher yield boreholes and perennial and high discharge springs are located close to the major faults and associated lineaments of the area and at the contacts between the Mesozoic sedimentary rocks and the Mekelle dolerite. Based on limited data of transmissivity of aquifers, there is a clue that higher transmissivity values are more frequent close to the major faults of the area. But there are also cases where adjacent deep wells (< 1.5 Km apart) drilled into the Adigrat Sandstone and Agula/Antalo formation on opposite sides of faults close to the Wukro and Mekelle fault belts show significantly differing hydraulic properties. These faults brought the Adigrat Sandstone and Agula Shale to be found adjacent to each other on the surface. And the wells drilled into the Adigrat formation are characterized by higher well yields (>50 L/s) and transmissivity values (around 400 m^2/day) while those on the Agula Shale indicate much lower well yields (< 3 L/s) and transmissivity values (< 3 m^2/day) regardless of their close location to the major faults of the area.

Based on the piezometric map, along with the relatively more depleted isotopic compositions, higher d-excess, and lower dissolved-ion concentrations of the groundwater samples, the highland areas (northwest, north, east and south of the study area) are characterized as recharge areas, while the narrow major river valleys of Giba, Illala, Chelekot and Fucea Mariam are found to be discharge areas.

Most groundwater samples from the area lay close to the Addis Ababa LMWL indicating meteoric origin. Slight shifts of some samples from this line are attributed to the altitude effect and the isotopic exchanges of rain droplets with the local air mass that have different isotopic

composition (more depleted and higher d-excess) from that of Addis Ababa. This effect also seen in a smaller slope of the LMWL of the study area ($\delta^2H = 6\times\delta^{18}O + 9.8$; $R^2 = 0.8$) that is plotted based on samples from the deep groundwater of the study area. The equation for the evaporation line for the area is $\delta^2H = 4.47\delta^{18}O + 6.42$; $R^2 = 0.8$. A depletion rate of -0.51 ‰/100m for the $\delta^{18}O$ has been observed from the shallow groundwater at different altitudes. In most cases, groundwater feeds the semi-perennial streams and rivers in the area. But isotopic signatures in some wells indicate that there are localities where river flow and seepage from micro-dams locally feed the adjacent aquifers.

Double isotopic measurement of groundwater samples from wells in the summer and dry seasons show that there is a significant amount of shallow (perched) subsurface flowing water that is pumped in wells during the summer season. This interflow (throughflow) disappears shortly after the rainy season passed because it is mostly discharged to springs and rivers in the form of baseflow and partly percolates down to the deeper aquifers in downstream areas.

Five groundwater groups have been identified from the EC – altitude – lithology cross plot. A similar pattern of categories is also identified from a preliminary hierarchical cluster analysis (HCA) based on major-ion chemistry (Li^+, Na^+, K^+, Mg^{2+}, Ca^{2+}, HCO_3^-, SO_4^{2-}, Cl^-), EC and altitude of the water samples collected in this study. Group I samples are collected from basalt, sandstone, tillite (sand dominated), dolerite and metavolcanic rock aquifers in the highland areas of Atsbi, Hawzien, AmbaAlaje and HagereSelam are characterized by low EC (76 to 705 µS/cm) and low concentration of all the major ions. Group II samples with a similar lower EC (99 to 719 µS/cm) and low concentrations of all the major ions are collected from highly fractured sandstone and limestone aquifers at lower altitudes around Wukro and Abi Adi.

Group III and Group IV samples are collected from from the Agula and upper Antalo formations and at their contact with dolerite. They are characterized by high EC values. The aquifers from which Group III (795 to 1390 μS/cm) samples collected are characterized by localized and shallow groundwater flow systems adjacent to fracture zones, and hence probably lesser residence time. But they have relatively higher concentrations of Na^{+}, Ca^{2+}, Cl^{-} and SO_4^{2-} as compared to groups I and II, which is mainly related to the difference in solubility of their respective aquifer lithologies. Group IV samples are collected from locations where the groundwater recharge areas are extensively covered with thick shale and marl dominated units, and patchy gypsum layers are exposed in some outcrops and in lithologic logs. In these rock units, groundwater movement is slow, which jointly with the presence of soluble minerals enhance rock-water chemical interaction giving rise to the highest EC range (1575 to 2714 μS/cm) and concentrations of Na^{+}, Mg^{2+}, Ca^{2+}, Cl^{-} and SO_4^{2-}. The residence time of most samples in this Group IV must be different from Group III.

The water samples of Group V (SG9 of the HCA) are collected from the lowland areas (below 1500 masl) towards the west and east of the study area. They are characterized by high concentrations of Na^{+}, Mg^{2+} and Cl^{-}. The EC values of the groundwater samples within this group are between 967μS/cm and 2546 μS/cm and increases towards the center of the Afar depression, where salt mining and potash deposits are evident. This indicates that deep groundwater circulation and higher residence time of groundwater is expected towards the center of the Denakil basin.

The lithostratigraphic, geomorphologic, isotopic and hydrochemical settings observed in this study have indicated that three groundwater flow systems (shallow/local, intermediate and deep/semi-regional) can exist in the study area. The highland plateau which is covered by the

Neoproterozoic basement terrains, Paleozoic glacial sediments, dolerites, basaltic highlands and the Agula Shale Formation is characterized by shallow groundwater flow with lower concentrations of dissolved ions (except in perched conditions and encountered lenses of gypsum in the Agulae shale and Edaga Arbi Tillites), depletion in heavy isotopes and higher d-excess. The intermediate groundwater flow in the Upper part of Antalo Limestone Formation has relatively higher dissolved ions concentration, relatively enriched in heavy isotopes and lower d-excess. And indications of the deeper semi-regional aquifers are identified within the lower Antalo Limestone and the Adigrat Sandstone Formation.

The groundwater divide between the Tekeze and the Denakil basins for all the three flow systems coincides with the surface water divide line of these two basins (i.e. the eastern boundary of the study area represents the groundwater divide line between the basins). Within the Denakil basin the regional groundwater flow in the lower-most Mesozoic sediments is in the ESE direction.

Tritium data indicate that the groundwater in the study area has generally short residence time and is highly dependent on modern precipitation. The range observed in the study area (1.73 to 3.66 TU) indicates components of pre- and post-1952 recharge. The ages of young groundwaters like in the study area can be more precisely determined by using a suit of tracers such as tritium, noble gasses (including tritium/^{3}He dating and ^{39}Ar), chlorofluorocarbons (CFCs), and sulphur hexafluoride (SF_6). Measurement of ^{14}C can also be required for groundwaters from the central part of the Denakil Depression. Future sample collection strategy for this dating purpose should consider sampling from wells screened only in target aquifers, from systematically selected springs, river points based on expected groundwater flow directions and from rainfalls in different altitudes along selected transects.

Reference

Abdelwassie Hussein (2000). Hydrogeology of the Aynalem well field. Unpublished M.Sc. Thesis, Addis Ababa University, Ethiopia. 103 pp.

Aggarwal, P.K., Froelich, K., Gonfiantini, R., Gat, J.R. (2005). Isotope hydrology: a historical perspective from the IAEA. In: Aggarwal, P.K., Gar, J.R., Froelich, K.F.O. (eds). Isotopes in the water cycle: past, present and future of a developing science. *Springer*, Berlin, 381 pp.

Andarge Yitbarek (2002). Hydrogeological investigation of the Megech river basin. Unpublished M.Sc. Thesis. Addis Ababa University, Ethiopia.

Andarge Yitbarek, Razack, M., Tenalem Ayenew, Engida Zemedagegnehu, Tilahun Azagegn (2012). Hydrogeological and hydrogeochemical framework of Upper Awash River basin, Ethiopia: with special emphasis on inter-basins groundwater transfer between Blue Nile and Awash River. *J. Afr. Earth Sci.* 65:46–60.

Arkin, V., Beyth, M., Dow, D.B., Levitte, D., Haile, T. (1971). Geological Map of Mekele Sheet (ND 37-11). Ethiopian Institute of Geological Survey (E.I.G.S.), Addis Ababa, Ethiopia.

Begemann, F., Libby, W.F. (1957). Continental water balance, ground water inventory and storage times, surface ocean mixing rates and world–wide circulation patterns from cosmic-ray and bomb tritium. *Geochim. Cosmochim. Acta.* 12:277–296.

Belay Desta (1978). Preliminary regional geological report on the Dodola area (NB 37-7) 1:250,000 scale. Unpublished data, E.I.G.S., Addis Ababa, Ethiopia.

Beyth, M. (1972). The Geology of central and western Tigre. PhD Thesis, University of Bon, Germany, 155 pp.

Beyth, M., Avigad, D., Wetzel, H., Matthews, A., Berhe, S. (2003). Crustal exhumation and indications for Snowball Earth in the East African Orogen: north Ethiopia and east Eritrea. *Precambrian Research* 123: 187–201.

Beyth, M., Shachnai, E. (1970). Hydrogeology of Mekelle area. Ethiopian Institute of Geological Survey (E.I.G.S.), Addis Ababa, Ethiopia. 10 pp.

Boehmer, W.K., Boonstra, J. (1987). Analysis of drawdown in the country rock of composite dike aquifers. *J. Hydrol.* 94: 199–214.

Bossellini, A., Russo, A., Fantozzy, P.L., Getaneh Assefa, Solomon Tadesse (1997). The Mesozoic succession of Mekelle Outlier (Tigre Province, Ethiopia). *Mem. Sci. Geol.* 49:95–116 .

Bromley, J., Mannstrom, B., Nisca, D., Jamtlid, A. (1994). Airborne Geophysics: Application to a groundwater study in Botswana. *Ground Water* 32(1): 79–90.

Chorowicz, J., Collet, B., Bonovia, F.F., Mohr, P.A., Parrot, J.F., Tesfaye Korme (1998). The Tana basin, Ethiopia: Inter-plateau uplift, rifting and subsidence. *Tectonophysics* 295:351–367.

Clark, I.D., Fritz, P. (1997). Environmental isotopes in hydrogeology. Lewis, Boca Raton, F.L., 328 pp.

Cook, G., (2003). Groundwater flow in fractured rock aquifers. *CSIRO Land and Water*, Glen Osmond, S.A., Australia. 108 pp.

Craig, H. (1961). Isotopic variations in meteoric waters. *Sci.* 133:1702–1703. doi:10.1126/science.133.3465.1702.

Dainelli, G. (1943). Geologia dell'Africa Orienta, Vol.4. Reale Acc, Italia, Roma.

Daniel Gemechu (1977). Aspects of climate and water budget in Ethiopia. *Addis Ababa University Press.* 71 pp.

Davidson, A. (1983). Reconnaissance Geology and Geochemistry of parts of Illubabor, Kafa, GemuGofa and Sidamo, Ethiopia. E.I.G.S., Bull No.2, Addis Ababa, Ethiopia.

Darling, G.W., Birhanu Gizaw, Arusel, M.K. (1996). Lake-groundwater relationships and fluid-rock interaction in the East African Rift Valley: isotope evidence. *J. Afr. Earth Sci.* 22:423–431.

Dereje Ayalew (2011). The relations between felsic and mafic volcanic rocks in continental flood basalts of Ethiopia: implication for the thermal weakening of the crust. Geological Society, London, Special Publications 357:253-264. doi:10.1144/SP357.13.

DH Consult (2010). Groundwater resources potential assessment of the Mekelle Outlier. Unpublished Phase II Report. Ministry of Water Resources, Addis Ababa, Ethiopia. 153 pp.

Dow, D.B., Beyth, M., Tsegaye Hailu (1971). Paleozoic glacial rocks recently discovered in northern Ethiopia. *Geol. Mag.* 108(1):53–60, Great Britain.

Engels, G.G. (1966). Mesozoic Stratigraphy of Northern Ethiopia. Mobilr Petrol. Ethiopia, Inc., Rep. No. ETG-18, Asmara.

E.I.G.S./Ethiopian Institute of Geological Survey (1993). Hydrogeological map of Ethiopia, 1:2,000,000 scale. Ministry of Mines and Energy and Ethiopian Institute of Geological Survey (E.I.G.S.), Addis Ababa, Ethiopia.

E.I.G.S./Ethiopian Institute of Geological Survey (1996). Explanation of the Geological map of Ethiopia (Scale 1:2,000,000), 2nd edition. Ethiopian Institute of Geological Survey (E.I.G.S.), Addis Ababa, Ethiopia, 79 pp.

E.M.A./Ethiopian Mapping Agency (1999). National Atlas of Ethiopia. Ethiopian Mapping Authority (E.M.A.), Addis Ababa, Ethiopia.

Fetter, C.W. (1994). Applied Hydrogeology. Prentice–Hall, Inc., Englewood Cliffs, New Jersey, USA. 604 pp.

F.W.W.D.S.E./Federal Water Works Design and Supervision Enterprise (2007). Evaluation of Aynalem Well Fields around Mekelle Town for Water Supply Source, Unpublished Final Report, Volume II. Addis Ababa, Ethiopia. 147 pp.

F.W.W.D.S.E./Federal Water Works Design and Supervision Enterprise (2009). Groundwater resources of the Upper Tekeze basin: resource description, assessment and model. Unpublished Phase one report (Hydrogeology report). Addis Ababa, Ethiopia. 72 pp.

Garland, C.R. (1980). Geology of the Adigrat area. Ministry of Mines, Addis Ababa. *Memoir*, No. 1. 51 pp.

Geukens, F. (1966). Geology of Arabian Peninsula-Yemen. *Geol. Surv. Prof. Paper*. 560-B, 23 pp. Washington.

Gibson, J.J., Edwards, T.W.D., Birks, S.J., St Amour, N.A., Buhay, W.M., McEachern, P., Wolfe, B.B., Peters, D.L. (2005). Progress in isotope tracer hydrology in Canada. *Hydrol Process* 19:303–327. doi: hyp.217/hyp.5766.

Griffiths, J. F. (1972). Climates of Africa. In: Griffiths, J.F. (Ed.), World Survey of Climatology. *Elsevier*, Amsterdam.

Gudmundsson, A., Gjesdal, O., Brenner S.l. (2003). Effects of linking up of discontinuities on fracture growth and groundwater transport. *Hydrogeol. J.* 11:84–99. *doi:10.1007/s10040-002-0238-0*.

Hailemichael G (2004). Study on groundwater and requirements for drilling and other systems tapping groundwater in Ethiopia (UNESCO study). Paper presented to the international conference and exhibition on groundwater in Ethiopia, 25-27 May 2004, Addis Ababa,

Ethiopia.

Hoefs, J. (2009). Stable isotope geochemistry. 6th Edition. *Springer*. Verlag, Berlin. 285 pp.

Hunkeler, D., Aravena, R., Butler, B. (1999). Monitoring microbial dechlorination of tetrachloroethene (PCE) in groundwater using compound-specific stable carbon isotope ratios: microcosm and field studies. *Environ. Sci. Technol.* 33:2733–2738.

Hutchinson, R.W. and Engels, G.G. (1970). Tectonic significance of regional geology and evaporite lithofacies in northereastern Ethiopia. Phil. Trans. Roy. Soc. London, A. V. 267:313-329.

IAEA/International Atomic Energy Agency (2011). Hydrogeology of the Nile Basin in Ethioipia, Review article. In press. International Atomic Energy Agengy, Addis Ababa, Ethiopia, 76 pp.

IWMI, Intenational Water Management Institute (2009). Overview of the groundwater resources and its use for the Nile Basin in Ethioipia, Review article. International Water Management Institute, Addis Ababa, Ethiopia.76 pp.

Jestin, F., Huchon, P. (1992). Cine´matique et de´formation de la jonction triple Mer Rouge-Golfe d'Aden-Rift Ethiopien depuis l'Oligoce`ne. *Bull. Soc. Geol. Fr.* 163:125–133.

Kazmin, V., 1972. The Geology of Ethiopia. Unpublished Report, E.I.G.S., Addis Ababa, Ethiopia.

Kazmin, V. (1975). Explanatory note to the Geology of Ethiopia. EIGS, *Bull No.2*, Addis Ababa, Ethiopia.

Kazmin, V. (1979). Stratigraphy and correlation of volcanic rocks of Ethiopia. E.I.G.S., Note number 106:1-26.

Kendall, C., Coplen, T.B. (2001). Distribution of oxygen-18 and deuterium in river waters across the United States. *Hydrol. Process* 15:1363–1393. doi:hyp.217/hyp.217.

Kieffer, B., Arndt, N., Lapierre, H., Bastien, F., Bosch, D., Pecher, A., Gezahegn Yirgu, Dereje Ayalew, Weis, D., Jerram, D.A., Keller, F., Meugniot, C. (2004). Flood and shield basalts from Ethiopia: Magmas from the African Superswell. *J. Petrol.* 45:793–834.

Kukillaya, J.P., Kunhi, A.M., Abdul Rahman, A.K. (1992). Basic and ultrabasic dykes as potential aquifers in hard rock terrains. *Bhu-Jal News.* 7(4): 14–19.

Kuster, D., Dwivedi, S.B., Kurkura Kabeto, Mehari k, Matheis, G. (2005). Petrograhic reconnaisance investigation of mafic sills associated with flood basalts, Mekelle basin, Northern Ethiopia: Implications for Ni-Cu Exploration. *J. Geochem. Exp*. 85:63–79 .

Matter, J., Morin, R. Goldberg, D., Stute, M., (2006). Contact zone permeability at intrusion boundaries: new results from hydraulic testing and geophysical logging in the Newark Rift Basin, New York, USA. *Hydrogeol. J.* 14:689–699.

Meert, J.G. (2003). A synopsis of events related to the assembly of eastern Gondwana. *Tectonophysics* 362: 1-40.

Menzies, M.A., Baker, J., Bosence, D., Dart, C., Davidson, I., Hurford, A., Al'Kadasi, M., McClay, K., Nichols, G., Al'Subbary, A., Yelland, A. (1992). The timing of magmatism, uplift and crustal extension: preliminary observations from Yemen. In: Storey, B.C., Alabaster, T., Pankhurst, R.J. (Eds.), Magmatism and the Causes of Continental Break-Up. Spec. Publ. - Geol. Soc. Lond., vol. 68, pp. 293 – 304.

Merla, J.G. and Munucci (1938). Missione geologica nel Tigrai, *Reale Accademia d'Italia*, Rome.

Merla, G., Abate, E., Azzaroli, A., Bruni, P., Fazzuoli, M., Sagri, M. (1979). Comments to the Geological map of Ethiopia and Somalia. *Consiglio Nazionaledeelle Ricerche*. 95pp, Frenze.

Mohr, P.A. (1962). The Geology of Ethiopia. Univ. Coll. of Addis Ababa Press (reprinted in 1971 at the Haile Silassie I University Press). Addis Ababa, Ethiopia. 268 pp.

Mohr, P.A. (1983). Ethiopian flood basalt province, review article. *Nature* 303:577-585, Department of Geology, University College Galway, Ireland.

Mohr, P.A., Zanettin, B. (1988). The Ethiopian flood basalt province. In: Macdougall, J. D. (Ed), Continental Flood Basalts. Kluwer, Dordrecht, pp. 63–110.

Molla Demilie, Wohnlich, S., Birhanu Gizaw, Stichler, W. (2006). Groundwater recharge in the Akaki catchment, Central Ethiopia: Evidence from environmental isotopes ($\delta^{18}O$, $\delta^{2}H$ and ^{3}H) and chloride mass balance. *Hydrol. Process* 21:807–818.

Molla Demilie, Wohnlich, S., Wisotzky, F., Birhanu Gizaw (2007). Groundwater recharge, flow and hydrochemical evolution in complex volcanic aquifer system, Central Ethiopia. *Hydrogeol. J.* 15:1169–1181 .

Molla Demlie, Wohnlich, S., Tenalem Ayenew (2008). Major ion hydrochemistry and environmental isotope signatures as a tool in assessing groundwater occurrence and its dynamics in a fractured volcanic aquifer system located within a heavily urbanized catchment, central Ethiopia. *J. Hydrol.* 353:175–88.

Moser H, Stichler W (1971) Die Verwendung des Deuterium und Sauerstoff-18 Gehalts bei Hydrologischen Untersuchungen. Geol. Bavarica 64:7–35

Mulugeta Alene (1998). Tectonomagmantic evolution of the Neoproterozoic rocks of the Mai Kenetal-Negash area, northern Ethiopia. PhD Thesis, University of Turin.

Mulugeta Alene, Jenkin, G.R.T., Leng, M.J., Darbyshire, D.P.F. (2006). The Tambien Group, Ethiopia: An early Cryogenian (ca. 800-735 Ma) Neoproterozoic sequence in the Arabian-Nubian Shield. *Precamberian Research* 147:79–99.

Mulugeta Alene, Ruffini, R., Sacchi, R. (2000). Geochemistry and Geotectonic setting of Neoproterozoic rocks from northern Ethiopia (Arabian-Nubian Shield), *Gondwana Res.* 3:333–347.

Mulugeta Alene and Sacchi, R. (2000). The Neoproterozoic low-grade basement of Tigrai, northern Ethiopia. Abstact: 18th Colloquium of African Geology, Graz. *J. Afr. Earth Sci.* 30 (4):5–6.

MWR/Ministry Water Resources (1998). Tekeze River Basin integrated development master plan project. Unpublished Sectoral Reports. Ministry of Water resources-Netherlands Engineering Consultants. Addis Ababa, Ethiopia.

Nata Tadesse (2003). Hydrogeological investigation and environmentally sound plans for the development of groundwater in the Werei River basin, Tigray, Ethiopia. Ph.D. Thesis, University of Natural Resources and Applied Life Sciences, Department of Applied Geology, Vienna, Austria.

Nata Tadesse, Miruts Hagos (2010). Geological and Structural Investigation: A Case Study on the Groundwater Potential Assessment in the Hantebet Catchment (Southern Mekelle, Tigray Region) (in press). Mekelle University, Mekelle, Ethiopia.

Neumann, E., Planke, S., and Malthe-Sørenssen, A. (2003). Emplacement mechanisms and magma flow in sheet intrusions in sedimentary basins. *Physics of Geological Processes*, University of Oslo, Norway.

Newman, B.D., Osenbrück, K., Aeschbach-Hertig, W., Solomon, D.K., Cook, P., Różański, K., Kipfer, R. (2010). Dating of 'young' groundwaters using environmental tracers: advantages, applications, and research needs. *Isot. Environ. Health Stud.* 46(3):259–278. doi:10.1080/10256016.2010.514339.

Pik, R., Deniel, C., Coulon, C., Gezahegn Yirgu, Hoffman, C., Dereje Ayalew (1998). The northwestern Ethiopian plateau flood basalts, Classification and spatial distribution of magma types. *J. Volc. and Geother. Res.* 81:91–111.

Rietti-Shati, M., Yam, R., Karlen, W., Shemesh, A. (2000). Stable isotope composition of tropical high-altitude fresh-waters on Mt. Kenya, Equatorial East Africa. *Chem. Geol.* 166:341–350.

Rochette, P., Endale T, Feraud, G., Pik, R., Courtillot, V., Endale Ketefo, Coulon, C., Hoffmann, C., Vandamme, D., Gezahegn Yirgu (1998). Stratigraphy and timing of the Oligocene Ethiopian traps. *Earth and Planetary Science Letters* 164:497–510.

Rozanski, K., Araguas-Araguas, L. (1995). The spatial and temporal variability of stable isotope composition of precipitation over the South American continent. In: Seifu Kebede, Travi, Y. (2012). Origin of the $\delta^{18}O$ and $\delta^{2}H$ composition of meteoric waters in Ethiopia. *Quatern. Int.*, 257:4–12.

Samuel Yihdego (2003). Hydrogeological Assessment of the Ellala-Aynalem Catchments with Particular Reference to the Chemical Variation and Aquifer Characterization, Northern Ethiopia. Unpublished M.Sc. thesis, Addis Ababa University, Ethiopia. 183 pp.

Sanford, W.A., Aeschbach-Hertig, W., Andrew, L., Herczeg, A.L. (2011). Insights from environmental tracers in groundwater systems. *Hydrogeol. J.* 19:1–3.

Schmidt, T.C., Zwank, L., Elsner, M., Berg, M., Meckenstock, R.U., Haderlein, S.B. (2004). Compound-specific stable isotope analysis of organic contaminants in natural environments: a critical review of the state of the art, prospects and future challenges. *Anal. Bioanal. Chem.* 378:283–300.

Seifu Kebede (2004). Vertical electrical sounding for groundwater exploration in volcanic terrain of central and North-Western Ethiopia. International conference and exhibition on groundwater, Addis Ababa, Ethiopia.

Seifu Kebede (2004). Approches isotopique et geochimique pour l'etude des eaux souterraines et des lacs: Exemples du haut bassin du Nil Bleu et du rift Ethiopien [Environmental isotopes and geochemistry in groundwater and lake hydrology: cases from the Blue Nile basin, main Ethiopian rift and Afar, Ethiopia], PhD thesis, University of Avignon, France. 162 pp.

Seifu Kebede, Travi, Y., Tamiru Alemayehu, Tenalem Ayenew (2005). Groundwater recharge, circulation and geochemical evolution in the source region of the Blue Nile River, Ethiopia. *Appl. Geochem.* 20:1658–1676.

Seifu Kebede, Travi, Y., Asrat, A., Tamiru Alemayehu, Tenalem Ayenew, Zenaw Tessema (2008). Groundwater origin and flow along selected transects in Ethiopian rift volcanic aquifers. *Hydrogeol. J.* 16:55–73.

Seifu Kebede, Travi, Y. (2012). Origin of the $\delta^{18}O$ and $\delta^{2}H$ composition of meteoric waters in Ethiopia. *Quatern. Int.*, 257:4–12.

Seifu Kebede (2013). Groundwater in Ethiopia features, numbers and opportunities. *Springer Hydrogeology*, Berline. 121 pp.

Shimelis Weldesenbet (2012). Hydrogeology, hydrochemistry and isotope hydrology of Central Main Ethiopian Rift. PhD thesis. Ruhr Universitat Bochum, Germany. 175 pp.

Singhal, B. and Gupta, R. (2010). Applied hydrogeology of fractured rocks: Second edition. *Springer* 408 pp.

SRK Consulting (2012). Karoo groundwater atlas: February 2012. Cape Town, S. Africa. 17 pp.

Stern, R.J. (1994). Arc assembly and continental collision in the Neoproterozoic East African Orogen: Implication for the consolidation of Gondwana. Anual Reviews Earth Sciences, 22:319–351.

Tamiru Alemayehu (2006). Groundwater occurrence in Ethiopia. Addis Ababa University Press, Ethiopia. 106 pp.

Tarekegn Tadesse (1997). Geology of the Axum area. Ethiopian Institute of Geological Survey. *Memoir No.9*. Addis Ababa.

Teklay Zereay (2007). Evaluating the potential of the Aynalem wellfield for the conjunctive use of surface and groundwater. Unpublished M.Sc. thesis, Mekelle University, Ethiopia. 113 pp.

Telford, R.J. (1998). The palaeoenvironmental record of Holocene environmental change in the Ethiopian rift valley. Ph.D. thesis, University of Wales.

Tenalem Ayenew (1998). The hydrogeological system of the Lake District basin. Central Main Ethiopian Rift. PhD Thesis, Free University of Amsterdam, The Netherlands. 259 pp.

Tenalem Ayenew, Tamiru Alemayehu (2001). Principles of hydrogeology. Addis Ababa University Press. 125 pp.

Tenalem Ayenew (2003). Environmental isotope-based integrated hydrogeological study of some Ethiopian rift lakes. *Journal of Radio-analytical and Nuclear Chemistry* 257(1):11–16.

Tenalem Ayenew, Seifu Kebede, Tamiru Alemyahu (2007). Environmental isotopes and hydrochemical study as applied to surface water and groundwater interaction in the Awash River basin. *J. Hydro.l pro.* 22(10):1548–1563.

Tenalem Ayenew (2009). Hydrogeological and geophysical investigation for Water well drilling site selection in Werii-Leke Woreda of central Tigray zone, northern Ethiopia. Unpublished report, Tigray Region Bureau of Water and Energy, Mekelle, Ethiopia.

Tesfamichael Gebreyohannes (2009). Regional groundwater flow model of Giba Basin, Northern Ethiopia. PhD Thesis, Vrije Universiteit Brussel, Belgium. 256 pp.

Tesfamichael Gebreyohannes, Smedt, F.D., Muruts Hagos, Kassa Amare, Kurkura Kabeto, Abdelwassie Hussein, Nyssen, J., Bauer, H., Moeyersons, J., Deckers, J., Taha, N. (2009). Large-scale Geological mapping of the Geba basin, Northern Ethiopia. VLIR – Mekelle University IUC program. *Tigray Livelihood Papers* pp. 9–46.

Tesfaye Chernet (1988). Hydrogeological map of Ethiopia, 1:2,000,000 scale. Ethiopian Institute of Geological Surveys, Addis Ababa, Ethiopia.

Tesfaye Chernet (1993). Hydrogeology of Ethiopia and water resources development. Unpublished report. EIGS, Addis Aaba, Ethiopia, 222pp.

Tesfaye Chernet, Gebretsadik Eshete (1982). Hydrogeology of Mekelle area (ND37 – 11). Ministry of Mines and Energy and Ethiopian Institute of Geological Survey, *memoir* No.2. 49 pp.

Verhagen BT (1991) Detailed geohydrology with environmental isotopes: A case study at Seroew, Botswana. In: Isotope Techniques in Water Resources Development, IAEA, Vienna, 345–362.

Wakgari Furi, Razack, M., Tenalem Ayenew, Seifu Kebede, Dagnachew Legese (2011). Hydrochemical characterization of complex volcanic aquifers in a continental rift zone: the Middle Awash Basin Ethiopia. *Hydrogeol. J.* 20:325–400.

Worash Getaneh (2002). Geochemistry province and depositional tectonic setting of the Adigrat Sandstone Northern Ethiopia. *J. Afr. Earth Sci.* 35:185–198.

Annex 1 Data of samples collected in the late dry season (April, 2013) ['BH' stands for bore hole; 'DW' stands for deep well; 'HDW' stands for had dug well; 'SP' stands for spring]

S.no	Sampling date	Sample ID	Easting	Northing	Elevation (masl)	Depth (m)	Yield (L/s)	Lithology	EC (µS/cm)	pH	T °C	Tritum (TU; σ = 0.5)	δ^2H ‰	$\delta^{18}O$ ‰	d-excess
1	28.04.2013	BH20	554086	1450963	2002	76	-	Shale, marl, limestone	1576	7.5	24	-	-4.67	-1.75	9.33
2	21.04.2013	DW10	557448	1445784	2135	104	-	Shale, marl, limestone	1946	7.8	23	2.36	17.47	-4.08	15.17
3			522527	1503854	2280	7	-	Shale, marl	1580	7.8	21	-	1.58	-0.79	7.9
4	28.04.2013	DW16	564925	1513383	2009	111	17	Limestone, gypsum	1811	7.3	22	3.3	-7.64	-3.03	16.6
5	19.04.2013	BH13	546672	1503269	1855	45	-	Limestone, shale	860	7.4	22	-	-1.13	-2.16	16.15
6	18.04.2013	BH11	559862	1484399	2300	54	-	Limestone, marl	975	7.3	19	-	-2.73	-1.95	12.87
7	27.04.2013	DW13	576657	1509342	2328	115	5	Marl, shale, limestone	935	7.4	19	-	-8.79	-3.67	20.57
8	21.04.2013	BH18	546523	1479676	1937	77	2	Limestone, shale, marl	2541	7.0	22	-	-6.35	-2.54	13.97
9	20.04.2013	BH15	547029	1489769	2130	50	-	Limestone, shale	849	7.3	20	-	-0.07	-1.46	11.61
10	23.04.2013	DW11	556473	1461799	2092	150	5	Limestone, shale, marl, dolorite	1076	7.7	21	-	5.55	-0.33	8.19
11	11.04.2013	SP3	562112	1501200	2213	-	0.3	-	1575	6.9	20	2.92	-6.39	-2.61	14.49
12	28.04.2013	BH30	564925	1513385	2008	28	1.5	Limestone	1339	7.4	23	-	-5.66	-2.77	16.5
13	21.04.2013	BH17	561610	1473000	2281	50	4	Limestone, shale, marl	990	7.3	18.5	-	-4.55	-2.94	18.97
14	21.04.2013	BH19	547163	1478877	1942	52	3	Limestone, shale, marl, dolorite	1898	7.2	20	-	1.88	-1.07	10.44
15	27.04.2013	BH14	544194	1495946	2002	56	0.8	Limestone, shale	1040	7.0	22	-	-2.45	-2.01	13.63
16	21.04.2013	BH16	557606	1476680	2240	54	0.5	Limestone	705	7.5	19.5	-	-0.92	-2.22	16.84
17	20.04.2013	DW8	544047	1495129	2009	-	-	Limestone, shale, marl alluvium, dolorite	2344	7.3	23	2.44	-0.68	-2.11	16.2
18	20.04.2013	DW7	556669	1494742	2037	-	6	Limestone, shale, marl, alluvium, dolorite	1929	7.0	23	-	-7.45	-2.64	13.67
19	21.04.2013	SP13	561153	1474287	2268	-	4	Limestone, shale, marl	843	7.2	20	-	-3.31	-2.25	14.69
20	21.04.2013	SP12	561708	1471764	2206	-	0.5	Limestone, shale, marl	3121	7.25	19	-	-3.46	-2.52	16.7
21	11.04.2013	SP2	569912	1514740	2062	-	12	Limestone, shale	898	-	-	-	-5.66	-2.47	14.1
22	11.04.2013	SP1	561562	1502579	2240	-	2	Limestone, shale	1875	-	-	-	-1.9	-2.01	14.18

S.no	Sampling date	Sample ID	Easting	Northing	Elevation (masl)	Depth (m)	Yield (L/s)	Lithology	EC (µS/cm)	pH	T °C	Tritum (TU; σ = 0.5)	δ^2H ‰	$\delta^{18}O$ ‰	d-excess
23	27.04.2013	HDW3	548193	1499338	1927	-	-	Limestone, shale	816	7.4	22	-	2.18	-1.01	10.26
24	18.04.2013	HDW2	567137	1482089	2367	-	-	Limestone, marl	1390	7.2	20	-	-7.24	-2.81	15.24
25	27.04.2013	SP7	569275	1492179	2362	-	2	Limestone	1039	7.4	20	-	-8.17	-3.16	17.11
26	18.04.2013	DW3	564341	1485674	2336	-	22	Limestone, marl, dolorite	1210	7.1	22	2.58	-8.42	-2.81	14.06
27	20.04.2013	SP9	547100	1486390	2100	-	2	Limestone, shale, alluvium	1112	7.3	20	-	-2.47	-1.91	12.81
28	21.04.2013	DW9	545387	1479732	1912	650	0	Limestone, shale, marl, dolorite	2611	6.9	22	3.14	-9.29	-2.79	13.03
29	18.04.2013	DW2	584182	1475467	1413	94	-	Limestone, alluvium	1650	7.6	25	2.78	-4.74	-2.33	13.9
30	27.04.2013	R7	546413	1505217	1796	-			1072	8.8	26	2.88	18.85	1.89	3.73
31	18.04.2013	SP5	580315	1473622	1511	-	17	Limestone	2546	7.1	23	2.67	3.03	-0.84	9.75
32	21.04.2013	R8	545423	1479560	1907	-		Limestone, shale, marl, dolorite	1584	8.3	22	3.01	3.65	-0.58	8.29
33	20.04.2013	SP11	545376	1487959	1953	-		Limestone	2713	8.2	24	2.26	-7.2	-2.88	15.84
34	20.04.2013	SP10	546497	1487309	2089	-	2	Limestone	1018	7.2	21	3.28	0.81	-1.77	14.97
35	24.04.2013	SP18	524097	1502834	2004	-	25	Limestone	719	7.3	20	3.66	-4.87	-2.85	17.93
36	17.08.2005	SP20	509933	1499261	2030	-	9	Limestone	797	7.9	21	2.35	-5.45	-2.83	17.19
37	24.04.2013	SP19	524684	1499014	1828	-		Sandstone, Limestone	625	7.7	24	2.61	-4.19	-2.86	18.69
38	27.04.2013	SP8	541415	1495507	1959	-	5		1038	7.1	20	2.75	-2.56	-2.28	15.68
39	28.04.2013	R14	564925	1513384	2006	-	30	Limestone	1020	8.6	23.5	-	3.31	-1.03	11.55
40	23.04.2013	R10	538590	1455740	1695	-	95	Limestone, dolorite	1200	8.5	21	2.5	-0.33	-1.12	8.63
41	23.04.2013	SP17	539168	1457006	1955	-	4	Limestone, dolorite	849	7.2	24	-	-2.05	-1.73	11.79
42	14.08.2005	SP16	552788	1452114	1977	-		Limestone, alluvium	859	7.9	20	3	-4.81	-1.5	7.19
43	27.04.2013	DW5	551690	1487551	2166	-		Limestone, dolorite	1251	7.2	21	-	-7.16	-2.69	14.36
44	18.04.2013	DW4	560970	1487145	2281	-	25	Limestone, dolorite	1263	7.3	20	3.45	-5.36	-2.38	13.68
45	27.04.2013	BH12	573454	1493195	2393	58	5	Dolorite	1160	7.3	19	-	-7.82	-2.91	15.46
46	18.08.2005	SP24	527613	1461672	2156	-		Limestone, dolorite	1577	7.3	23	-	-7.12	-2.16	10.16
47	27.04.2013	R6	563566	1491851	2235	-			1375	7.7	19	-	-0.92	-1.85	13.88
48	18.04.2013	SP6	559195	1490431	2217	-		Limestone, dolorite	830	7.2	20	-	-4.41	-2.12	12.55

S.no	Sampling date	Sample ID	Easting	Northing	Elevation (masl)	Depth (m)	Yield (L/s)	Lithology	EC (µS/cm)	pH	T °C	Tritum (TU; σ = 0.5)	δ^2H ‰	$\delta^{18}O$ ‰	d-excess
49	26.04.2013	BH25	541397	1475175	2150	50	2	Dolorite	585	7.6	19	-	-7.96	-2.69	13.56
50	13.04.2013	BH8	549205	1549161	2227	-	-	Sandstone	595	7.1	20	-	-7.63	-2.71	14.05
51	13.04.2013	BH5	560345	1549683	2349	-	-	Sandsone	433	7.3	19	-	-4.59	-3.03	19.65
52	13.04.2013	BH4	558900	1551925	2353	-	-	Sandstone	365	6.9	20	-	-3.06	-2.79	19.26
53	27.04.2013	DW6	546692	1505523	1792	-	-	Sandstone	947	7.0	24	2.75	-20.39	-4.05	12.01
54	04.08.2005	DW1	560528	1567193	2832	92	-	Sandstone	76	7.8	19	3.21	-6.26	-3.39	20.86
55	28.04.2013	DW15	564921	1525889	2018	168	6	Sandstone	336	7.3	21	-	-0.27	-1.77	13.89
56	25.04.2013	SP22	501355	1505847	1676	-	-	Sandstone	99	8.1	21	-	4.97	-0.59	9.69
57	25.04.2013	SP21	506401	1497693	1673	-	45	Sandstone	287	7.9	24	1.73	-17.3	-4.06	15.18
58	14.04.2013	R5	555377	1530529	1948	-	-	Sandstone	550	8.3	28	-	9.63	0.45	6.03
59	12.04.2013	R2	561297	1562503	2536	-	-	Sandstone	225	7.2	20	-	-3.9	-1.98	11.94
60	12.04.2013	SPD	570432	1571347	2832	-	1	Sandstone	185	7.4	18	-	-7.9	-2.74	14.02
61	26.04.2013	DW12	504611	1463560	1610	-	-	Sandstone, alluvial Alluvual sand	550	7.6	25	-	-5.25	-2	10.75
62	27.04.2013	BH26	576828	1520257	2158	70		Alluvial sand, sandstone, meta-volcanics	569	7.6	21	-	-9.41	-3.74	20.51
63	27.04.2013	R13	573864	1518871	2116	-		Alluvial sand, Sandstone	481	9.2	24.5	-	-1.45	-2.38	17.59
64	11.04.2013	HDW1	554031	1508599	1899	12			1070	6.9	21	2.94	2.28	-1.36	13.16
65	14.04.2013	BH10	549004	1532486	2121	42		Sandstone/tillite	290	7.6	21	-	-1.9	-2.03	14.34
66	13.04.2013	BH7	550693	1555711	2320	93		Tillite	760	7.9	20	2.43	-18.62	-4.15	14.58
67	13.04.2013	BH6	551606	1547085	2247	-		Sandstone/tillite	395	7.2	19	-	-6.62	-2.9	16.58
68	12.04.2013	BH3	562453	1559822	2578	50		Sandstone/tillite	169	7.2	19	-	-4.79	-2.39	14.33
69	13.04.2013	R3	551446	1558814	2334	-	2	Sandstone, tillite, Alluvial sand	920	8.5	26	-	-3.03	-1.74	10.89
70	11.04.2013	R1	555838	1509273	1906	-			1008	8.0	25	-	7.37	-0.44	10.89
71	28.04.2013	HDW6	563009	1529716	2063	-		Sandstone, tillite	754	7.5	22	-	-2.61	-2.34	16.11

S.no	Sampling date	Sample ID	Easting	Northing	Elevation (masl)	Depth (m)	Yield (L/s)	Lithology	EC (µS/cm)	pH	T °C	Tritum (TU; σ = 0.5)	δ^2H ‰	$\delta^{18}O$ ‰	d-excess
72	24.04.2013	HDW4	519595	1506502	2530	5	-	Basalt	564	7.2	17	-	-2.25	-2.24	15.67
73	21.04.2013	SP15	558283	1444110	2116	-	-	Sandstone, basalt	530	7.7	30	-	-11.74	-3.23	14.1
74	21.04.2013	SP14	558912	1435750	2703	-	-	Basalt	297	8.2	15	2.73	-11.39	-3.65	17.81
75	21.04.2013	R9	555450	1440599	2516	-	13	Basalt, Sandstone	567	8.8	25	2.43	-4.65	-2.59	16.07
76	25.04.2013	BH22	513204	1502111	2637	40	1.5	Basalt/mudstone	436	7.9	17	-	-9.2	-2.96	14.48
77	25.04.2013	BH21	513779	1509482	2562	60		Basalt/mudstone	437	7.4	17	-	-3.53	-2.28	14.71
78	28.04.2013	BH29	565424	1530159	2118	50	1	Meta-dolomite	927	7.6	22	-	-5.73	-2.53	14.51
79	28.04.2013	BH28	566630	1541538	2487	45	2	Meta-sediment, meta-volcanics	825	7.8	20	-	-9.84	-2.96	13.84
80	27.04.2013	BH27	578856	1531354	2638	40	1.2	Meta-basalt	467	7.5	17	1.92	-13.69	-3.4	13.51
81	26.04.2013	BH24	503281	1471416	1518	45	1.5	phyllite	967	7.3	27	-	0.53	-1.56	13.01
82	25.04.2013	BH23	499161	1484004	1454	48	2	phyllite	1827	7.2	27	-	-4.33	-2.01	11.75
83	14.04.2013	BH9	542662	1542595	2084	85	-	slate	795	7.5	21	-	-7.67	-3.12	17.29
84	12.04.2013	BH2	570337	1573556	2771	65	-	Phyllite	610	7.5	16	2.06	-8.34	-4.61	28.54
85	12.04.2013	BH1	576544	1579098	1300	67	-	Slate	1560	7.0	20	2.12	-18.46	-4.88	20.58
86	28.04.2013	DW14	563806	1535118	2333	-	-	Metabasic	605	7.4	19	3.18	-6.83	-2.8	15.57
87	27.04.2013	SP26	580109	1533673	2674	-	-	Phyllite	435	7.9	18	1.97	-14.08	-3.82	16.48
88	27.04.2013	SP25	578740	1531354	2627	-	-	Meta-basalt	478	7.5	18	2.1	-13.23	-4.17	20.13
89	26.04.2013	SP23	515087	1456933	1736	-	1.5	Meta-limestone	1534	7.5	25	-	-0.79	-0.28	1.45
90	12.04.2013	SP4	577967	1579515	1294	-	2	Meta-limestone	1395	7.8	25	2.06	-13.03	-4.77	25.13
91	26.04.2013	R12	502301	1469976	1465	-	-	Meta-limestone	1157	8.9	21	-	11.02	0.64	5.9
92	14.04.2013	R4	543889	1536833	1984	-	-	slate	852	8.0	21	-	2.9	-0.63	7.94
93	27.04.2013	HDW5	576497	1524687	2415	13	-	Phyllite	661	7.6	18.5	-	-9.38	-3.93	22.06
94	25.04.2013	R11	502835	1488216	1363	-	-	Alluvium, slate	815	9.0	29	-	-0.17	0.4	-3.37

Annex 2 Data of samples collected in the end of rainy season (August-October, 2012) ['BH' stands for shallow bore hole; 'DW' stands for deep well; 'SP' stands for spring]

S.no	Sampling date	Sample ID	Easting	Northing	Elevation (masl)	Depth (m)	Yield (L/s)	Lithology	EC (µS/cm)	pH	T °C	Tritum (TU; σ = 0.5)	δ^2H ‰	$\delta^{18}O$ ‰	d-excess
1	14.07.2012	DW17	552414	1489444	2196	-	-	Dolerite, limestone	-	-	-	-	-7.86	-2.46	11.82
2	14.07.2012	DW5	552125	1487865	2174	-	-	Dolerite, limestone	-	-	-	-	-5.72	-2.09	11
3	14.07.2012	DW18	557706	1488148	2247	-	-	Limestone, marl	-	-	-	-	-1.37	-1.84	13.35
4	19.07.2012	DW3	564350	1485683	2324	-	-	Marl, shale, limestone	1490	7.8	-	-	-8.39	-2.64	12.73
5	19.07.2012	DW19	560159	1487626	2272	-	-	Limestone, Dolerite	1310	8.0	-	-	-7.07	-2.37	11.89
6	14.09.2012	DW6	546547	1505354	1800	-	-	Sandstone	974	7.7	-	-	-12.2	-2.78	10.04
10	17.07.2012	BH31	563899	1485842	2318	65	2.5	Marl, shale, limestone	740	7.8	-	-	-3	-1.84	11.72
11	04.09.2012	BH32	550172	1500492	1984	-	-	Marl, shale, limestone	1030	7.6	-	-	-1.27	-1.43	10.17
12	05.09.2012	BH13	546681	1503281	1875	-	-	Marl, shale, limestone	850	7.8	-	-	-1.51	-1.33	9.13
13	08.09.2012	BH14	540700	1485374	1778	45	0.5	Limestone, Marl	1190	7.7	-	-	-1.25	-1.3	9.15
14	08.09.2012	BH15	543750	1482903	1911	42	0.8	Limestone, Marl	1215	7.7	-	-	-0.6	-1.31	9.88
15	08.09.2012	BH16				-	-	Limestone, Marl			-	-	4.93	-0.25	6.93
16	16.07.2012	SP6	559200	1490284	2212	-	-	Limestone, Dolerite	780	7.8	-	-	-2.63	-2	13.37
17	09.09.2012	SP27	546828	1481229	1987	-	-	Limestone, Marl	1250	7.7	-	-	-3.63	-2.18	13.81
18	14.09.2012	SP28	551084	1489474	2163	-	-	Marl, shale, limestone	848	8.5	-	-	3.23	-1.44	14.75
19	14.09.2012	SP29	551573	1489933	2135	-	-	Marl, shale, limestone	1020	8.3	-	-	-3.21	-1.92	12.15
20	14.09.2012	SP30	551620	1490415	2113	-	-	Marl, shale, limestone	1640	7.8	-	-	-7.26	-2.39	11.86

Annex 3 Generated hydrochemical data of systematically selected samples collected in the late dry season (April, 2013) ['BH' stands for bore hole; 'DW' stands for deep well; 'HDW' stands for had dug well; 'SP' stands for spring]

Code	**X**	**Y**	**Z**	**Depth**	**EC**	**PH**	**T**	**Li^+**	**Na^+**	**K^+**	**Mg^{++}**	**Ca^{++}**	**HCO_3^-**	**SO_4^-**	**NO_3^-**	**Cl^-**	**F^-**
BH1	576544	1579098	1300	67	1560	7	20	0	101.0	2.0	101.0	190.0	421.04	334.0	206.0	134.0	0.2
BH2	570337	1573556	2771	65	610	7.5	16	0	26.5	1.0	32.0	81.8	384.43	62.8	3.4	34.0	0.5
BH3	562453	1559822	2578	50	169	7.2	19	0	6.3	1.7	6.2	21.6	91.53	9.2	28.0	4.7	0.3
BH4	558900	1551925	2353		365	6.9	20	0	15.3	0.7	12.0	47.0	213.57	20.2	9.7	19.5	0.4
BH5	560345	1549683	2349		433	7.3	19	0	12.8	4.8	21.0	52.5	256.28	30.0	6.6	17.4	0.5
BH6	551606	1547085	2247		395	7.2	19	0	22.8	0.6	10.4	52.6	237.98	30.0	11.5	14.3	0.6
BH7	550693	1555711	2320	93	760	7.9	20	0	113.0	5.3	21.0	31.9	396.63	73.7	0.6	48.0	0.6
BH8	549205	1549161	2227		595	7.1	20	0	23.0	2.2	23.0	77.8	311.20	57.7	15.2	32.0	0.7
BH9	542662	1542595	2084	85	795	7.5	21	0	39.2	2.7	45.0	65.4	500.36	27.0	8.1	25.0	0.8
BH10	549004	1532486	2121	42	290	7.6	21	0	5.7	0.9	5.0	46.0	176.96	7.4	20.2	7.3.0	0.4

BH11	559862	1484399	2300		975	7.3	19	0	21.7	1.8	30.0	137.0	384.43	144.0	61.0	60.4	0.4
BH12	573454	1493195	2393	58	1160	7.3	19	0	39.1	3.0	33.0	172.0	482.06	286.0	23.0	60.8	0.5
BH13	546672	1503269	1855		860	7.4	22	0	27.2	3.8	25.0	130.0	323.41	128.0	70.2	43.0	0.5
BH14	544194	1495946	2002	56	1040	7	22	0	13.2	0.5	13.0	235.0	463.75	303.0	16.4	9.9	0.3
BH15	547029	1489769	2130		849	7.3	20	0	12.1	1.3	31.0	128.0	439.34	115.0	43.0	10.5	0.5
BH16	557606	1476680	2240	54	705	7.5	19.5	0	12.4	1.8	16.0	125.0	396.63	39.0	42.0	13.1	0.5
BH17	561610	1473000	2281	50	990	7.3	18.5	0	51.1	1.7	27.0	146.0	439.34	170.0	36.0	45.0	0.6
BH18	546523	1479676	1937	77	2541	7	22	0.1	45.0	3.6	83.0	510.0	396.63	1550.0	6.9	55.1	0.8
BH19	547163	1478877	1942	52	1898	7.2	20	0.3	54.6	1.9	60.0	364.0	323.41	1070.0	50.8	121.0	0.7
BH20	554086	1450963	2002	76	1576	7.5	24	0	47.0	2.4	61.0	287.0	372.22	870.0	4.0	27.0	0.7
BH21	513779	1509482	2562	60	437	7.4	17	0	15.2	0.8	18.0	54.1	292.90	9.2	19.2	5.5	0.8
BH22	513204	1502111	2637	40	436	7.9	17	0	20.6	2.3	23.0	46.0	317.30	14.5	1.1	3.3	1.0
BH23	499161	1484004	1454	48	1827	7.2	27	0.2	97.2	1.2	97.0	288.0	524.77	1110.0	3.0	22.0	1.2

BH24	503281	1471416	1518	45	967	7.3	27	0	81.8	1.3	32.0	90.5	506.47	41.0	96.6	35.0	2.0
BH25	541397	1475175	2150	50	585	7.6	19	0	15.6	0.9	28.0	78.9	457.65	35.0	14.3	11.4	0.9
BH26	576828	1520257	2158	70	569	7.6	21	0	31.5	1.1	18.0	68.7	378.32	27.0	13.5	20.8	0.6
BH27	578856	1531354	2638	40	467	7.5	17	0	16.9	0.5	15.0	68.5	280.69	19.4	7.9	15.1	0.3
BH28	566630	1541538	2487	45	825	7.8	20	0	16.1	1.1	56.1	82.4	402.73	58.3	60.5	37.0	0.6
BH29	565424	1530159	2118	50	927	7.6	22	0	30.9	0.5	40.0	84.5	585.79	56.3	7.6	30.0	0.7
BH30	564925	1513385	2008	28	1339	7.4	23	0	56.6	2.4	42.0	195.0	366.12	554.0	3.7	60.8	0.6
DW1	560528	1567193	2832	92	76	7.8	19	0	2.7	1.0	5.7	18.1	54.92	5.9	7.8	3.7	0.2
DW2	584182	1475467	1413	94	1650	7.6	25	0	64.9	3.9	78.0	254.0	274.59	910.0	20.5	79.4	0.5
DW3	564341	1485674	2336		1210	7.1	22	0	28.3	3.6	33.0	242.0	390.53	613.0	0.3	13.9	0.5
DW4	560970	1487145	2281		1263	7.3	20	0	24.1	1.4	40.0	261.0	378.32	645.0	18.2	17.0	0.4
DW5	551690	1487551	2166		1251	7.2	21	0.1	54.4	2.3	41.0	215.0	384.43	608.0	0.6	22.0	0.5
DW6	546692	1505523	1792		947	7	24	0	33.8	6.3	24.0	157.0	445.45	167.0	167	47.0	0.4

DW7	556669	1494742	2037		1929	7	23	0	46.0	3.1	64.0	424.0	335.61	1410.0	0	22.0	1
DW8	544047	1495129	2009		2344	7.3	23	0	76.7	2.2	51.6	454.0	323.41	1380.0	2.0	78.0	1
DW9	545387	1479732	1912	650	2611	6.9	22	0.1	81.4	5.3	71.0	548.0	396.63	1580.0	0	42.0	1
DW10	557448	1445784	2135	104	1946	7.8	23	0	53.0	5.5	30.0	502.0	146.45	1610.0	2.0	14.0	2
DW11	556473	1461799	2092	150	1076	7.7	21	0	85.2	2.2	42.0	85.5	384.43	283.0	1.4	43.0	1.3
DW12	504611	1463560	1610		550	7.6	25	0	15.4	0.8	17.3	72.0	400.00	19.0	17.6	12.4	0.6
DW13	576657	1509342	2328	115	935	7.4	19	0	26.1	2.5	31.3	92.7	604.10	61.4	0.6	20.0	0.5
DW14	563806	1535118	2333		605	7.4	19	0	27.0	0.3	26.0	67.6	500.36	23.0	4.5	21.0	0.3
DW15	564921	1525889	2018	168	336	7.3	21	0	11.3	7.2	10.3	41.4	158.65	30.0	11.3	15.4	0.1
DW16	564925	1513383	2009	111	1811	7.3	22	0	62.8	2.9	39.0	394.0	335.61	1070.0	1.7	72.9	0.5
HDW1	554031	1508599	1899	12	1070	6.9	21	0	52.3	2.4	36.0	153.0	341.71	245.0	32.0	53.8	0.3
HDW2	567137	1482089	2367		1390	7.2	20	0.1	46.0	1.7	64.0	202.0	530.87	356.0	38.0	66.1	0.5
HDW3	548193	1499338	1927		816	7.4	22	0	38.0	1.2	26.0	114.0	494.26	85.1	70.1	33.0	0.4

HDW4	519595	1506502	2530	5	564	7.2	17	0	14.6	0.7	21.0	86.8	366.12	16.4	20.0	8.5	0.3
HDW5	576497	1524687	2415	13	661	7.6	18.5	0	24.2	0.8	25.0	87.5	150.00	17.9	10.2	17.5	0.4
HDW6	563009	1529716	2063		754	7.5	22	0	27.6	0.6	43.0	77.9	378.32	25.0	21.0	11.0	0.7
R1	555838	1509273	1906		1008	8	25	0	53.8	3.0	31.0	133.0	384.43	297.0	6.0	59.1	0.4
R2	561297	1562503	2536		225	7.2	20	0	7.9	1.8	6.7	28.8	140.35	14.9	1.3	12.7	0.3
R3	551446	1558814	2334		920	8.5	26	0	54.9	2.9	48.0	77.4	329.51	76.0	0.6	76.2	0.2
R4	543889	1536833	1984		852	8	21	0	88.9	1.9	28.0	56.0	396.63	40.0	0	95.2	1.4
R5	555377	1530529	1948		550	8.3	28	0	31.4	7.7	19.0	50.2	317.30	25.0	3.14	28.0	0.6
R6	563566	1491851	2235		1375	7.7	19	0	48.0	2.1	36.0	262.0	408.83	618.0	1.4	51.4	0.5
R7	546413	1505217	1796		1072	8.8	26	0	69.1	5.0	37.0	124.0	158.65	460.0	7.2	80.8	0.4
R8	545423	1479560	1907		1584	8.3	22	0	45.0	2.3	54.0	305.0	256.28	960.0	7.8	56.5	1
R9	555450	1440599	2516		567	8.8	25	0	25.0	1.4	28.0	54.6	484.43	34.0	10.7	12.1	0.5
R10	538590	1455740	1695		1200	8.5	21	0	65.0	2.6	56.0	146.0	317.30	500.0	4.0	53.4	1

R11	502835	1488216	1363		815	9	29	0	49.0	5.9	27.0	90.3	237.98	246.0	3.2	51.2	0.5
R12	502301	1469976	1465		1157	8.9	21	0	152.0	2.9	38.0	68.4	396.63	278.0	3.8	80.8	1.8
R13	573864	1518871	2116		481	9.2	24.5	0	25.9	0.9	21.0	51.4	244.08	43.0	1.2	26.0	0.2
R14	564925	1513384	2006		1020	8.6	23.5	0	50.0	2.4	31.0	131.0	475.96	284.0	3.8	53.4	0.3
SP1	561562	1502579	2240		1875			0	56.8	2.6	34.8	486.0	219.67	1450.0	0	68.2	0
SP2	569912	1514740	2062		898			0	27.0	2.2	29.0	143.0	421.04	194.0	15.2	31.0	0.5
SP3	562112	1501200	2213		1575	6.9	20	0	63.4	5.5	36.0	301.0	396.63	684.0	42.0	74.7	1
SP4	577967	1579515	1294		1395	7.8	25	0	67.7	0.8	65.0	170.0	494.26	273.0	110.0	110.0	0.4
SP5	580315	1473622	1511		2546	7.1	23	0	97.1	7.7	84.0	422.0	250.18	1530.0	6.8	111.0	1
SP6	559195	1490431	2217		830	7.2	20	0	16.7	1.0	20.0	147.0	472.22	163.0	39.0	21.0	0.3
SP7	569275	1492179	2362		1039	7.4	20	0	26.1	1.2	31.0	177.0	445.45	270.0	34.0	30.0	0.7
SP8	541415	1495507	1959		1038	7.1	20	0	25.8	1.1	29.0	188.0	408.83	279.0	44.0	30.0	0.5
SP9	547100	1486390	2100		1112	7.3	20	0	27.1	0.9	35.0	210.0	421.04	381.0	32.0	21.0	0.6

SP10	546497	1487309	2089		1018	7.2	21	0	16.4	2.1	19.0	196.0	372.22	325.0	63.5	20.0	0.6
SP11	545376	1487959	1953		2713	8.2	24	0	33.8	3.7	34.0	608.0	256.28	1740.0	0	18.0	0
SP12	561708	1471764	2206		3121	7.25	19	0.2	257.0	8.6	207.0	358.0	543.08	1670.0	61.2	308.0	0
SP13	561153	1474287	2268		843	7.2	20	0	38.8	1.4	26.0	125.0	402.73	120.0	30.0	46.0	0.8
SP14	558912	1435750	2703		297	8.2	15	0	12.8	0.3	11.0	45.0	213.57	7.5	3.0	4.0	0.3
SP15	558283	1444110	2116		530	7.7	30	0	15.8	0.8	19.0	79.9	378.32	16.7	11.8	8.9	0.4
SP16	552788	1452114	1977		859	7.9	20	0	31.7	2.4	44.0	111.0	372.22	238.0	13.9	21.0	0.5
SP17	539168	1457006	1955		849	7.2	24	0	38.9	0.9	24.0	126.0	433.24	72.8	56.7	32.0	0.7
SP18	524097	1502834	2004		719	7.3	20	0	18.7	1.7	21.0	119.0	439.34	56.2	16.3	15.0	0.8
SP19	524684	1499014	1828		625	7.7	24	0	15.4	1.9	18.0	94.3	414.94	30.0	16.1	9.3	0.6
SP20	509933	1499261	2030		797	7.9	21	0	24.6	2.5	25.0	123.0	488.16	52.1	34.0	15.0	0.5
SP21	506401	1497693	1673		287	7.9	24	0	9.2	3.0	7.8	43.0	170.86	18.2	4.3	8.1	0.4
SP22	501355	1505847	1676		99	8.1	21	0	2.3	4.7	4.1	17.0	85.43	7.2	8.1	3.6	0.3

SP23	515087	1456933	1736		1534	7.5	25	0	66.5	4.1	38.0	278.0	414.94	657.0	7.9	133.0	2
SP24	527613	1461672	2156		1577	7.3	23	0	21.9	1.5	57.0	319.0	439.34	817.0	0	14.0	1
SP25	578740	1531354	2627		478	7.5	18	0	16.4	0.4	14.0	68.2	280.69	15.9	15.5	14.2	0.4
SP26	580109	1533673	2674		435	7.9	18	0	13.2	0.6	11.0	69.1	250.18	26.0	19.2	14.0	0.4
SPD	570432	1571347	2832		185	7.4	18	0	32.6	0.5	39.0	65.5	80.00	58.3	6.4	29.0	0.7

Annex 4 Data of field measurements of different geological structures in different parts of the study area and in different rock units

X	Y	Z	Type	Strike	Dip/dip direction	Spacing	Aperture	Infilling	Continuity	Rock type	Formation	Remark 1	Remark 2
555191	1526783		Bedding plane	290	28/200					Fossiliferrous and/or lithic limestone	Antalo limestone	Intercalation of thin and thick limestone beds, cliff forming beds where the joint spacing are wide	Beb thickness= 2.25cm,3.36cm,4.5cm, 1.4m,10m
555191	1526783		Joint set 1	280	70/10	6.6cm,7.8cm,40cm,565cm	few mm	Silty-clay soil	Contineous	"	"		
555191	1526783			10	Vertical/100	1.4cm,4.45cm,6.66cm,70cm,1m,1.2m	few mm	Silty-clay soil	Non contineous	"	"		
556695	1488439		Joint	325	Vertical/235	Irregular	less than a mm	None	Contineous	Dolerite	Mekelle Dolerite	Miderately weathered with spherodal weathering	
556695	1488439			350	"/260	"	"	None	"	"	"	"	
556695	1488439			345	"/255	"	"	None	"	"	"	"	
556695	1488439			330	"/240	"	"	None	"	"	"	"	
556695	1488439			325	"/235	"	"	None	"	"	"	"	

556695	1488439			325	"/235	"	"	None	"	"	"	"	
560381	1483832	2326	Dolerite dyke/5.2 m wide	220	75/130								
560381	1483832		Joints in the dyke	325	Vertical/235	5cm,10cm,12cm, 26cm,32cm	few mm	Quartz	Contineous	Dolerite	Dyke	Slightly to moderately weathered	
561012	1483414	2344	Joint Set 1	290	70/200	20cm,32cm,40cm ,125cm, 125cm,155cm	8mm	None	Contineous	Marly shale	Agulae shale	Blocks in between joints are fractured	Horizontal beds
561012	1483414		Joint Set 2	200	74/290	16cm,30cm,34cm ,53cm,90cm,134cm	few mm to 1cm	Calcite	"	"	"	"	Horizontal beds
564459	1484574	2338	Joint Set 1	295	80/205	66cm,101cm,105cm,109cm	1mm,5mm,1cm	Silty-clay soil	"	Fissiliferous limestone (intercalated with marly limestone)	"	The marly limestones are fractured	Bed thickness=50cm to 31cm
564459	1484574		Joint Set 2	226	87/136	Iregular	"	Silty-clay soil	"	"	"		
564459	1484574		Bedding plane	360	13/270					"	"	381	
564399	1485633	2318	Joint Set 1	200	Vertical/110	2m,3m	few mm to 1cm	Silty-clay soil	Contineous	Fosiliferous Limestone (intercalated with marl)	"	95.25	Horizontal beds, Bed thickness=15cm to 1m
564399	1485633		Joint Set	292	Vertical/2	120cm,3	few mm	Silty-	"	Fosiliferous	"		

			2		02	40cm	to 1cm	clay soil		Limestone (intercalated with marl)			
564399	1485633	2318	Joint Set 1	305	Vertical/215	8 cm to 60cm	less than a mm	None	"	Marl	"		Horizonral beds, Bed thickness=18cm to 1m
564399	1485633		Joint Set 2	346	Vertical/256	"	"	"	"	"	"		
564399	1485633		Joint Set 3	335	Vertical/245	"	"	"	"	"	"		
564562	1485766	2322	Joint Set 1	190	Vertical/100	68cm,80cm,82cm,96cm	few mm	Quartz	"	Dolerite sill	Mekelle Dolerite	Minor joints with similar orientation and joint spacing 1cm to 15cm	
564562	1485766		Joint Set 2	280	Vertical/190	1cm,6cm,30cm,42cm	"	"	"	"	"		
550223	1500462	1985	Joint Set 1	325	Vertical/235	1m	few mm	None	"	Limestone	Agulae shale		Horizontal beds
550223	1500462		Joint Set 2	306	Vertical/216	25cm,60cm	"	"	"	"	"		
541548	1483438	1809	Dolerite dyke/17m wide	40	Vertical/130								
541548	1483438		Joints in the dyke	310	25 to 90/40	50cm,80cm,90cm	few mm	Quartz	Non contineous	Dolerite	Dyke	Shearing in similar trend as the dykes	
540650	1484319	1810	Joint Set 1	340	Vertical/250	137cm	few mm	None	Contineous	Marl	Antalo limestone		Beds slightly

													dipping toward SE
540650	1484319		Joint Set 2	300	Vertical/210	21cm	"	"	"	"	"		
540650	1484319		Joint 3	80	Vertical/170	Very scattered	"	"	"	"	"		
540650	1484319		Joint 4	50	Vertical/140	"	"	"	"	"	"		
540244	1485595	1838	DolerIte dyke/175 cm wide	83	Vertical/173								Slightly to moderately weathered
542706	1483698	1925	Joint Set 1	294	Vertical/204	40cm, 70 cm	0.5cm,7cm	Silty-clay soil	Contineous	Limestone	Antalo limestone		Thichly beded, Slightly dipping to the SE
542706	1483698		Joint Set 2	18	Vertical/108	36cm,76 cm	"	Silty-clay soil	"	"	"		
542344	1482484	1888	Joint Set 1	280	Vertical/190	23cm,25 cm,38cm ,40cm,70cm	few mm to 5cm	None	"	Black limestone	"	Bed thickness ranges 1m to 4m	Horizontal beds, Found just on top of thick dolerote sill
542344	1482484		Joint Set 2	70	Vertical/160	5m	"	"	"	"	"	"	
542344	1482484		Joint Set 3	17	Vertical/107	40cm, 190cm	"	"	"	"	"	"	
543773	1482563	1907	Joint Set 1	87	Vertical/177	110cm,165cm,210cm	few mm to 3cm	Silty-clay soil	"	Limestone	"	Bed thickness in cms	Horizontal beds

543773	1482563		Joint Set 2	317	Vertical/227	270cm	"	"	Non contineous	"	"	"	
564288	1537965	2427	Joint set 1	84	82/354	40mm,37mm,75mm,44cm,20cm	1mm to 2mm	None	Contineous	Phylite	Tsaliet group		cleavage (strike N-S, dip 78, dip direction 265)
			Joint set 2	288	82/18	Very scattered	"	"	"	"	"		"
			Joint set 3		Sub-horizontal	34cm	"	"	"	"	"		
562462	1537751	2367	Joint set 1	170	22/90	15cm to 30cm	"	"	"	"	"		Folliation (strike 10, dip Vertical)
562222	1537782	2339	Joint set 1	110	Vertical/200	40cm to 60cm	less than a mm	None	Contineous	Shist	"		Folliation (strike 0, dip 80 dip direction 280)
			Joint set 2	90	Vertical/360	"	"	"	"	"	"		
565455	1535520	2403	Massive carbonate marble							Carbonate marble	Tembien group		
564749	1533964	2333	Joint set 1	256	Vertical/166	2m to 3m	less than a mm	None	Contineous	Metabasic	Tsaliet group		
			Joint set 2	232	43/322	2m to 3m	"	"	"	"	"		
			Joint set 3	360	52/270	1m	"	"	"	"	"		

			Joint set 1		42/325	10cm to 1m	"	"	"	"	"		
			Joint set 2		82/260	"	"	"	"	"	"		
			Joint set 3	227	Vertical/317	"	"	"	"	"	"		
			Joint set 4		Sub-horizontal	Scattered							
564777	1533560	2325	Apilitic dyke	240	Vertical/330								
564768	1533491	2320	Joint set 1	260	50/350	1.5m to 2m	"	"	"	Metabrecia	"		
			Joint set 2	170	10/260	5cm to 1m	"	"	"	"	"		
			Joint set 1 (prominent)	270	Vertical/360	1m	"	"	"	Slate	Tembien group		Foliation (Strike 207)
			Joint Set 2	10	Vertical/100	15cm	"	"	"	Slate	Tembien group		
			Joint set 3		Sub-horizontal		"	"	"	Slate	Tembien group		
564762	1533372	2305	Fault (with fault guage and intense fracturing, displacement 3m)	315	25/225								

564785	1533322	2307	Gradition al Contact b/n metavolc anics and metasedi ments										
564995	1531854	2227	Sharp contact b/n slate and dolostone				"	"	"	Slate	Tembien group		Slaty cleavage (Strike 28, dip 60, dip direction 118)
565199	1530143	2132	Massive dolostone outcrop										Bedding strike N-S and steeply dipping
565857	1529760	2090	Massive black limestone										Bedding strike N-S and steeply (70 to west) dipping
			Strike slip fault	90	Vertical/1 80								
566238	1529612	2081	Pebbly slate outcrop										Bedding strike N-S and steeply dipping
570559	1516382	2077	Joint set 1	360, 340, 22	Vertical/2 60	Irregular	2cm to less than a mm	Silty-sand soil	Non contineous	Fossilifereous limestone	Agula shale	Bed thickneses 50cm to less than a mm	Bedding horizontal
			Joint set 2	66	Vertical/1 56	Irregular	"	"	"	"	"		

571429	1516986	2094	Fault/parallel to Agula river)	76	Vertical/166								
573243	1517736	2129	Fault contact b/limestone and sandstone	318	Vertical/228								
573461	1518326	2132	Major joint set	282, 294, 310	Vertical/205	35cm to 2m	50cm to less than a mm	Sandy soil	Contineous	Sandstone	Adigrat sandstone		
574427	1520718	2185	Joint set 1	260	Vertical/350	2cm to 5cm with non-systematic intense fracturing	less than a mm	None	Contineous	Phylite/Slate	Tsaliet/Tembien group		
			Joint set 2	210	25/120	"	"	"	"	"	"		
			Joint set 3	50	10/320	"	"	"	"	"	"		
			Joint se 4 (minor)	235	Vertical/325	Very scattered	"	"	"	"	"		
576267	1524259	2398	Joint set 1	298	Vertical/208	2cm to 50cm	"	"	"	"	"		
			Joint set 2	10	Vertical/100	"	"	"	"	"	"		
			Joint set 3		Sub-horizontal	30cm	"	"	"	"	"		

579058	1532228	2649	Joint set 1	290	Vertical/200	1m	"	"	"	"	"		
			Joint set 2	290	20/20	1m	"	"	"	"	"		
			Cleavage	20	60/113					"	"		
569752	1523598	2520	Joint set 1	350	Vertical/260	3m to 4m	"	"	"	Sandstone	Adigrat sandstone		
			Joint set 2	286	Vertical/196	"	"	"	"	Sandstone	Adigrat sandstone		
???	???	???	Dolerite dyke	300	75/210								
			Joint set 1 (prominent)	10	Vertical/100		"	"	"	Dolerite	Mekelle Dolerite		
550352	1489015	2160	Ambaradem Sandstone outcrop										
548860	1483911	2184	Dolerite dyke (13m wide)	20	Vertical/110								
			Joint set 1 (prominent)	20	Vertical/110			quart/calcite					
			Joint set 2	110	Vertical/200			"					
548233	1482652	2199	Dolerite dyke (20m wide)	36	Vertical/126								

			Joint set 1	36	Vertical/126	Irregular	"	"	"	Dolerite	Mekelle Dolerite		
			Joint set 2	308	Vertical/218	20cm	"	"	"	Dolerite	Mekelle Dolerite		
			Joint set 3		Sub-horizontal	20cm	"	"	"	Dolerite	Mekelle Dolerite		
548233	1482652	2199	Joint set 1	100, 78	Vertical/179	20cm	"	"	"	Marly limestone	Agula shale		
			Joint set 2	8	Vertical/98	30cm	"	"	"	Marly limestone	Agula shale		
548233	1482652	2199	Joint set 1	210	Vertical/300		"	"	"	Dolerite	Mekelle Dolerite		
546652	1480716	1969	Dolerite dyke	26	66/135								
			Joint set 1	230	Vertical/320		"	"	"	Dolerite	Mekelle Dolerite		
			Joint set 2	60	Vertical/150		"	"	"	Dolerite	Mekelle Dolerite		
			Joint set 3	288	Vertical/198		"	"	"	Dolerite	Mekelle Dolerite		
546562	1480578	1963	Joint set 1	318	Vertical/228	1m	2cm to less than a mm	"	"	Limestone	Antalo limestone		Bedding strike 96, dip 28, dip direction 360
			Joint set 2	50	Vertical/140	"	"	"	"	"	"		
557602	1499925	2338	Joint set 1	336	Vertical/2	100cm,	Tight		Contineous	Limestone	Antalo		Horizontal

					46	120 cm, 275 cm					limestone		bedding, Bed thickness (1m to 1.5m)
			Joint set 2	256	Vertical/346	17cm, 50cm, 100cm, 130cm, 170cm	"		"	"	"		
557118	1512409	2089	Joint set 1 (old)	315	Vertical/220	120cm, 130cm, 160cm, 230cm	Tight to 13 cm		"	"	"		
			Joint set 2 (oldest)	35	Vertical/125	Irregular			Discontineous	"	"		
			Joint set 3 (young)	80	Vertical/170	220cm			"	"	"		
577967	1579515	2294	Joint set 1	150,165	Vertical/248	27cm, 38cm, 77cm	Tight		Contineous	Blacklimestone	Tambien Group		
			Joint set 2	64	Vertical/154	40cm, 70cm, 120cm	"		"	"	"		
560528	1567193	2661	Dolerite dyke	155	Vertical/245	80acm central & massive with 1m wide contact zones on its left and right				Cutting Sandstone			

560363	1563163	2558	Dolerite dyke	155	Vertical/245	1.5m wide				Cutting phyllite			
562453	1559822	2578	Joint set 1	25	Vertical/115					Sandstone	Enticho sandstone		
			Joint set 2	102	Vertical/192					"	"		
			Joint set 3	176	Vertical/266					"	"		
560345	1549683	2349	Joint set 1 (young)	20	72/115	3cm, 6.3cm, 7.5cm, 8cm, 23cm	Tight to 1cm		Contineous	Sandstone	"		
			Joint set 2 (old)	150	Vertical/240					"	"		
			Joint set 3		Horizontal	10cm, 15cm, 20cm, 50cm	Tight		Contineous	"	"		
549962	1553889	2306	Joint set 1 (young)	126	Vertical/216	9cm, 10cm, 20cm	Tight		Contineous	Tillite	Edaga-Arbi tillite		Tillite of marly nature, sub horizontal, layering, bed thickness 5cm-10cm
			Joint set 2 (old)	36	Vertical/126	3cm, 4.5cm, 8cm, 17cm	"		Contineous	"	"		
543788	1536836	1996	Joint set 1	46	40/120	37cm	Tight		Contineous	Slate	Tambien		

											Group		
			Foliation	11	60/110		"		"	"	"		
561612	1526058	2043	Joint set 1	163	Vertical/253	130cm to 280cm	5cm to 20cm		"	Fossilifereous limestone	Antalo limestone		
			Joint set 2	85	Vertical/175	200cm and greater	"		Contineous	"	"		
			Bedding plane	150	22/240					"	"		
580315	1473622	1511	Joint set 1	5 to 10	Vertical/98	5cm to 73cm	Tight to 3cm		Contineous	Limestone	"		
			Joint set 2	127	Vertical/217	5cm to 15cm	Tight to few mm		Contineous	"	"		
568326	1479886	2386	Joint set 1	165	Vertical/255	11cm, 18cm, 45cm	Tight		Contineous	Dolerite	Mekelle Dolerite		
			Joint set 2	103	Vertical/193	Irregular	Tight		Contineous	"	"		
568326	1479886	2386	Joint set 1	172	Vertical/262	15cm to 20cm	Tight		Contineous	Marl	Antalo limestone		
			Joint set 2	28	Vertical/118	"	"		"	"	Antalo limestone		
			Joint set 3	92	Vertical/182	"	"		"	"	Antalo limestone		
			Joint set 4	140	Vertical/230	"	"		"	"	Antalo limestone		
573454	1493195	2393	Joint set 1	47	Vertical/1	19cm to	Tight		Contineous	Dolerite	Mekelle		

					37	200cm					Dolerite		
			Joint set 2	143	Vertical/233	"	"		"	"	"		
551953	1489779	2198	Joint set 1	5	Vertical/95	32cm, 115cm	Tight		Contineous	Dolerite	Mekelle Dolerite		
			Joint set 2	61	Vertical/151	12cm, 26cm, 45cm	"		"	"	"		
547100	1486390	2100	Major joint set	134	Vertical/224	50cm to 1m	Tight to 1cm		Contineous	Limestone	Antalo limestone		
546497	1487309	2089	Joint set 1	0	Vertical/90	133cm	Tight to 2.3cm		Contineous	Blacklimestone	Antalo limestone		
			Joint set 2	80	Vertical/170	16cm, 24cm, 43cm, 1.2m	"		"	"	Antalo limestone		
545376	1487959	2093	Joint set 1	116	Vertical/206	9cm, 24cm, 30cm, 0.5m	Tight		Contineous	Dolerite	Mekelle Dolerite		
			Joint set 2	25	Vertical/115	Irregular	"		"	"	"		
561708	1471764	2206	Major joint set	110	Vertical/200	35cm	Tight		Contineous	Limestone	Agulae shale		
560901	1474449	2265	Dolerite dyke	40	Vertical/130	7.1m thick				Dolerite	Mekelle Dolerite		Intense jointing on the marl in contact with the dolerite dyke strike similar to

													the dyke, dams both surface water and groundwater
546451	1479056	1930	Dolerite dyke	30	Vertical/120	13.5m				Dolerite	Mekelle Dolerite		"
538708	1455957	1806	Major joint set	116	Vertical/206	2cm to 50cm	Tight		Contineous	Dolerite	Mekelle Dolerite		
539168	1457006	1955	Joint set 1	82	Vertical/172	0.3m to 1.5m	Tight		Contineous	Limestone	Antalo limestone		
			Joint set 2	35	Vertical/125	"	"		"	"	"		
539687	1461502	2086	Joint set 1	156	Vertical/246	1cm to 20cm	Tight		Contineous	Marl	"		
			Joint set 2	38	Vertical/128	"	"		"	"	"		
			Joint set 3	97	Vertical/187	"	"		"	"	"		
524684	1499014	1851	Joint set 1	97	Vertical/187	90cm to 1m	Tight		Contineous	Sandstone	Adigrat Sandstone		
			Joint set 2	42	Vertical/132	1.6m to 2m	"		Discontineous	"	"		
524684	1499014	1851	Joint set 1	97	Vertical/187	40cm to 1m	Tight		Contineous	Sandy limestone (calcarinite)	Antalo limestone		
			Joint set 2	360	Vertical/270	80cm to 1.7m	"		"	"	"		

			Bedding plane		21/115								
510786	1500631	2444	Joint set 1	10	Vertical/100	10cm to 1.5m	Tight		Contineous	Mudstone	Amba aradem formation		
			Joint set 2	124	Vertical/214	8cm, 38cm, 60cm	"		"	"	"		
508232	1498169	1775	Joint set 1	80	Vertical/170	Irregular	Tight		Contineous	Sandstone	Adigrat sandstone		
			Joint set 2	140	Vertical/230	"	"		"	"	"		
502301	1469976	1465	Joint set 1 (major,old)		Vertical/59	5cm, 13cm, 50cm	Tight		Contineous	Metabasalt	Tsaliet group		
			Joint set 2 (young)		62/54	3.17m	"		"	"	"		
			Filiation		Vertical/44		"		"	"	"		
503281	1471416	1518	Joint set 1 (major,old)		Vertical/78	5cm, 19cm	Tight		Contineous	Phyllite	Tsaliet group		
			Joint set 2 (young)		Vertical/42	8cm, 15cm, 21cm	"		"	"	"		
			Filiation	53	Vertical/143								
572971	1489868	2392	Joint Set 1	45	Vertical/135	50-100cm	5-20mm	None	Contineous	Limestine, shale, marl intercalation	Agulae shale		

572971	1489868		Joint Set 2	360	Vertical/270	30-50cm	5-10mm	Clay	"	"	"		
572971	1489868		Joint Set 3	280	Vertical/190	20-60cm	2-5mm	None-clay	"	"	"		
572971	1489868		Joint Set 4	330	Vertical/240	60cm	2-5mm	None	"	"	"		
572939	1489898	2398	Joint Set 1	285	Vertical/195	50-100cm	2-20mm	None	"	"	"		
572939	1489898		Joint Set 2	15	Vertical/105	50-100cm	2-20mm	None	"	"	"		
572939	1489898		Joint Set 3	310	Vertical/220	30-50cm	5mm	None	"	"	"		
572903	1489934	2402	Joint Set 1	280	Vertical/190	150cm	5mm	None	"	"	"		
572903	1489934		Joint Set 2	30	Vertical/120	100cm	10mm	Calcite	"	"	"		
572941	1489884	2399	Joint Set 1	290	60^0/200	50cm	1-20mm	None	"	"	"		
572941	1489884		Joint Set 2	40	Vertical/130	20-50cm	2-10mm	None	"	"	"		
573142	1490212	2401	Joint Set 1	280	Vertical/180	2m	Tight	None	Non contineous	Dolerite	Mekelle dolerite		
573142	1490212		Joint Set 2	340	Vertical/250	3m	Tight	None	Contineous	"	"		
573142	1490212		Joint Set 3	30	40^0/120	30cm-1m	Tight	None	Contineous	"	"		
544894	1496350	1985		80	Vertical	3-80cm	20-	Clay	"	Limestine,	Agulae		

							220mm			shale, marl intercalation	shale		
544916	1496343	1987		50	Vertical	30-110cm	20-100mm	None	"	"	Agulae shale		
544855	1496328	1984		30	25^0?	5-25 cm	10-100mm	Clay	"	"	Agulae shale		
544760	1496231	1987		280	60	10-25cm	10-50mm	Clay	"	"	Agulae shale		
544726	1496393	1982		60	Vertical	2.5-27cm	20-250mm	None	"	"	Agulae shale		
544706	1496415	1981		120	80	4-60cm	20-50mm	Calcite	"	"	Agulae shale		
544590	1496520	1986		85	Vertical	7-100cm	40-250mm	Calcite and open	"	"	Agulae shale		
544466	1496402	1990		30	Vertical	15-40cm	50-100mm	None	"	"	Agulae shale		
544427	1496359	1988		Horizontal	0	10-65cm	40-250mm	None	"	"	Agulae shale		
544703	1496612	1994		140	85	5-15cm	10-120mm	None	Non contineous	"	Agulae shale		
544804	1496501	1990		80	Vertical	7-30cm	20-150mm	None	Contineous	"	Agulae shale		
549218	1501986	1914		300	20	5-20cm	10-500mm	Clay	Non contineous	"	Agulae shale		
549182	1501975	1913		70	10	13-25cm	20-30mm	None	Contineous	"	Agulae shale		
549183	1501950	1918		30	10	4-14cm	5-50mm	Clay	Contineous	"	Agulae shale		

549079	1502095	1919		320	5	3.5-60cm	15-80mm	Clay	Contineous	"	Agulae shale		
548937	1502173	1923		310	5	1-5cm	5-60mm	None	Non contineous	"	Agulae shale		
548912	1502200	1920		325	35	1-5cm	5-60mm	None	Contineous	"	Agulae shale		
549166	1502463	1921		300	20	2-5cm	5-75mm	None	Contineous	"	Agulae shale		
549109	1502492	1917		270	Vertical	3.5-8cm	20-110mm	Clay	Contineous	"	Agulae shale		
549088	1502495	1911		60	20	2-13cm	15-80mm	None	Contineous	"	Agulae shale		
549039	1502455	1908		80	10	5-15cm	15-50mm	Clay	Non contineous	"	Agulae shale		
548726	1502329	1897		320	5	2-10cm	10-80mm	Clay	Contineous	"	Agulae shale		
548683	1502368	1894		330	10	2-18cm	15-50mm	None	Contineous	"	Agulae shale		

Annex 5 Groundwater level and well yield data collected from different sources

S.No	X	Y	Z	Total Depth	Water Strike Depth (mbgl)	SWL (mbgl)	Well Yield (L/S)	Source
1	533420	1543700	1852	41		7	1.5	DH Consult
2	547251	1560492	2438	44		8	3	DH Consult
3	538062	1544127	1956	36		3.5	6	DH Consult
5	548158	1549299	2224	61		4.5	5	DH Consult
6	535792	1539813	1973	33		12.5	3	DH Consult
7	541075	1543692	2093	37		16	1.8	DH Consult
8	552046	1552205	2282	41		3.2	2.5	DH Consult
9	543586	1544508	2108	52		23	0.5	DH Consult
11	540625	1550094	1943	44		21	2.5	DH Consult
12	543627	1563445	2164	60				DH Consult
13	537171	1543813	1936	45		4	0.7	DH Consult
17	604745	1531701	800	89		13.5	4	DH Consult
20	563592	1539646	2422	36		10	0.8	DH Consult
21	562859	1536796	2351	45		20	0.8	DH Consult
22	563856	1540472	2406	33		3.5	2	DH Consult
23	570308	1516103	2075	36		10	4	DH Consult
24	558049	1560370	2398	49		29	1.5	DH Consult
25	567855	1570617	2766	45		21	2	DH Consult
26	547591	1496226	1988	44		Artesian	10	DH Consult
28	547935	1492503	2124	46		13	1	DH Consult
32	551760	1478919	2045	78		24	2	DH Consult
33	550475	1499314	1968	37		3	5	DH Consult
35	543898	1497970	2010	37		4.8	0.8	DH Consult
36	556075	1478033	2199	41		3	2.5	DH Consult
37	555751	1478341	2185	37		4.2	1.8	DH Consult
38	572508	1482762	2091	45		15	0.8	DH Consult
40	555487	1491484	2255	41		1.5	1	DH Consult
41	546050	1478454	1955	53		18	1.8	DH Consult
43	582368	1523296	2426	63		27	1.5	DH Consult
44	580585	1541225	2993	43		11	1.5	DH Consult
45	573010	1524113	2545	43		3	1.5	DH Consult
46	578102	1538233	2724	43		12.6	1	DH Consult
48	535033	1508388	1952	60		17	0.5	DH Consult
49	553378	1498065	2141	55		19	0.8	DH Consult
58	499041	1525646	1752	54		30	0.6	DH Consult

59	512839	1526738	1615	43		7.6	2.5	DH Consult
60	499846	1519024	1875	51		3.9	0.7	DH Consult
61	515746	1528339	1642	31		3.3	3	DH Consult
64	547671	1548784	2212	74		5	3	DH Consult
65	555901	1543966	2234	37		3.15	2	DH Consult
67	525770	1537187	1624	45		12.4	1.5	DH Consult
68	551290	1534057	2080	40		8	0.8	DH Consult
69	545200	1536880	2053	32		4.7	0.3	DH Consult
71	527183	1534431	1673	36		5.3	1.6	DH Consult
72	562908	1524766	1994	30		19	3	DH Consult
73	542706	1531127	1982	108		8	5	DH Consult
75	572700	1511430	2233	36		7	1	DH Consult
77	563053	1501971	2254	49		18.6		DH Consult
79	566850	1514874	2046	57		40	0.5	DH Consult
80	557013	1530254	1982	51		4	10	DH Consult
82	522203	1473873	2131	33		3	1.5	DH Consult
88	544264	1464722	2128	41		15.4	0.8	DH Consult
91	551070	1471122	2338	36		10	1.2	DH Consult
93	549723	1470746	2144	33		5	1.8	DH Consult
94	561340	1459859	2143	52		13.5	2.5	DH Consult
95	561731	1462431	2129	28		7	10	DH Consult
96	572887	1437532	2115	120		1.5	7	DH Consult
98	555121	1448285	2055	60		7	5	DH Consult
99	558547	1460352	2118	51		0	3	DH Consult
103	541745	1405176	2227	52		11.3	5	DH Consult
104	545695	1467677	2150	50		6.5	0.8	DH Consult
105	547591	1496226	1968	44		Artesian	10	DH Consult
107	572508	1482762	2091	45		15	0.8	DH Consult
108	546050	1478454	1955	52		18	1.8	DH Consult
109	555487	1491484	2255	40		1.5	1	DH Consult
110	547255	1503382	1867	114		5.3	25	DH Consult
119	556075	1480330	2199	41		3	2.5	DH Consult
120	543898	1497970	2014	37		4.8	0.8	DH Consult
122	555751	1478341	2185	37		4.2	1.8	DH Consult
123	564070	1486356	2323	43		13	0.8	DH Consult
124	541483	1491682	2231	35		12	0.5	DH Consult
125	563060	1474870	2307	51		10	1	DH Consult
127	561643	1478813	2284	58		20	4	DH Consult
128	555901	1486423	2252	44		5.3	4	DH Consult
129	546242	1503342	1883	38		12	4	DH Consult
130	547128	1501090	1938	62		30	3.16	DH Consult

131	556707	1496957	2081	50		7.1	3.37	DH Consult
132	548820	1492435	2070	62		13	3.56	DH Consult
134	545504	1489984	2131	44		14	2.6	DH Consult
135	553320	1488680	2203	133		37		DH Consult
136	559405	1487676	2262	94		24		DH Consult
137	557487	1488680	2248	150		28		DH Consult
138	559410	1487663	2259	128		24.1		DH Consult
139	559405	1487676	2262	101		24		DH Consult
140	557108	1487962	2232	151		46		DH Consult
141	556050	1487809	2211	120		11		DH Consult
142	556722	1487915	2227	118		31.3		DH Consult
143	553941	1488821	2214	120		20		DH Consult
144	553706	1488251	2210	120		15		DH Consult
145	554336	1487216	2189	104		13		DH Consult
146	555520	1487648	2221	75		19.7		DH Consult
147	557115	1487967	2233	65		8.1		DH Consult
148	557809	1488359	2237	90		19		DH Consult
149	558268	1488286	2243	72		16		DH Consult
151	552490	1489376	2208	75		9.8		DH Consult
152	552945	1488948	2208	80		14		DH Consult
153	553207	1488955	2206	100		16		DH Consult
154	552490	1489376	2208	84		6.6		DH Consult
155	552945	1488663	2202	69		17		DH Consult
156	550604	1499441	1974	71		12		DH Consult
157	551239	1499241	1970	58		16		DH Consult
158	550560	1498426	1966	73		8.3		DH Consult
160	552970	1488153	2206	145		51	18	DH Consult
161	557116	1487879	2245	104		25		DH Consult
164	552970	1488153	2206	147		29	25	DH Consult
167	553426	1487393	2204	286		36		DH Consult
169	561057	1487352	2277	250		15.8	36.7	DH Consult
170	564439	1485877	2311	300		6.3	30	DH Consult
171	561060	1480957	2327	210		8	0.8	DH Consult
172	557234	1488028	2228	244		50	25	DH Consult
173	552970	1488153	2206	250		56	22	DH Consult
174	549453	1485160	2133	320		16.8	6	DH Consult
187	572090	1490331	2377	62	22	19	30	TWWCE
188	571887	1492008	2378	60	18	12	20	TWWCE
189	574424	1494243	2423	58	11	5.5	9	TWWCE
191	560389	1474914	2253	70	19	5	25	TWWCE
193	560389	1474914	2253	70	8	6	8	TWWCE

194	561133	1477040	2255	70	9	6	7	TWWCE
202	569894	1492889	2391	64	12	4	20	TWWCE
217	555135	1526845	1925	350	14	4	3	TWWCE
223	551701	1487541	2174	84	12.5	7.4	8	TWWCE
224	562713	1522903	1982	88	12	16	10	TWWCE
225	562482	1522447	1984	79	13	16	4	TWWCE
228	566691	1522354	2042	46	15	12.5	4	TWWCE
233	561684	1533936	2345	45	7	5	2	TWWCE
234	563212	1536331	2347	42	12	11	0.5	TWWCE
235	565070	1538880	2461	45	18	13	2	TWWCE
236	566208	1541183	2468	45	20	10	5	TWWCE
237	566567	1540508	2482	45	16	16	3	TWWCE
238	563092	1542043	2422	54	17	12.2	1	TWWCE
240	562703	1537590	2357	54	16	15	1	TWWCE
241	562283	1535625	2324	42	6	3.2	2	TWWCE
243	550319	1520767	1988	38	13	15	5	TWWCE
244	562726	1537620	2358	45	28	21	0.4	TWWCE
245	547422	1533794	2105	54	7	6	5	TWWCE
247	557044	1536693	2003	51	22	7	1	TWWCE
248	603493	1534967	850	105	24	19.7	3.5	TWWCE
249	595110	1534628	1463	151	88	48	11	TWWCE
250	575255	1544676	2776	38	9	4	0.7	TWWCE
251	576235	1545262	2799	44	13	8.3	0.6	TWWCE
252	577493	1545873	2812	44	6	3	0.5	TWWCE
253	577072	1549117	2862	56	30	6	0.7	TWWCE
254	578786	1548053	2838	44	9	4.8	1.8	TWWCE
255	579582	1547810	2873	50	41	8	0.13	TWWCE
256	573267	1548028	2731	43	13	8	5	TWWCE
257	573833	1545245	2761	41	22	5	2	TWWCE
258	574154	1548917	2757	50	9	8	0.06	TWWCE
259	573990	1533381	2673	46	18	15	1.5	TWWCE
260	577023	1524079	2418	46	10	10	2	TWWCE
261	578323	1528596	2576	40	8	8	0.3	TWWCE
262	579031	1533678	2716	34	6	4	4	TWWCE
264	581318	1530211	2612	37	6	6	0.8	TWWCE
266	572814	1526110	2532	49	15	15	0.2	TWWCE
267	575175	1527128	2614	52	30	14	0.4	TWWCE
268	575627	1533676	2716	34	10	8	3	TWWCE
269	572589	1532358	2633	51	34	22	1	TWWCE
271	573802	1529882	2604	45	31	23	1.5	TWWCE
272	574599	1531243	2646	49	18	13	2	TWWCE

274	576634	1539087	2713	45	21	11	2	TWWCE
276	575227	1551202	2807	60	27	33		TWWCE
278	573206	1537578	2771	45	9	15	0.4	TWWCE
279	572205	1537895	2759	45	7	4	2.5	TWWCE
282	582368	1523296	2426	63	45	27	1.5	TWWCE
283	580585	1541225	2993	43	18	11	1.5	TWWCE
284	573010	1524113	2545	43	4	3	1.5	TWWCE
285	578102	1538233	2724	43	12	12.6	1	TWWCE
287	572841	1546616	2738	46	8	7	1.5	TWWCE
292	572838	1542471	2741	45	8	14		TWWCE
293	573202	1549059	2692	48	10	19		TWWCE
294	572515	1541618	2726	36	7	8.2	1.45	TWWCE
295	581427	1530926	2646	43	18	20	0.8	TWWCE
296	576010	1547135	2777	48	9	5	2	TWWCE
298	577782	1534977	2708	33	9	6	0.8	TWWCE
300	583805	1548460	2809	45	27	14	0.35	TWWCE
301	581580	1522966	2410	45	24	13	0.35	TWWCE
302	576979	1545326	2805	44	9	9	1.5	TWWCE
303	582976	1522364	2387	37	6	4	2	TWWCE
304	571001	1517476	2115	42	22	20	2	TWWCE
305	574536	1519380	2133	33	11	9	4	TWWCE
306	575027	1535033	2690	36	5	6	1	TWWCE
307	549795	1582305	2430	72	6	3	6	TWWCE
308	548812	1582355	2446	120	11	9	15	TWWCE
309	551018	1565700	2400	54	12	8	1	TWWCE
312	552970	1572386	2485	69	12	11.5	0.4	TWWCE
318	550011	1574059	2493	69	16	32	2.5	TWWCE
322	549200	1582327	2442	113	3	3	15	TWWCE
323	547960	1582207	2454	144	18	21	2	TWWCE
324	549206	1582327	2440	114	3	3	18	TWWCE
326	523132	1534863	1632	54	35	32	0.5	TWWCE
329	544574	1540629	2082	45	11	6	0.3	TWWCE
330	542358	1544398	2083	51	27	17	0.8	TWWCE
331	534233	1545920	1890	51	13	10	1	TWWCE
333	551277	1562503	2375	58	21	10	3	TWWCE
334	548315	1552994	2380	21	14	13	1.5	TWWCE
335	550017	1554072	2301	52	24	7	0.8	TWWCE
336	542662	1557337	2134	45	29	13	0.6	TWWCE
337	541591	1557414	2124	51	21	20	0.4	TWWCE
339	550832	1555029	2311	58	12	6	2	TWWCE
341	557765	1543343	2276	49	12	5.5	2	TWWCE

342	557323	1542672	2262	46	11	7	1	TWWCE
345	549707	1549115	2240	49	9	10	0.3	TWWCE
346	555525	1543664	2244	46	12	4	0.8	TWWCE
347	554744	1554619	2335	50	9	6.4	0.8	TWWCE
348	542289	1542800	2086	48	11	11	5	TWWCE
351	546776	1541872	2147	40	3	2	1.5	TWWCE
352	547877	1547948	2260	49	15	10	1	TWWCE
353	547620	1551210	2229	58	30	27	1.5	TWWCE
354	546818	1554455	2226	46	15	6	1.8	TWWCE
355	549743	1560902	2361	58	9	15	0.4	TWWCE
356	549815	1557251	1355	58	33	21	2.5	TWWCE
357	542685	1541768	2078	37	25	17	0.5	TWWCE
359	520775	1464253	1740	60	22	13	10	TWWCE
360	527075	1464651	1751	63	22	13	20	TWWCE
361	513063	1473847	1737	59	15	12	20	TWWCE
362	512931	1474211	1727	57	10	13	20	TWWCE
363	512415	1473937	1716	55	12	8	4	TWWCE
364	520302	1465712	1732	60	13	8	5	TWWCE
365	520528	1465805	1728	60	9	7	15	TWWCE
366	520073	1465110	1720	67	9	7	4.5	TWWCE
368	520288	1464523	1735	60	14	7	10	TWWCE
369	519563	1463601	1718	62	8	5	6	TWWCE
370	520980	1463587	1759	60	8	10	12	TWWCE
371	528571	1462414	2212	50	11	7	5	TWWCE
372	512727	1474609	1722	52	12	8	10	TWWCE
373	512924	1474785	1727	52	10	7	10	TWWCE
374	512511	1474128	1738	55	12	9	10	TWWCE
375	522738	1473815	1727	58	14	10	6	TWWCE
376	517902	1474955	1722	56	13	10	10	TWWCE
377	513226	1474988	1732	52	12	8	10	TWWCE
378	527355	1462019	2120	92	12	28	15	TWWCE
383	524262	1456482	1790	44	18		0.4	TWWCE
384	517471	1451440	1513	48	12		0.4	TWWCE
385	512076	1474223	1711	44	9		0.4	TWWCE
386	512335	1474597	1711	47	7	6	2	TWWCE
393	522264	1465634	1768	48	29	25	2	TWWCE
394	510025	1442403	1461	42	9	4	1.5	TWWCE
395	521870	1462709	1786	41	10	11	2	TWWCE
396	524689	1464133	2261	37	12	20	1.5	TWWCE
399	512140	1477921	1545	38	9	5	2	TWWCE
400	526338	1447057	1654	46	12	12	2.5	TWWCE

401	526938	1441111	1658	52	10	10	2.6	TWWCE
402	528047	1444067	1686	49	19	22	2.5	TWWCE
404	513478	1444068	1479	37	6	2.2	2	TWWCE
407	529334	1454117	1757	52	9	7	0.5	TWWCE
408	514431	1468049	1646	37	10	15	1	TWWCE
409	529610	1454427	1771	60	9	3	1	TWWCE
411	528702	1452130	1698	43	9	18	1	TWWCE
412	534133	1448870	1682	51	24	21	5	TWWCE
413	532789	1446843	1700	50	7	4	10	TWWCE
423	522203	1473873	2131	33	5	3	1.5	TWWCE
424	520209	1458282	1911	72	18	18		TWWCE
431	529334	1454117	1757	52	9	7	0.5	TWWCE
432	522341	1465933	1770	41	5	4	2	TWWCE
433	521746	1465919	1761	42	10	5	2	TWWCE
434	521562	1466558	1743	42	11	10	2.5	TWWCE
435	509192	1481405	2197	82	39	6	0.8	TWWCE
438	559545	1507939	2109	427	72	32	20	DH Consult
439	555157	1528161	1941	204	50	Artesian	50	DH Consult
440	555135	1526855	1930	350	4	3	3	DH Consult
445	538486	1523128	1981	324	9	12	40	DH Consult
449	539594	1467513	2095	70	6	4	3	
453	551248	1464202	2059	43	9	8	1	
456	554637	1460404	2065	70	6	4	10	
457	554185	1459472	2087	58	12	9	20	
458	554114	1559955	2072	70	15	11	6	
460	560628	1462483	2129	64	15	Artesian	40	
461	560343	1462723	2126	70	15	2	20	
462	559446	1462079	2119	60	18	Artesian	35	
463	559732	1461812	2120	70	30	Artesian	25	
464	559911	1461450	2123	70	18	Artesian	10	
465	558626	1451833	2161	58	17	16	1.5	
466	557401	1463309	2066	60	12	11.5	0.7	
467	555280	1450077	2024	57	12	11	1.2	
468	551977	1473534	2128	41	9	8	15	
482	555280	1450077	2024	57	12	11	1.2	
483	558626	1451833	2161	58	17	16	1.5	
484	538963	1476498	2142	41	6	0.5	20	
486	541457	1474940	2156	43	9	9	0.8	
489	549980	1465795	2065	70	30	7	30	
490	544817	1464242	2112	58	14	12	15	
491	544987	1465448	2120	70	18	18	40	

492	558244	1460352	2112	64	10	7	3	
493	554482	1464672	2089	70	12	12	30	
494	557401	1463309	2066	60	12	11.5	0.7	
495	562129	1463386	2126	46	9	9	0.8	
496	536238	1470499	2333	40	6	0.45	10	
497	551977	1473534	2128	41	9	8	15	
498	549939	1470367	2137	46	15	11.6	20	
499	562821	1461536	2150	58	40	39	1	
503	555685	1557123	2379	46	24	17	1	
504	555285	1556971	2373	42	15	18	1.5	
505	560011	1559470	2504	42	12	11.2	1	
509	562155	1542704	2376	40	15	12	1.5	
511	564620	1543265	2436	42	23	21	1.5	
512	562332	1560608	2532	37	9	9	1	
515	564881	1557716	2566	34	17	14	0.4	
517	556180	1561614	2432	46	24	11	0.8	
518	553322	1562335	2434	46	13	27	0.3	
519	558550	1560926	2443	43	15	12	0.8	
520	575164	1577387	2381	31	13	11	2	
523	578741	1578996	2344	43	33	28	0.5	
525	559527	1545697	2308	39	6	1.5	1	
526	563766	1542111	2419	60	37	36	2	
563	494753	1472310	1457	45	12	4	1.5	
565	491183	1483974	1424	52	33	28	0.6	
569	487662	1473174	1302	49	9	21.5	1	
570	486954	1469964	1309	67	39	63	0.3	
572	499660	1485694	1408	40	7	4.5	2	
574	491268	1475720	1417	73	29	29	2	
575	493221	1498623	1628	73	19	13	2.5	
576	561562	1502579	2240	spring				
577	569912	1514740	2062	spring				
578	562112	1501200	2213	spring				
579	577967	1579515	1294	spring				
580	580315	1473622	1511	spring				
581	559195	1490431	2217	spring				
582	569275	1492179	2362	spring				
583	541415	1495507	1959	spring				
584	547100	1486390	2100	spring				
585	546497	1487309	2089	spring				
586	545376	1487959	1953	spring				
587	561708	1471764	2206	spring				

588	561153	1474287	2268	spring				
589	558912	1435750	2703	spring				
590	558283	1444110	2116	spring				
591	552788	1452114	1977	spring				
592	539168	1457006	1955	spring				
593	524097	1502834	2004	spring				
594	524684	1499014	1828	spring				
595	509933	1499261	2030	spring				
596	506401	1497693	1673	spring				
597	501355	1505847	1676	spring				
598	515087	1456933	1736	spring				
599	527613	1461672	2156	spring				
600	578740	1531354	2627	spring				
601	580109	1533673	2674	spring				
602	570432	1571347	2832	spring				

Annex 6 Well hydraulic parameters collected from different sources

Object-ID	Main aquifer	X	Y	Z	Well depth m	Transmissivity m^2/day	Aquifer thickness m	Hydraulic conductivity m/day	Data source
Bubu Hotel	Limestone					4.33		0.72	EMD
Kalamino2002	Limestine, Dolerite					119		5.23	EMD
Mekelle University	Limestine, Dolerite					1.49		0.07	TWWCE
Mesebo 3	Marl with limestone	550130	1498944	1945		7.62		1.27	EMD
Mesebo 4	Marl with limestone	551238	1499237	1991		104		9.32	EMD
Mesebo 5	Marl with limestone	550608	1499440	1976		434		22.80	EMD
Quiha town	Limestone					336		18.60	TWWCE
Sewhi Nugus	Limestone, Marl					83.5		3.48	TWWCE
Tesfa Livestock	Limestone	552112	1484834	2226		402		57.50	EMD
TW-1	Dolerite	553845	1487586	2193		23.3		1.25	DEVECON
TW-4	Dolerite	553140	1488452	2178		24.4		1.28	DEVECON
TW-5	Dolerite, Limestone, Snadstone	552880	1489018	2183		146		4.54	DEVECON
PB-1	Sandstone, Dolerite	555814	1487575	2213		145		4.83	TWWCE
PB-2	Dolerite	556716	1487915	2229		20.7		0.99	TWWCE
PB-3	Dolerite	553936	1488190	2218		2630		49.70	TWWCE
PB-4	Limestone, Dolerite	553704	1488248	2205		293		11.70	TWWCE
PB-5	Dolerite	554288	1487046	2181		0.97		0.02	TWWCE
PB-6	Limestone, Dolerite	555524	1487644	2218		2260		74.40	TWWCE
PB-7	Limestone, Dolerite	557111	1487964	2230		888		44.40	TWWCE
PB-8	Limestone, Gravel	557800	1488354	2243		500		14.70	TWWCE
PB-9		558268	1488286	2243	71.5	51.04		3.20	Guesh
PB-10	Limestone, Sandstone					15.7		0.95	TWWCE
PB-11	Sandstone, Limestone	552485	1489381	2197		967		74.40	TWWCE
PB-12	Limestone, Dolerite	553534	1488943	2197		1360		85.40	TWWCE
PW1	Limestone	556050	1487809	2211	120	280.8		9.36	Teklay
PW2	Dolerite	556722	1487915	2224	117.5	21.024		1.45	Teklay
PW3	Limestone	553941	1488821	2214	120	1429		35.70	Teklay
PW4	Dolerite	553706	1488251	2210	120	91.67			FWWDSE

PW5	Dolerite	554336	1487216	2189	104	1.02			FWWDSE
PW6	Limestone	555526	1487648	2221	75	1641		43.18	Teklay
PW7	Dolerite	557115	1487967	2233	65	552.9		25.00	Teklay
PW8	Marl with limestone	557809	1488359	2237	89.9	432		27.00	Teklay
PW9	Marl with limestone	558268	1488286	2243	71.5	19		0.68	Teklay
TW1-2005	Limestone	551965	1487745			1935		8.20	Tesfamichael
TW2-2005	Limestone	552132	1487873	2135		15.6		0.13	
TW4-2005	Limestone	557116	1487879	2206		39.5		0.20	
TW5-2005	Limestone	553207	1488955	2203		183.1		1.40	
TW6-2005	Limestone					23.7		0.12	
Adi seleste		555901	1486423	2252		217		18.10	
AR-1		556406	1488604	2215		409		14.00	Guesh
AR-2		555787	1489875	2256		723		18.00	Guesh
LESPER		551526	1487025	2143		27.4		24.00	Guesh
TW4	Dolerite	553140	1488452	2178		24.4		19.00	Guesh
TW5		552880	1489018	2183		127		28.00	Guesh
TW1-2005		561057	1487352		250	2130		6.20	FWWDSE
TW2-2005		564439	1485877		300	357		1.00	FWWDSE
TW3-2005		561660	1480957			357		1.00	FWWDSE
TW4-2005		557234	1488028		243.5	100		0.30	FWWDSE
TW5-2005		553074	1488354		250	186		0.50	FWWDSE
TW6-2006		549453	1485160		320	65.3			FWWDSE
TW7-2006		568500	1492331		336	151		0.40	FWWDSE
TW8-2006		543880	1506057		321	dry			FWWDSE
MU_Well		552413	1489446			150		0.40	FWWDSE
Igrewonber (MW)		554168	1489449			229		0.70	FWWDSE
WW-1/ Endagabir	Limestone, Dolerite				70	65.62			FWWDSE
WW-2/ Romanat	Marl				110	19.78			FWWDSE
BH-92/ Kuiha hospital	Dolerite	558144	1490672			5.53		0.04	FWWDSE
BH-74/ Cement - 4		551239	1499241	2202	56	110.74			FWWDSE
BH-20/ Aynalem(PW-12)		553549	1488948	2208	80	1138.4			FWWDSE
BH-75/ Cement-6		550560	1498426	1966	73	136.27			FWWDSE
BH-8/ Aynalem(PW-3)		553941	1488821	2214	120	3120.63			FWWDSE
BH-77/ Cement-5		550604	1499441	1974	70.5	245.96			FWWDSE
BH-78/ Enda kidana		556707	1496957	2081	60	15.67			FWWDSE
BH-13/ Aynalem(PW-11)		552490	1489376	2208	75	91.67			FWWDSE
BH-49/ Chinferes		546242	1503342	1883	45	143.46			FWWDSE
BH-50/ Adi bahakel		547128	1501090	1938	61.6	525.93			FWWDSE

BH-63/ Adi dairo		548820	1492435	2070	61.55	296.25			FWWDSE
BH-59/ Adi amiku		545504	1489984	2131	43.45	708.78			FWWDSE
BH-60/ Negodi		544382	1490857	2147	68.48	436.17			FWWDSE
Hawelti BH1		548776	1491289	2085	100	62.49	48	1.30	Tekeze drilling PLC
Ministry of defence well		562150	1528939	2043	138	2110.3	120	17.59	Tekeze drilling PLC
Illala slaughter		552791	1497261	1999	145	81.54	115	0.71	Tekeze drilling PLC
Ashago/BH1 (FPW-9)		560145	1487643		252	470.2	48.68	9.66	Tekeze drilling PLC
Chinferes/BH1					254	369.67	135.5	2.73	Tekeze drilling PLC
Messebo/BH-1		551068	1498562	1874	98	28.12			Tekeze drilling PLC
Messebo/BH-2		551617	1498923	1984	146.5	26.73			Tekeze drilling PLC
Messebo/BH-3		550855	1500131	1977	152.5	385.9			Tekeze drilling PLC
Messebo/BH-4		552500	1499429	2022	128.6	2.61			Tekeze drilling PLC
Messebo/BH-5		552122	1499182	2002	100	1219.93			Tekeze drilling PLC
Messebo/BH-6		551901	1498949	1989	110	3.94			Tekeze drilling PLC
Messebo/BH-7		551901	1498949	1989	204	3.5			Tekeze drilling PLC
Messebo/BH-8		576764	1390173	1475	128.6	8.83			Tekeze drilling PLC
MO-TW10 (MariamDehan)	dolerite, limestone, marl, gypsum	548531	1499142	1935	612	2.59	300	0.01	DH-consult
MO-TW4 (Kihen)	limestone	559545	1507939	2109	427	8.27	200	0.04	DH-consult
SH-BH3 (Sheba leather factory)	limestone	562713	1522903	1982	86	92.4	68	1.36	DH-consult
SH-BH2 (Sheba leather factory)	limestone, marl	562482	1522447	1984	76	19.5	63	0.31	DH-consult
Chinferes	sandstone	546692	1505523	1792	180	421	100		DH-consult
Agulae TW	limestone	566830	1513889	2030	375	432			DH-consult
SifraJeganu	limestone, marl	564839	1526060	2004	100	2			DH-consult
MO-TW5 (Tsigereda)	limestone, sandstone	538486	1523128	1981	324	60.9		0.15	DH-consult